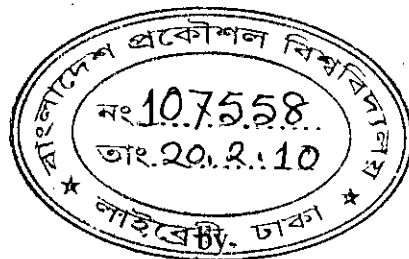
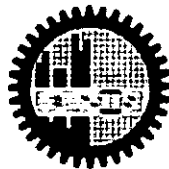


**CROSSTALK MODELING AND ANALYSIS OF
FBG-OC-BASED BIDIRECTIONAL OPTICAL CROSS CONNECTS
IN A WDM NETWORK**

A thesis submitted in partial fulfillment of the requirements for the degree of
MASTER OF SCIENCE
IN
ELECTRICAL AND ELECTRONIC ENGINEERING



Mohammad Rezaul Karim




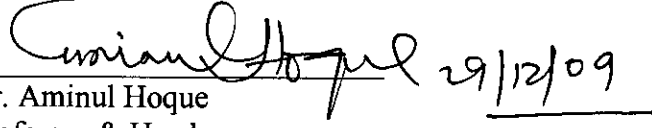
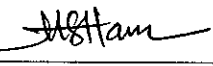

DEPARTMENT OF ELECTRICAL AND ELECTRONIC ENGINEERING
BANGLADESH UNIVERSITY OF SCIENCE AND TECHNOLOGY

2009

Approval Certificate

The Thesis titled “**CROSSTALK MODELING AND ANALYSIS OF FBG-OC-BASED BIDIRECTIONAL OPTICAL CROSS CONNECTS IN A WDM NETWORK**” submitted by Mohammad Rezaul Karim, Roll No. 040506211P, Session: April 2005 has been accepted as satisfactory in partial fulfillment of the requirements for the degree of MASTER OF SCIENCE IN ELECTRICAL AND ELECTRONIC ENGINEERING on December 29, 2009.

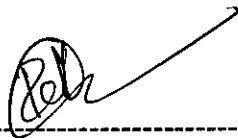
Board of Examiners

1. 
Dr. Satya Prasad Majumder
Professor
Department of EEE, BUET, Dhaka
Chairman
(Supervisor)
3.  29/12/09
Dr. Aminul Hoque
Professor & Head
Department of EEE, BUET, Dhaka
Member
&
(Ex-Officio)
4. 
Dr. Md. Shah Alam
Associate Professor
Department of EEE, BUET, Dhaka
Member
5. 
Dr. Md. Hossam-e-Haider
Wing Commander
Instructor Class-A
Dept. of Electrical, Electronics and Communication Engineering
Military Institute of Science and Technology (MIST)
Mirpur Cantonment, Dhaka
Member
(External)

Declaration

This is to certify that the thesis titled “**CROSSTALK MODELING AND ANALYSIS OF FBG-OC-BASED BIDIRECTIONAL OPTICAL CROSS-CONNECTS IN A WDM NETWORK**” is the result of my study in partial fulfillment of the M.Sc. Engineering degree under the supervision of Dr. Satya Prasad Majumder, Professor, Department of Electrical and Electronic Engineering (EEE), Bangladesh University of Science and Technology (BUET), and it has not been submitted elsewhere for any other degree or diploma.

Signature of the Candidate



(Mohammad Rezaul Karim)
Roll No. 040506211P

DEDICATED
TO
MY PARENTS

Contents

List of Figures	viii
List of Tables	xiii
List of Symbols	xiv
List of Abbreviations	xvi
Acknowledgement	xvii
Abstract	xviii
Chapter 1: Introduction	1
1.1 The Evolution of Fiber Optic Systems	2
1.2 Introduction of WDM systems	4
1.3 All-Optical Network	4
1.4 Background of this Study	5
1.5 Literature Review	6
1.6 Objectives	8
1.7 Research Methodology	9
1.8 Organization of the Thesis	9
Chapter 2: WDM Concepts and Components	11
2.1 Principles of WDM	12
2.2 Couplers	14
2.3 Star Couplers	15
2.4 Mach-Zehnder Interferometer Multiplexers	16
2.5 Isolators and Circulators	18
2.6 Fiber Bragg Gratings	19
2.7 Arrayed Waveguide Grating	22

2.8	Optical Amplifiers	25
	2.8.1 Semiconductor Optical Amplifiers	27
	2.8.2 Erbium-doped Fiber Amplifiers	27
	2.8.3 Raman Amplifiers	28
2.9	Summary	30
 Chapter 3: WDM Networks		31
3.1	WDM Network Elements	31
	3.1.1 Optical Line Terminals	31
	3.1.2 Optical Add/Drop Multiplexers	32
	3.1.3 Optical Cross Connects	34
3.2	Network Topologies	36
3.3	SONET/SDH Networks	38
3.4	Broadcast-and-Select WDM Networks	39
	3.4.1 Broadcast-and-Select Single-Hop WDM Networks	40
	3.4.2 Broadcast-and-Select Multi-Hop WDM Networks	40
3.5	Wavelength-Routed Networks	41
3.6	Unidirectional versus Bidirectional WDM Networks	42
3.7	System Model	44
3.8	Summary	45
 Chapter 4: Crosstalk Modeling and Analysis		46
4.1	Introduction	46
	4.1.1 Interband Crosstalk	46
	4.1.2 Intraband Crosstalk	47
	4.1.3 Crosstalk in Optical Networks	48
	4.1.4 Bidirectional Systems	49
4.2	FBG-OC-Based BOXC Architectures	50

4.3	Intraband Crosstalk arising from FBGs operation	53
4.4	Analysis of Intraband Crosstalk in BOXCs	55
4.5	Expression of Bit-Error Rate	64
4.6	Impact of Intraband Crosstalk induced by BOXC on BER	65
	4.6.1 PP due to Intraband Crosstalk induced by BOXC	67
	4.6.2 BER and PP due to Optical Amplifier	68
4.7	Summary	70
 Chapter 5: Results and Discussion		71
5.1	Impact of Intraband Crosstalk	71
5.2	Impact of Optical Amplifier	83
5.3	Summary	90
 Chapter 6: Conclusion and Scope of Future Work		91
6.1	Conclusion	91
6.2	Scope of Future Work	92
 Bibliography		93
 Index		96

List of Figures

	Page
Figure 1.1	Increase in the BL product over the period 1975 to 2000 through several generations of optical fiber communication systems 2
Figure 2.1	The transmission bandwidths in the 1310 nm and 1550 nm windows allow the use of many simultaneous channels for sources with narrow spectral widths 12
Figure 2.2	Implementation of a typical WDM network 13
Figure 2.3	Cross-sectional view of a fused-fiber coupler having a coupling region W and two tapered regions of length L 14
Figure 2.4	Shows an 8×8 star coupler formed by interconnecting twelve 2×2 coupler 16
Figure 2.5	Layout of a basic 2×2 Mach-Zehnder interferometer 17
Figure 2.6	Four-channel wavelength multiplexer using three 2×2 Mach-Zehnder interferometers 17
Figure 2.7	Functional representation of circulators: (a) three-port and (b) four-port. The arrows represent the direction of signal flow 18
Figure 2.8	Principle of operation of an isolator that works only for a particular state of polarization of the input signal 19
Figure 2.9	Shows basic parameters in reflection grating 20
Figure 2.10	Formation of a Bragg grating in a fiber core by means of two intersecting ultraviolet light beams 21
Figure 2.11	Simple concept of demultiplexing function using fiber Bragg grating and optical circulator 22
Figure 2.12	Top view of a typical arrayed waveguide grating used as a highly versatile passive WDM device 22
Figure 2.13	Geometry of the star coupler used in arrayed waveguide grating WDM device 24
Figure 2.15	Basic operation of a generic optical amplifier 26

Figure 2.16	Block diagram of semiconductor optical amplifier (SOA)	27
Figure 2.17	An erbium-doped fiber amplifier (EDFA)	28
Figure 2.18	SRS gain coefficient as a function of channel separation	29
Figure 2.19	Distributed Raman amplifier using a backward propagating pump, shown operating along with discrete EDFAs	30
Figure 3.1	Block diagram of optical line terminal (OLT)	32
Figure 3.2	Different OADM architectures. (a) parallel; (b) modular version of the parallel architecture; (c) serial; and (d) band drop	33
Figure 3.3	Schematic of optical cross-connect (OXC) based on optical switches	35
Figure 3.4	Three common topologies used for fiber optic networks (a) bus, (b) ring, and (c) star	37
Figure 3.5	Generic configuration of a large SONET network consisting of linear chains and various types of interconnected rings	38
Figure 3.6	Dense WDM deployment of n wavelengths in an OC-192 trunk ring	39
Figure 3.7	Two alternate physical architectures for a WDM-based local network: (a) star, (b) bus	40
Figure 3.8	Architecture and traffic flow of a multihop broadcast-and-select WDM network	41
Figure 3.9	Wavelength reuse on a mesh network	42
Figure 3.10	(a) Unidirectional and (b) bidirectional transmission systems	43
Figure 3.11	(a) Two unidirectional systems using four fibers, and (b) two bidirectional systems using two fibers	44
Figure 3.12	Bidirectional WDM ring networks interconnected by BOXCs	44
Figure 3.13	Schematic diagram of a 2×2 BOXC using four-port OCs and FBGs	45
Figure 4.1	Source of interband crosstalk. (a) An optical demultiplexer and	

	(b) an optical switch with inputs at different wavelengths	47
Figure 4.2	Sources of intraband crosstalk. (a) A cascaded wavelength demultiplexer and a multiplexer, and (b) an optical switch	48
Figure 4.3	Separating the two directions in a bidirectional system: (a) using a WDM mux/demux, and (b) using an optical circulator (OC). Both methods can introduce crosstalk, as shown by dashed lines in the figure	50
Figure 4.5	A bidirectional transmission system	49
Figure 4.6	BOXCs based on FBGs and OCs. (a) 2×2 BOXC using six-port ROCs and FBGs, and (b) 4×4 BOXC consists of six 2×2 BOXC	52
Figure 4.7	Illustration of the mechanism generating intraband crosstalk in the operation of tunable FBG. (a) The reflection mode of FBG, (b) The transmission mode of FBG, and (c) The consequent spectrum	54
Figure 4.8	Transmission and reflection spectra of FBGs. (L_{FT} : Transmission loss outside the Bragg wavelength, L_{FR} : Reflection loss at the Bragg wavelength, R_{FG} : Reflectivity at the Bragg wavelength, I_{FG} : Isolation of FBGs)	55
Figure 5.1	BER vs. received power at the bar-state of (a) 2×2 BOXC, and (b) 4×4 BOXC with the different number of wavelength channels, m . Component crosstalk, $X_f = -22\text{dB}$ and backscattering-induced crosstalk, $X_R = -25\text{dB}$ are assumed	72
Figure 5.2	BER performance in presence of intraband crosstalk with varying number of wavelength channels, m with different component crosstalk, X_f in the bar-state of 2×2 BOXC. Backscattering-induced crosstalk, $X_R = -25\text{dB}$ is assumed	73
Figure 5.3	BER performance in presence of intraband crosstalk with varying number of wavelength channels, m with different component crosstalk, X_f in the bar-state of 4×4 BOXC.	

	Backscattering-induced crosstalk, $X_R = -25\text{dB}$ is assumed	74
Figure 5.4	Power penalty as a function of component crosstalk at the bar-state of (a) 2×2 BOXC and, (b) 4×4 BOXC with the different number of wavelength channels, m . BER = 10^{-9} is assumed	75
Figure 5.5	Power penalty as a function of wavelength channels, m at the bar-state of (a) 2×2 BOXC and, (b) 4×4 BOXC with the different number of component crosstalk, X_f . BER = 10^{-9} is assumed	76
Figure 5.6	BER vs. received power at the cross-state of (a) 2×2 BOXC, and (b) 4×4 BOXC with the various positions, n of the wavelength channels while the number of wavelength channels, $m = 32$ is fixed. Component crosstalk, $X_f = -22\text{dB}$ and backscattering-induced crosstalk, $X_R = -25\text{dB}$ is assumed	77
Figure 5.7	BER performance in presence of intraband crosstalk with various position of wavelength channels, n while the total number of wavelength channels, $m = 32$ is fixed with different component crosstalk, X_f in the cross-state of 2×2 BOXC. Backscattering-induced crosstalk, $X_R = -25\text{dB}$ is assumed	78
Figure 5.8	BER performance in presence of intraband crosstalk with various position of wavelength channels, n while the total number of wavelength channels, $m = 32$ is fixed with different component crosstalk, X_f in the cross-state of 4×4 BOXC. Backscattering-induced crosstalk, $X_R = -25\text{dB}$ is assumed	79
Figure 5.9	Power penalty as a function of component crosstalk at the cross-state of (a) 2×2 BOXC and, (b) 4×4 BOXC with the various positions of the wavelength channels, n while the number of wavelength channels, $m = 32$ is fixed. BER = 10^{-9} is assumed . . .	80
Figure 5.10	Power penalty as a function of position of the wavelength channels, n at the cross-state of (a) 2×2 BOXC and, (b) 4×4 BOXC with the different amount of component crosstalk, X_f ,	

	while the number of wavelength channels, $m = 32$ is fixed. BER = 10^{-9} is assumed	81
Figure 5.11	BER vs. received power at the bar-state of (a) 2×2 BOXC, and (b) 4×4 BOXC with the different number of optical amplifiers, N_a while the number of wavelength channels, $m = 32$ is fixed. Component crosstalk, $X_f = -22\text{dB}$ assumed	85
Figure 5.12	Power penalty as a function of number of optical amplifiers, N_a at the bar-state of (a) 2×2 BOXC and, (b) 4×4 BOXC with the number of wavelength channels, $m = 32$ is fixed. Component crosstalk, $X_f = -22\text{dB}$ and BER = 10^{-9} is assumed. Data is obtained from the plot of figure 5.11	86
Figure 5.13	BER vs. received power at the cross-state of (a) 2×2 BOXC, and (b) 4×4 BOXC with the varying number of optical amplifiers, N_a while the wavelength channel position, $n = 4$ and the total number of wavelength channels, $m = 32$ is fixed. Component crosstalk, $X_f = -22\text{dB}$ assumed	87
Figure 5.14	Power penalty as a function of number of optical amplifiers, N_a at the cross-state of (a) 2×2 BOXC and, (b) 4×4 BOXC with the number of wavelength channels, $m = 32$ and position of wavelength channel, $n = 4$ is fixed. Component crosstalk, $X_f = -22\text{dB}$ and BER = 10^{-9} is assumed. Data is obtained from the plot of figure 5.13	88

List of Tables

4.1	Number of crosstalk fields generated in the 2×2 BOXC and combined with the main signal λ_{2n-1} for the bar state (Port I to Port III)	56
4.2	Number of crosstalk fields generated in the 2×2 BOXC and combined with the main signal λ_{2n-1} for the cross state (Port I to Port IV)	57
4.3	Number of crosstalk fields generated in the 4×4 BOXC and combined with the main signal λ_{2n-1} for the bar state (Port I to Port V)	57
4.4	Number of crosstalk fields generated in the 4×4 BOXC and combined with the main signal λ_{2n-1} for the cross state (Port I to Port VI)	57
4.5	Number of crosstalk fields generated in the 4×4 BOXC and combined with the main signal λ_{2n-1} for the cross state (Port I to Port VII)	58
4.6	Number of crosstalk fields generated in the 4×4 BOXC and combined with the main signal λ_{2n-1} for the cross state (Port I to Port VIII)	58
5.1	Received power and power penalty due to intraband crosstalk in the 2×2 BOXC	82
5.2	Received power and power penalty due to intraband crosstalk in the 4×4 BOXC	82
5.3	Received power and power penalty due to optical amplifier in the 2×2 BOXC	89
5.4	Received power and power penalty due to optical amplifier in the 4×4 BOXC	90

List of Symbols

σ_{th}^2	Thermal noise power of optical receiver
σ_{co}^2	Coherent crosstalk noise power
σ_{ico}^2	Incoherent crosstalk noise power
σ_X^2	Intraband crosstalk noise power
σ_{tx}^2	FBGs transmission noise power
σ_{re}^2	FBGs reflection noise power
σ_R^2	Backscattered-induced crosstalk noise power
n_{eff}	Effective refractive index
Λ	Period of Bragg grating
β	Propagation constant
σ_1^2	Total noise power of receiver
k	Boltzman constant
T	Room temperature in Kelvin
e	Electron charge
h	Plank constant
B_e	Electrical bandwidth of receiver
B_o	Optical bandwidth of receiver
X_R	Backscattering-induced crosstalk coefficient
X_f	Component crosstalk coefficient
R	Reflectivity of backscattering
G	Gain of optical amplifier
λ	Wavelength
λ_{Bragg}	Bragg wavelength
m	Number of wavelength channels
n	Position of wavelength channels
σ_s^2	Receiver shot noise power
σ_{sig-sp}^2	Signal-ASE beat noise power

σ_{sp-sp}^2	ASE-ASE beat noise power
n_{sp}	Spontaneous emission factor
f_c	Optical carrier frequency
F_n	Noise-figure
R_d	Responsivity of a photodiode
σ_{1A}^2	Amplifier noise power
P_s	Optical power of the main signal
σ_0^2	Thermal and shot noise power of receiver

List of Abbreviations

WDM	Wavelength Division Multiplexing
OXC	Optical Cross-Connect
BOXC	Bidirectional Optical Cross-Connect
FBG	Fiber Bragg Grating
EDFA	Erbium Doped Fiber Amplifier
AWG	Arrayed Waveguide Grating
BWRN	Bidirectional WDM Ring Network
OADM	Optical Add/Drop Multiplexer
BOADM	Bidirectional Optical Add/Drop Multiplexer
OC	Optical Carrier/Optical Circulator
ASE	Amplified Spontaneous Emission
MZI	Mach-Zehnder Interferometer
BER	Bit-Error Rate
PP	Power Penalty
OLT	Optical Line Terminal
SONET	Synchronous Optical Network
SDH	Synchronous Digital Hierarchy
LAN	Local Area Network
MAN	Metropolitan Area Network
SOA	Semiconductor Optical Amplifier
BL	Bandwidth Length product
PMD	Polarization Mode Dispersion
ROC	Rotatable Optical Circulator
dB	Decibel
SOP	State of Polarization
TWA	Traveling Wave Amplifier

Acknowledgement

This is immense pleasure to express my profound gratitude to my supervisor Professor Dr. Satya Prasad Majumder, Department of Electrical and Electronic Engineering (EEE), Bangladesh University of Engineering and Technology (BUET), Dhaka, for providing me the opportunity to conduct graduate research in recent research area of optical fiber communication. I wish to convey my heartfelt thank to him for his continuous guidance, kind help and wholehearted encouragement during the course of the work, without which this work would never be possible.

I would like to thank Prof. Dr. Aminul Hoque, Dr. Shah Alam, Dr. Hossam-e Haider for being the part of my defense committee.

I wish to express my profound indebtedness and thanks to my wife Salina Karim for her assistance during the writing of this dissertation and her continuous support during my work. I would like to express my gratitude to my parents and all family members for their encouragement and love during my course of work. I am grateful to all the respected teachers and officials of Electrical and Electronic Engineering department of BUET as well for helping all the students like me in many different ways.

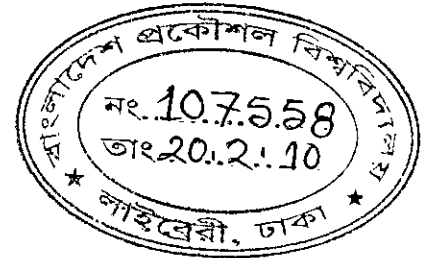
Finally, I would like to express my heartiest gratitude to Almighty Allah for enabling me to the successful completion of my master's thesis.

Abstract

Bidirectional optical cross connects (BOXCs) using a fiber Bragg gratings (FBGs) and optical circulators (OCs) have been considered for bidirectional wavelength division multiplexing (WDM) ring networks. Theoretical analysis is carried out to evaluate the performance of BOXCs in a WDM transmission system in the presence of intraband crosstalk due to FBGs. The analytical expression of in-band crosstalk due to FBG-based BOXCs is developed. The expression of BER and power penalty is derived considering the effect of in-band crosstalk for the operation BOXC in a WDM system. Analysis is also extended considering the impact of amplified spontaneous emission (ASE) noise due to optical amplifier used in a WDM ring network. We analyzed here two configurations of FBG-based bidirectional optical cross connects: 2×2 BOXC and 4×4 BOXC for bidirectional WDM ring networks and evaluate the bit-error-rate (BER) and power penalty (PP) of these configurations. It is found that the BER and PP, due to linear homodyne crosstalk induced by FBGs, both are increased with the number of wavelength channels increased for both bar and cross state of BOXCs. BER and PP are not affected with the position of the wavelength channels in the bar state while in the cross state, if the position of the wavelength channels is increased, the BER and PP both are increased. Performance degradation in terms of BER and PP due to BOXC induced crosstalk and also due to the effect of ASE noise is evaluated and optimum system design parameters are determined for operation of WDM network at BER of 10^{-9} .

CHAPTER ONE

Introduction



Ever since ancient times, one of the principle needs of people has been to communicate. This need created interest in devising communication systems for sending message from one distant place to another. Many forms of communication systems have appeared over the years. The basic motivations behind each new form were either to improve the transmission fidelity, to increase the data rate so that more information could be sent, or to increase the transmission distance between relay stations. Before the nineteenth century, all communication systems operated at a very low information rate and involved only optical or acoustical means, such as signal lamps or horns. One of the earliest known optical transmission links, for example, was the use of fire signal by the Greeks in the eighth century B.C. for sending alarms, calls for help, or announcements of certain events.

Telecommunication networks based on optical fiber technology have become a major information-transmission system, with high-capacity optical fiber links encircling the global in both terrestrial and undersea installations. In the early days of optical fiber communications, the applications involved basically only the optical fiber, a light source, and a photodetector. Now, there are numerous passive and active optical devices within a light-wave link that perform complex networking functions in the optical domain, such as signal restoration, routing, and switching. Along with the need to understand the functions of these devices comes the necessity to measure both component and network performance, and to model and simulate the complex behavior of reliable high-capacity networks.

As we see the new millennium, we are seeing dramatic changes in the telecommunications industry that have far-reaching implications for our lifestyles. There are many drivers for these changes. First and foremost is the continuing, relentless need for more capacity in the network. This demand is fueled by many factors. The tremendous growth of the Internet and the World Wide Web, both in terms of number of

users as well as the amount of time and thus bandwidth taken by user, is a major factor. Businesses today rely on high-speed networks to conduct their business. These networks are used to interconnect multiple locations within a company as well as between companies for business-to-business transactions. These factors have driven the development of high-capacity optical networks and their remarkably rapid transition from the research laboratories into commercial deployment.

1.1 The Evolution of Fiber Optic Systems

The research phase of fiber-optic communication systems started around 1975. The enormous progress realized over the 25-year period extending from 1975 to 2000 can be grouped into several distinct generations. Figure 1.1 shows the increase in the bandwidth-length (*BL*) product over this time period as quantified through various laboratory experiments. The straight line corresponds to a doubling of the *BL* product every year. In every generation, *BL* product increases initially but then begins to saturate as the technology matures. Each new generation begins a fundamental change that helps to improve the system performance further.

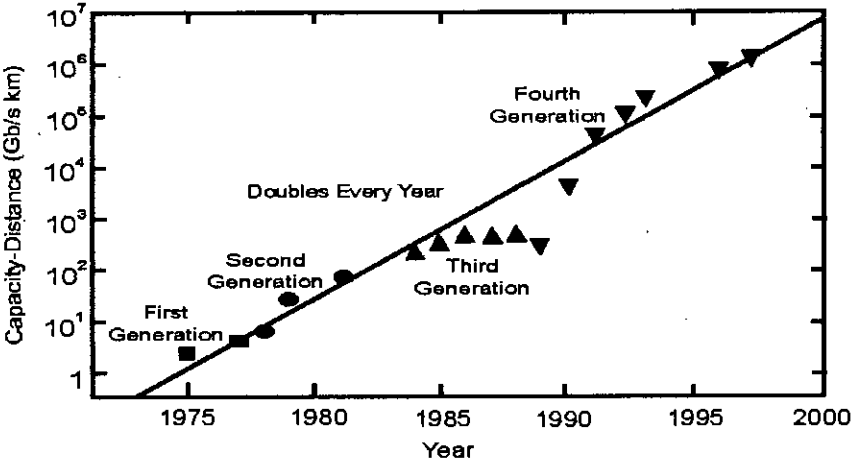


Figure 1.1: Increase in the *BL* product over the period 1975 to 2000 through several generations of optical fiber communication systems.

The first generation of fiber optic communication systems operated near 800nm and used GaAs semiconductor lasers. After several field trials during the period 1977-79, such

systems become available commercially in 1980. They operated at bit rate of 45 Mb/s and allowed repeater spacing of up to 19 km. The larger repeater spacing compared with 1 km spacing of coaxial cable systems was an important motivation for system designers because it decreased the installation and maintenance costs associated with each repeater.

The second generation of fiber-optic communication systems became available in the early 1980s, but the bit rate of early systems was limited to below 100 Mb/s because of dispersion in multimode fibers. This limitation was overcome by the use of single-mode fibers. By 1987, second generation fiber-optic communication systems, operating at bit rates of up to 1.7Gb/s with a repeater spacing of about 50 km, were commercially available.

The introduction of third generation fiber-optic communication systems operating at 1550 nm and operating at 2.5 Gb/s became available commercially in 1990. Such systems are capable of operating at a bit rate up to 10 Gb/s. The best performance is achieved using dispersion-shifted fibers in combination with laser oscillating in a single longitudinal mode. A drawback of third generation 1550 nm systems is that signal is regenerated periodically by using electronic repeaters spaced apart typically 60-70 km.

The fourth generation of fiber-optic communication systems makes use of optical amplification for increasing the repeater spacing and of wavelength division multiplexing (WDM) for increasing the bit rate. The advent of the WDM technique started a revolution that resulted in doubling of the system capacity every six months or so and led to fiber-optic communication systems operating at bit rate of 10 Tb/s by 2001. Clearly, the fourth-generation systems have revolutionized the whole field of fiber-optic communications.

The fifth generation of fiber-optic communication systems is concerned with extending the wavelength range over which a WDM system can operate simultaneously. A new kind of fiber, known as the dry fiber, has been developed with the property that fiber losses are small over the entire wavelength region extending from 1300 to 1650 nm. Availability of such fibers and new amplification schemes may lead to fiber-optic communication systems with thousands of WDM channels.

1.2 Introduction of WDM systems

The rapid growth of the Internet is strengthening demands for broadband services in access networks. To satisfy these demands, the introduction of WDM technologies is one of the most attractive solutions. A powerful aspect of WDM systems in optical communication is that many different wavelengths can be sent along a single fiber simultaneously. The technology of combining a number of wavelengths onto the same fiber is known as wavelength division multiplexing or WDM. Conceptually, the WDM scheme is the same as frequency division multiplexing (FDM) used in microwave radio and satellite systems. WDM system has potential for exploiting the large bandwidth offered by optical fibers. For example, hundreds of 10 Gb/s channels can be transmitted over the same fiber when channel spacing is reduced to below 100 GHz. If the OH peak can be eliminated using dry fibers, the total capacity of a WDM system can ultimately exceed 30 Tb/s.

The concept of WDM has been pursued since the first commercial fiber-optic communication system became available in 1980. In its simplest form, WDM was used to transmit two channels in different transmission windows of an optical fiber. However, it was during the decade of the 1990s that WDM systems were developed most aggressively. Commercial WDM systems first appeared around 1995, and their total capacity exceeded 1.6 Tb/s by the year 2000. Several laboratory experiments demonstrated in 2001 a system capacity of more than 10 Tb/s although the transmission distance was limited to below 200 km. Clearly, the advent of WDM has led to virtual revolution in designing optical fiber communication systems.

1.3 All-Optical Network

All-optical networks have emerged as a solution to keep up with the always increasing throughput demand. In today's transport networks, data are transmitted over optical fibers and optical-electro-optical conversion is needed at the nodes to perform routing. These networks can achieve a throughput of up to several hundreds of Gb/s using WDM channels. Yet optical fibers have a potential capacity of several tens of Tb/s per channel.

Electronic switches are not able to sustain such transmission rates and have become complex and costly, making it highly desirable to replace them with all-optical switches where no electric conversion is needed at all. Deploying such all-optical networks is promising but also challenging and novel issues have to be anticipated. In this dissertation, we study one of these issues, impairment by optical leaks, called node crosstalk, which takes place in optical switches.

All-optical switches, or optical cross-connects (OXCs), remove the electrical conversion step in switching hardware. In addition to the gain in network data rate, all-optical switches are expected to become simpler to implement and therefore cheaper than their electrical counterparts. Moreover, all-optical switches allow for improved data rate flexibility in networks. All-optical switches have been the subject of much research in the recent years and some are already commercially available. The function of all-optical switch is to transmit an incoming signal arriving along a certain optical fiber on a certain wavelength to a different optical fiber. All-optical switches contain the same functional elements: demultiplexers, a switching fabric, optical wavelength converters, and multiplexers. In our work, we do not consider any wavelength conversion device.

1.4 Background of this Study

WDM optical networks are very promising due to their large bandwidth, their large flexibility and the possibility to upgrade the existing optical fiber networks to WDM networks to provide increased capacity [1]. OXCs are key components to enable all-optical networks based on WDM technology [2]. A number of unidirectional and bidirectional OXC architectures have been proposed in [3]-[9], each of which has its own unique features, strengths, and limitations. Imperfections of the optical components used in these architectures give rise to optical crosstalk [8]-[9].

Crosstalk is one of the major limitations for the practical implementation of OXCs in all optical networks [1], [3], [8]. Different kinds of linear crosstalk such as interband/out-of-band crosstalk and in-band/intraband crosstalk exist even in a perfectly linear channel due to imperfect nature of various WDM components. The network performance will be

limited due to the intraband crosstalk which gives rise to a significant signal degradation and power penalty that leads to an increased bit error probability [1].

Bidirectional optical cross connects (BOXCs) are key switching elements in bidirectional WDM ring networks (BWRNs), which could selectively interchange wavelength channels among the BWRNs in both directions [9]. Several types of BOXCs are reported in [4]-[9].

Though a number of research works reported to investigate the effect of crosstalk in WDM network design, the crosstalk modeling and systematic analysis of FBG-OC-based BOXC and its impact on transmission performance of WDM system is yet to be reported.

1.5 Literature Review

Fiber optic communication networks have provided us with high speed communications with enormous bandwidth potential. WDM enables the utilization of a significant portion of the available fiber bandwidth by allowing many independent signals to be transmitted simultaneously on one fiber, with each signal being on a different wavelength. BOXCs are the essential element of WDM systems and crosstalk that arises due to the leak in BOXC is our main focus of the study.

Tim *et al.* [1] presented the results of crosstalk analysis of four optical WDM OXC topologies and compared the performances among them. An optimal set of parameters is determined to reduce the total crosstalk.

Shen *et al.* [2] studied the impact of coherent and incoherent crosstalk induced in OXCs in a WDM network. They have shown that incoherent crosstalk always causes noise but coherent crosstalk either causes noise or not depending on the optical delay differences between the signal and crosstalk and bit duration of the signal.

Wu *et al.* [3] studied FBG-OC-based unidirectional OXC and established an analytical model of intraband optical crosstalk for this configuration. They have shown that under different switching states of OXC, coherent crosstalk much higher than the incoherent

crosstalk. An improved unidirectional OXC along with isolators is proposed to meet different requirements of practical systems.

Simmons *et al.* [4] shown a bidirectional OXC connection by using a novel micromirror switch and bidirectional connection offered in pairs.

Park *et al.* [5] proposed a multiwavelength bidirectional OXC based on FBGs and PBSs. A 2×2 BOXC is implemented using four pairs of FBGs and two PBSs, in order to experimentally evaluate the performance of the proposed BOXC. They have shown the BER performance of the BOXC considering crosstalk and insertion loss.

Kim *et al.* [6] proposed an independently switchable BOXC based on ON-OFF mirrors and a pair of AWGs which can eliminate Rayleigh Backscattering (RB) noise and optical reflection. In this structure, independent bidirectional connectivity is offered using two separate conventional unidirectional OXCs.

Kim *et al.* [7] proposed a BOXC using an AWGR and tunable FBGs for multiwavelength BWRNs. Two types of configurations: fold-back and loop back have been demonstrated experimentally. The performances of two proposed configurations have been investigated and compared in terms of crosstalk characteristics and backscattering suppression capability.

Jalal *et al.* [8] studied the impact of crosstalk due to unidirectional and bidirectional OXCs in a WDM network. Unidirectional OXC based on conventional MUX/DEMUX and bidirectional OXC based on AWGR and FBGs are considered and crosstalk limitations of above structures have been evaluated. Optimum system design parameters are determined to achieve specific operation.

Zhong *et al.* [9] proposed a new BOXC based on FBGs and OCs for bidirectional WDM ring networks which has small insertion loss. Dynamic and independent wavelength routing is achieved by employing cascaded tunable FBGs. They have studied the inband coherent and incoherent crosstalk generated in the BOXC.

Moon *et al.* [10] proposed highly channel-scalable multiwavelength unidirectional OXC based on tunable FBGs and OCs and its performances were investigated by using experiments and numerical simulations. They have shown from the numerical simulations that, signal-crosstalk beat noise is found to be the most critical limiting factor of the OXC size.

Cheng *et al.* [12] analyzed several classes of unidirectional OXC architectures for intraband crosstalk. They derive the expression for the power penalty imposed by crosstalk so that various OXC architectures can be evaluated in a systematic way. They have shown that the tradeoffs between the crosstalk requirements of the switches and the filters/demultiplexers may be exploited to yield most cost-effective OXC designs.

Olsson *et al.* [15] investigated theoretically and experimentally the performance of optical amplifiers in fiber optic communication systems. The noise and BER characteristics of optical networks with optical amplifiers are calculated and the dependence of system performance on amplifier characteristics is shown.

1.6 Objectives

The objectives of this research are:

- (i) To make detail analysis of inband coherent and incoherent crosstalk due to BOXCs based OCs and FBGs. To extend the analysis, the effect of ASE due to optical amplifier will be considered.
- (ii) To carry out BER performance analysis of a WDM system considering the above crosstalk limitations.
- (iii) To determine PP in a WDM system considering the above crosstalk limitation and to find the optical system parameters at a given BER.

1.7 Research Methodology

BOXCs using FBGs and OCs will be used in the crosstalk modeling and analysis. To evaluate the impact of inband crosstalk in BOXCs, analytical expression for the coherent and incoherent crosstalk arising in the BOXCs based on FBGs and OCs will be derived. To extend the analysis, the effect of ASE due to optical amplifier will be included. Crosstalk due to backscattering in BOXCs will also be considered. The expression for BER of a WDM system will be derived considering the component crosstalk, amplifier crosstalk and backscattering induced crosstalk. The BER performance results of BOXCs will be evaluated in terms of the received power, number of wavelength channels and the different component crosstalk by simulation. PP due to the crosstalk at a given BER will be evaluated from the results obtained above. Optimum system design parameters will be determined to achieve a given BER.

1.8 Organization of the Thesis

Chapter 2 addresses the operating principles of WDM and describes the basic characteristics of different WDM components needed for its realization.

Chapter 3 explore the brief architectural aspects of the network elements which are the part of the WDM networks and give brief description of some basic topologies that are possible for fiber optic WDM networks and examine the design tradeoffs among them.

Chapter 4 starts with the different crosstalk present in BOXCs. The theoretical analysis and the analytical expression of intraband such as coherent and incoherent crosstalk are given thereafter. After that the effect of crosstalk in the BER performance and power penalty is presented analytically. Finally the analytical expressions of ASE noises of optical amplifier are given and the effect of these noises on BER is presented analytically.

Chapter 5 presents the results and discussion. The BER and the PP are observed without and with optical amplifier noises separately in presence of intraband crosstalk present in BOXCs.

Chapter 6 presents the conclusive remarks of this thesis along with the limitation and the scope of future work.

CHAPTER TWO

WDM Concepts and Components

A powerful aspect of an optical communication link is that many different wavelengths can be sent along a single fiber simultaneously in the 1300-to-1600 nm spectral band. The technology of combining a number of wavelengths onto the same fiber is known as wavelength-division multiplexing or WDM. Conceptually, the WDM scheme is the same as frequency-division multiplexing (FDM) used in microwave radio and satellite systems. Just as in FDM, the wavelengths (or optical frequencies) in WDM must be properly spaced to avoid interchannel interference. The key system features of WDM are as follows:

- *Capacity upgrade.* The classical application of WDM has been to upgrade the capacity of existing point-to-point fiber optic transmission links. If each wavelength supports an independent network signal of perhaps a few Gb/s, then WDM can increase the capacity of a fiber network dramatically.
- *Transparency.* An important aspect of WDM is that each optical channel can carry any transmission format. Thus, using different wavelength, fast or slow asynchronous and synchronous digital data and analog information can be sent simultaneously, and independently, over the same fiber, without the need for a common signal structure.
- *Wavelength routing.* In addition to using multiple wavelengths to increase link capacity and flexibility, the use of wavelength-sensitive optical routing devices makes it possible to use wavelength as another dimension, in addition to time and space, in designing communication networks and switches. Wavelength routed networks use the actual wavelength of a signal as the intermediate or final address.
- *Wavelength switching.* Whereas wavelength-routed networks are based on a rigid fiber infrastructure, wavelength-switched architectures allow reconfigurations of the

optical layer. Key components of implementing these networks include optical add/drop multiplexers, optical cross-connects, and wavelength converters.

In this chapter, we will discuss the physical principles behind the operation of the most important components of optical communication systems. For each component, we will give a simple descriptive treatment in the following.

2.1 Principles of WDM

In standard point-to-point links a single fiber line has one optical source at its transmitting end and one photodetector at the receiving end. Signals from different light sources use separate and uniquely assigned optical fibers. Since an optical source has a narrow linewidth, this type of transmission makes use of only a very narrow portion of the transmission bandwidth capability of a fiber and the two low-loss windows provide many additional operating regions. By using a number of light sources, each emitting at a different peak wavelength that is sufficiently spaced from its neighbor so as not to create interference, the integrities of the independent messages from each source are maintained for subsequent conversion to electrical signals at the receiving end.

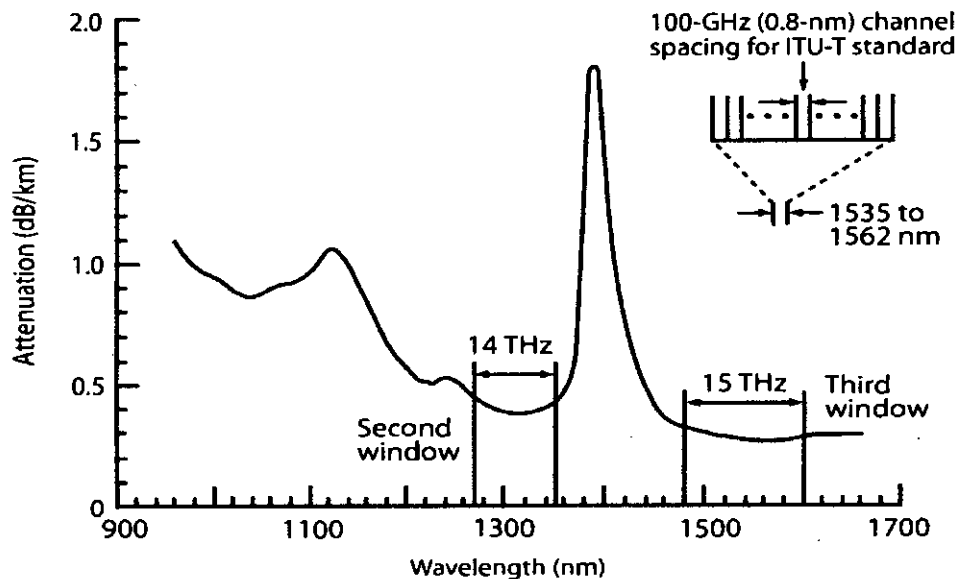


Figure 2.1: The transmission bandwidths in the 1310 nm and 1550 nm windows allow the use of many simultaneous channels for sources with narrow spectral widths.

A key feature of WDM is that the discrete wavelengths form an orthogonal set of carriers that can be separated, routed, and switched without interfering with each other. This holds as long as the optical intensity is kept sufficiently low to prevent nonlinear effects, such as stimulated Brillouin scattering and four-wave mixing processes, from degrading the link performance.

The implementation of WDM networks requires a variety of passive and /or active device to combine, distribute, isolate, and amplify optical power at different wavelengths. Passive device require no external control for their operation, so they are somewhat limited in their application in WDM networks. These components are mainly used to split and combine or tap off optical signals. The performance of active devices can be controlled electronically, thereby providing a large degree of network flexibility. Active WDM components include tunable optical filters, tunable sources, and optical amplifiers.

Figure 2.2 shows the use of such components in a typical WDM link containing various types of optical amplifiers. At the transmitting end, there are several independently modulated light sources, each emitting signals at a unique wavelength. Here, a multiplexer is needed to combine these optical outputs into a serial spectrum of closely spaced wavelength signals and couple them onto a single fiber. At the receiving end, demultiplexer is required to separate the optical signals into appropriate detection

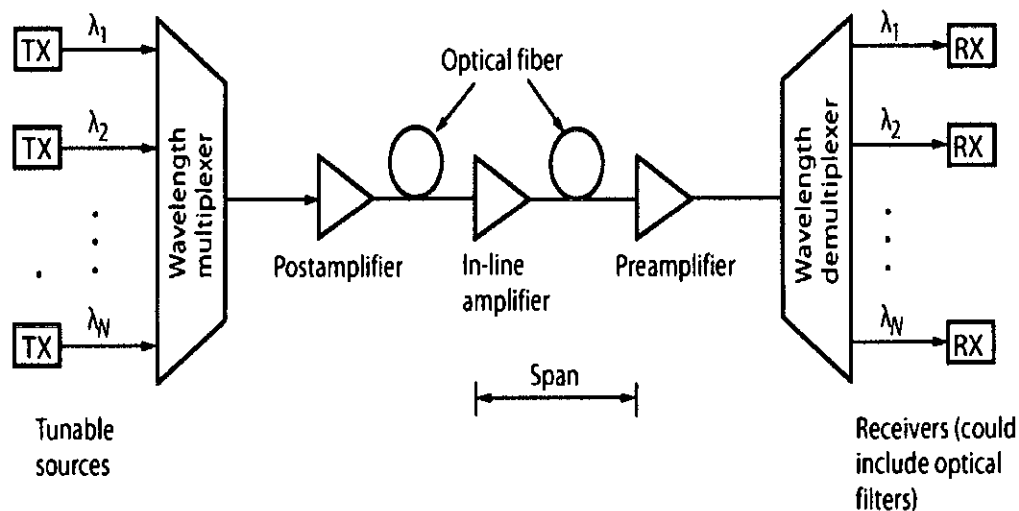


Figure 2.2: Implementation of a typical WDM network.

channels for signal processing. At the transmitting end, the basic design challenge is to have the multiplexer provide a low-loss path from each optical source to the multiplexer output. Since the optical signals that are combined generally do not emit any significant amount of optical power outside of the designed channel spectral width, interchannel crosstalk factors are relatively unimportant at the transmitting end.

2.2 Couplers

When discussing couplers and splitters, it is customary to refer to them in terms of the number of input and output ports on the device. For example, a device with two inputs and two outputs would be called a 2×2 coupler. In general, an $N \times M$ coupler has N inputs and M outputs.

The 2×2 coupler is a simple fundamental device that we will use here to demonstrate the operational principles. A common construction is the fused-fiber coupler. This is fabricated by twisting together, melting, and pulling two single-mode fibers so they get fused together over a uniform section of length W , as shown in figure 2.3. Each input and output has a long tapered section of length L , since the transverse dimensions are gradually reduced down to that of the coupling region when the fibers are pulled during the fusion process. The total draw length is $\mathcal{L} = L + W$. The device is known as a fused biconical tapered coupler. Here, P_0 is the input power, P_1 is throughput power, and P_2 is

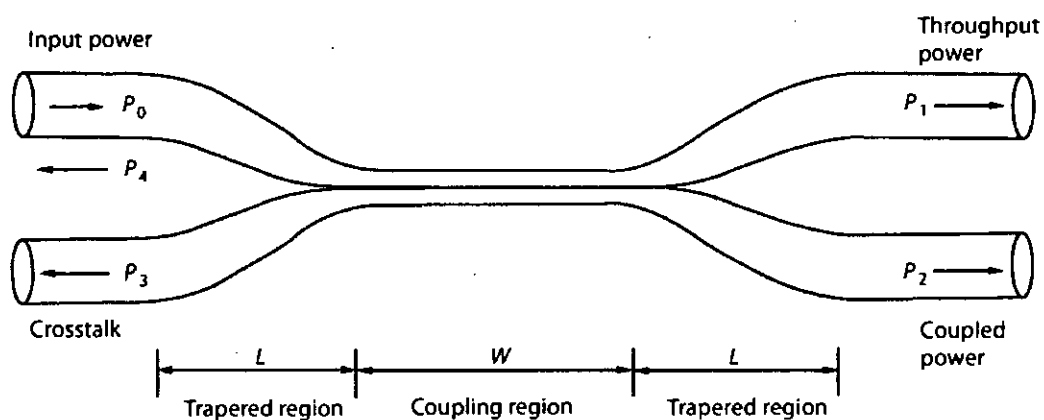


Figure 2.3: Cross-sectional view of a fused-fiber coupler having a coupling region W and two tapered regions of length L .

power coupled to the second fiber. The parameters P_3 and P_4 are extremely low signal levels resulting from backward reflections and scattering due to bending in and packaging of the device.

Assuming that the coupler is lossless, the expression for the power P_2 coupled from one fiber to another over an axial distance z is

$$P_2 = P_0 \sin^2(kz) \quad (2.1)$$

where k is the coupling coefficient describing the interaction between the fields in the two fibers. By conservation of power, for identical-core fibers we have

$$P_1 = P_0 - P_2 = P_0 [1 - \sin^2(kz)] = P_0 \cos^2(kz) \quad (2.2)$$

This shows that the phase of the driven fiber always 90° behind the phase of the driving fiber. Thus, when power is launched into fiber 1, at $z = 0$ the phase in fiber 2 lags 90° behind that in fiber 1. This lagging phase relationship continues for increasing z , until at a distance that satisfy $kz = \pi/2$, all of the power has been transferred from fiber 1 to fiber 2. Now fiber 2 become the driving fiber, so that for $\pi/2 \leq kz \leq \pi$ the phase in fiber 1 lags behind that in the fiber 2, and so on. As a result of this phase relationship, the 2×2 coupler is a directional coupler. That is, no energy can be coupled into a wave traveling in the negative z direction in the driven waveguide.

2.3 Star Couplers

The principal role of all star couplers is to combine the powers from N inputs and divide them equally among M output ports. Techniques for creating star couplers include fused fibers, gratings, micro-optic technologies, and integrated-optics schemes. The fiber-fusion technique has been a popular construction method for $N \times N$ star couplers. Large scale fabrication of these devices for $N > 2$ is limited because of the difficulty in controlling the coupling response between the numerous fibers during the heating and pulling process. Figure 2.4 shows an 8×8 star coupler formed by interconnecting twelve 2×2 coupler.

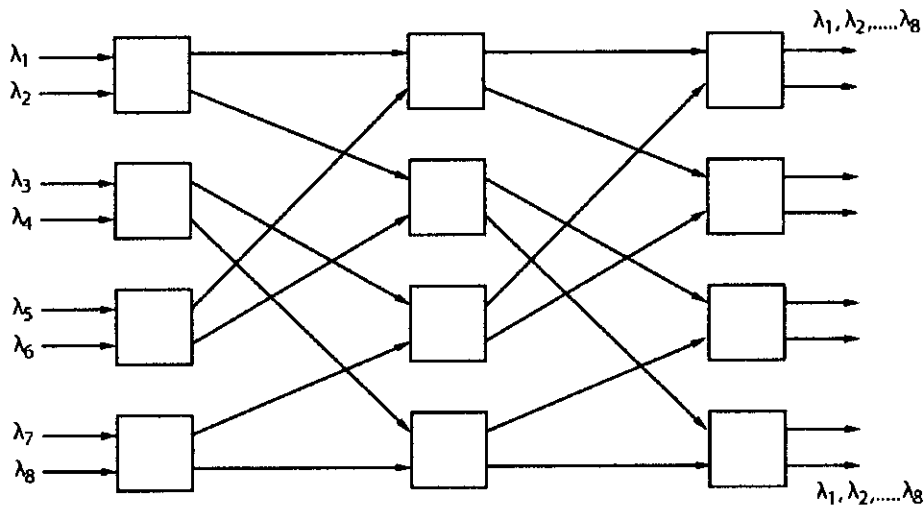


Figure 2.4: Shows an 8×8 star coupler formed by interconnecting twelve 2×2 coupler.

In an ideal star coupler, the optical power from any input is evenly divided among the output ports. The total loss of the device consists of its splitting loss plus the excess loss in each path through the star. The splitting loss is given in decibels by

$$\text{Splitting loss} = -10 \log \left(\frac{1}{N} \right) = 10 \log N$$

For a single input power P_{in} and N output powers, the excess loss in decibels is given by

$$\text{Fiber star excess loss} = 10 \log \left(\frac{P_{in}}{\sum_{i=1}^N P_{out,i}} \right)$$

Thus, the total loss experienced by a signal of the $N \times N$ star is given by

$$\text{Total loss} = \text{splitting loss} + \text{excess loss}$$

2.4 Mach-Zehnder Interferometer Multiplexers

Wavelength-dependent multiplexers can be also be made using Mach-Zehnder interferometry techniques. These devices can be either active or passive. Here, we look

first at passive multiplexers. Figure 2.5 illustrates the constituents of an individual Mach-Zehnder interferometer (MZI). This 2×2 MZI consists of three stages: an initial 3-dB directional coupler which splits the input signals, a central section where one of the waveguides is longer by ΔL to give a wavelength dependent phase shift between the two arms, and another 3-dB coupler which recombines the signals at the output. By splitting

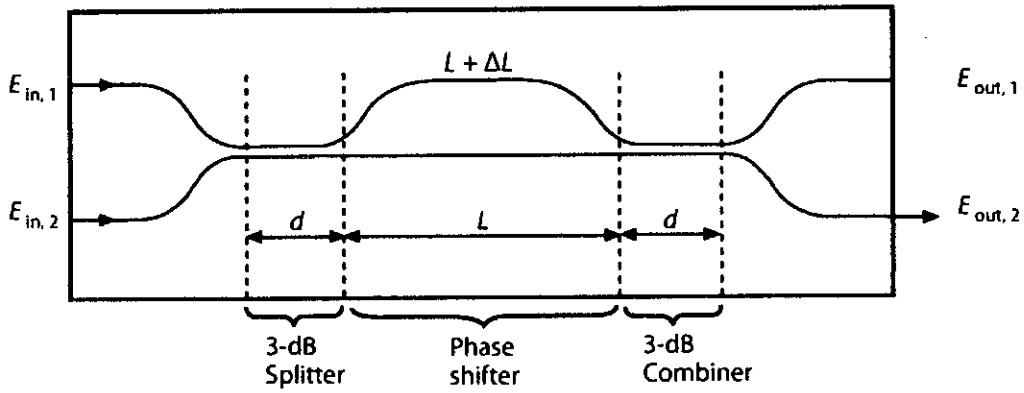


Figure 2.5: Layout of a basic 2×2 Mach-Zehnder interferometer.

the input beam and introducing a phase shift in one of the paths, the recombined signals will interfere constructively at one output and destructively at the other. The signals then finally emerge from only one output port.

Using basic 2×2 MZIs, any size $N \times N$ multiplexer can be constructed. Figure 2.6 gives an example for a 4×4 multiplexer. Here the inputs to MZI_1 are ν and $\nu + 2\Delta\nu$ (which we

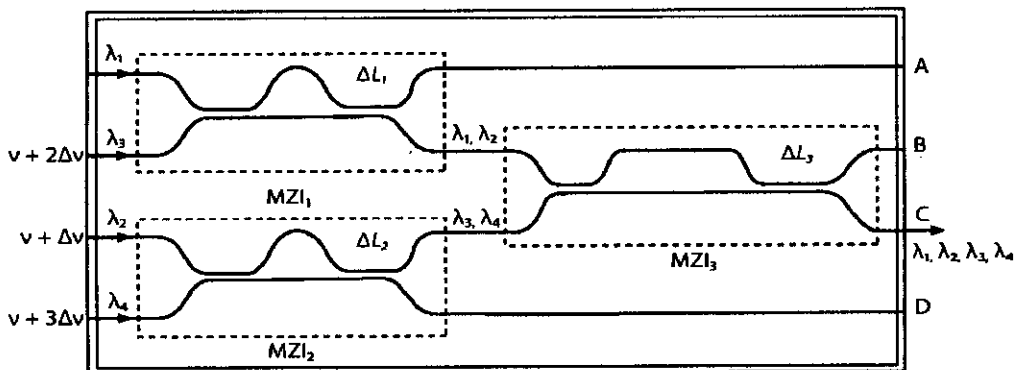


Figure 2.6: Four-channel wavelength multiplexer using three 2×2 Mach-Zehnder interferometers.

will call λ_1 and λ_3 , respectively), and the inputs to MZI_2 are $\nu + \Delta\nu$ and $\nu + 3\Delta\nu$ (λ_2 and λ_4 , respectively). In this way we can easily design N -to-1 MZI multiplexer. The N -to-1 MZI multiplexer can also be used as a 1-to- N demultiplexer by reversing the light-propagation direction.

2.5 Isolators and Circulators

Couplers and most other passive optical devices are reciprocal devices, in that the devices work exactly the same way if their inputs and outputs are reversed. However, in many systems there is a need for a passive nonreciprocal device. Isolators and circulators are example of such devices. The main function of isolator is to allow transmission in one direction through it but block all transmission in the other direction. Isolators are used in systems at the output of optical amplifiers and lasers primarily to prevent reflections from entering these devices, which would otherwise degrade their performance. The two key parameters of an isolator are its insertion loss, which is the loss in the forward direction, and which should be as large as possible. The typical insertion loss is around 1 dB, and the isolation is around 40-50 dB.

A circulator is similar to an isolator except that it has multiple ports, three or four as shown Figure 2.7. In a three port circulator, an input signal on port 1 is sent out on port 2, an input signal on port 2 is sent out on port 3, and an input signal on port 3 is sent out on port 1. Circulators operate on the same principle as isolators; therefore we only describe the details of how isolators work next.

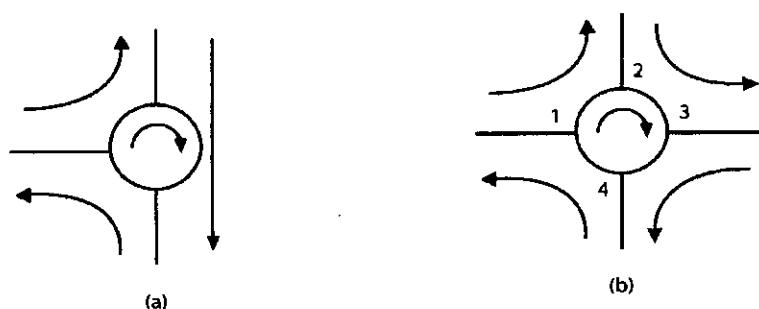


Figure 2.7: Functional representation of circulators: (a) three-port and (b) four-port. The arrows represent the direction of signal flow.

The principle of operation of an isolator is shown in Figure 2.8. Assume that the input light signal has the vertical state of polarization (SOP) shown in the figure. It is passed through a polarizer, which passes only light energy in the vertical SOP and blocks light energy in the horizontal SOP. Such polarizer can be realized using crystals, called dichroics, which have the property of selectively absorbing light with one SOP. The polarizer is followed by a Faraday rotator. A Faraday rotator is a nonreciprocal device, made of a crystal that rotates the SOP, say, clockwise, by 45° , regardless of the direction of propagation. The Faraday rotator is followed by another polarizer that passes only SOPs with this 45° orientation. Thus the light signal from left to right is passed through the device without any loss. On the other hand, light entering the device from the right due to a reflection, with the same 45° SOP orientation, is rotated another 45° by the Faraday rotator, and thus blocked by the first polarizer.

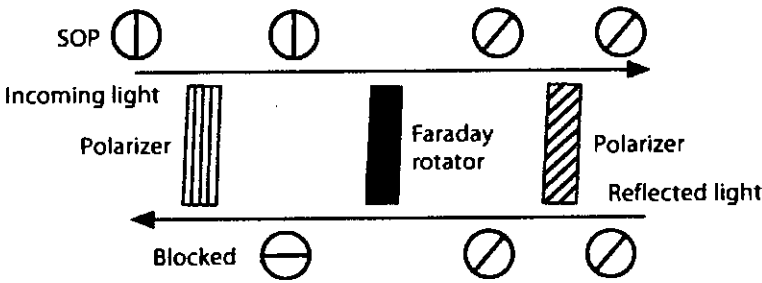


Figure 2.8: Principle of operation of an isolator that works only for a particular state of polarization of the input signal.

2.6 Fiber Bragg Gratings

A grating is an important element in WDM systems for combining and separating individual wavelengths. Basically, a grating is a periodic structure or perturbation in a material. This variation in the material has the property of reflecting or transmitting light in a certain direction depending on the wavelength. Thus, gratings can be categorized as either transmitting or reflecting gratings. Figure 2.9 defines various parameters for a reflection grating. Here, θ_i is the incident angle of the light, θ_d is the diffracted angle, and Λ is the period of the grating. In a transmission grating consisting of a series of equally spaced slits, the spacing between two adjacent slits is called the pitch of the grating. Constructive

interference at a wavelength λ occurs in the imaging plane when the rays diffracted at the angle θ_d satisfy the grating equation given by

$$\Lambda (\sin \theta_i - \sin \theta_d) = m \lambda \quad (2.3)$$

Here, m is called the order of the grating. In general, only the first-order diffraction condition $m = 1$ is considered. A grating can separate individual wavelengths since the grating equation is satisfied at different points in the imaging plane for different wavelengths.

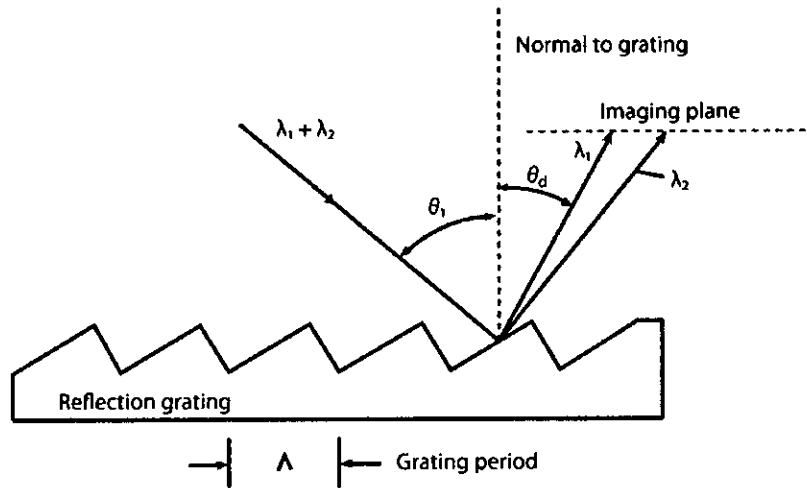


Figure 2.9: Shows basic parameters in reflection grating.

A Bragg grating constructed within an optical fiber constitutes a high-performance device for accessing individual wavelengths in the closely spaced spectrum of dense WDM systems. Since this is all fiber device, its main advantages are low cost, low loss (around 0.1 dB), ease of coupling with other fibers, polarization insensitivity, low temperature coefficient ($< 0.7 \text{ pm}^\circ\text{C}$), and simple packaging. A fiber grating is a narrowband reflection filter that is fabricated through a photoimprinting process. The technique is based on the observation that germanium-doped silica fiber exhibits high photosensitivity. This means that one can induce a change in the refractive index of the core by exposing it to 244 nm ultraviolet radiation. Optical bandwidths of 100 GHz and less have been demonstrated in such photoinduced gratings.

Several methods can be used to create a fiber phase-grating. Figure 2.10 demonstrates the so-called external-writing technique. The grating fabrication is accomplished by means of two ultraviolet beams transversely irradiating the fiber to produce an interference pattern in the core. Here, the regions of high intensity cause an increase in the local refractive index of the photosensitive core, where it remains unaffected in the zero-intensity regions. A permanent reflective Bragg grating is thus written into the core. When a multiwavelength signal encounters the grating, those wavelengths that are phase-matched to the Bragg reflection condition are not transmitted.

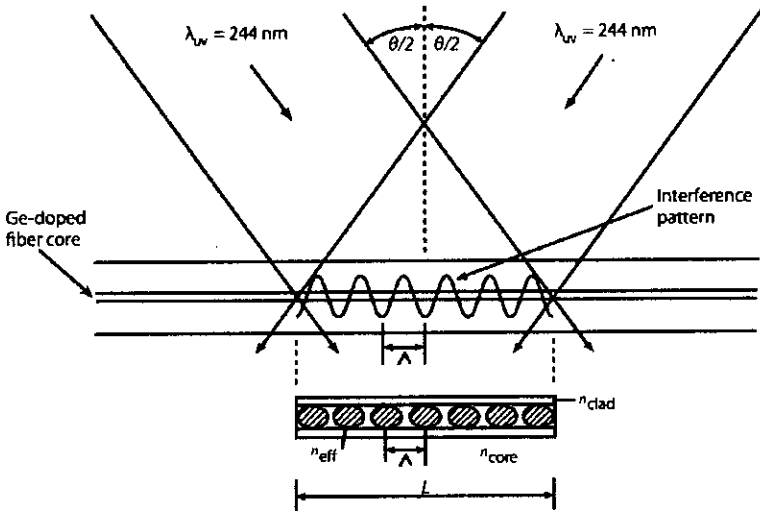


Figure 2.10: Formation of a Bragg grating in a fiber core by means of two intersecting ultraviolet light beams.

The maximum reflectivity R of the grating occurs when the Bragg condition holds; that is, at a reflection wavelength λ_{Bragg} where

$$\lambda_{\text{Bragg}} = 2 \Lambda n_{\text{eff}} \tag{2.4}$$

and n_{eff} is the mode effective index of the core.

Figure 2.11 shows a simple concept of demultiplexing function using a fiber Bragg grating. To extract the desired wavelength, a circulator is used in conjunction with grating. In a three-port circulator, an input signal on one port exits at the next port. For example, an input signal at port 1 is sent out at port 2. Here, the circulator takes the four

wavelengths entering port 1 and send them out at port 2. All wavelengths except λ_2 pass through the grating. Since λ_2 satisfies the Bragg condition of the grating, it gets reflected, enters port 2 of the circulator, and exits at port 3. More complex multiplexing and demultiplexing structures with several gratings and several circulators can be realized with this scheme.

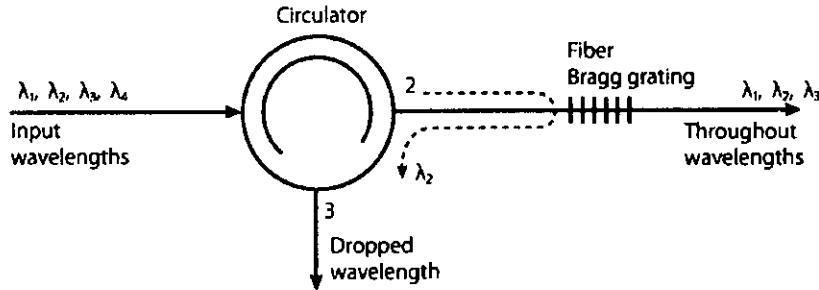


Figure 2.11: Simple concept of demultiplexing function using fiber Bragg grating and optical circulator.

2.7 Arrayed Waveguide Grating

A highly versatile WDM device is based on using an arrayed waveguide grating. This device can function as a multiplexer, a demultiplexer, a drop-and-insert element, or a wavelength router. The arrayed waveguide grating is a generalization of the 2×2 Mach-Zehnder interferometer multiplexer. One popular design consists of M_{in} input and M_{out}

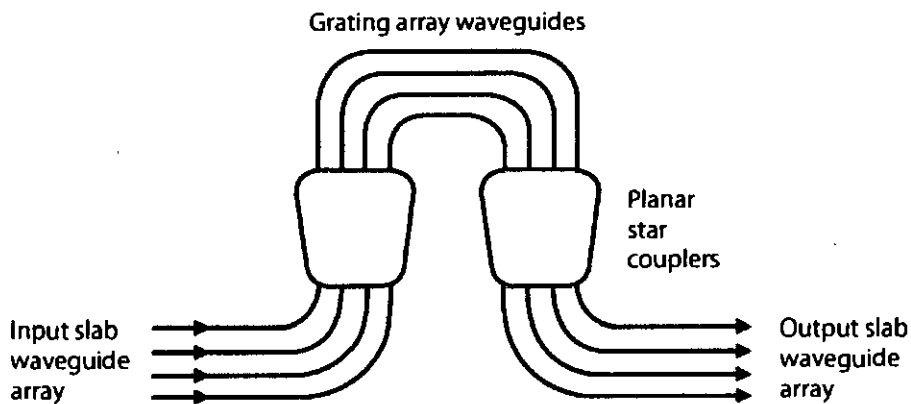


Figure 2.12: Top view of a typical arrayed waveguide grating used as a highly versatile passive WDM device.

output slab waveguides and two identical focusing planar star couplers connected by N uncoupled waveguides with a propagation constant β . The lengths of adjacent waveguides in the central region differ by a constant value ΔL , so that they form a Mach-Zehnder type grating, as Figure 2.12 shows. For a pure multiplexer, we can take $M_{in} = N$ and $M_{out} = 1$. The reverse holds for a demultiplexer; that is $M_{in} = 1$ and $M_{out} = N$. In the case of a network routing application, we can have $M_{in} = M_{out} = N$.

Figure 2.13 depicts the geometry of the star coupler. The coupler acts as a lens of focal length L_f so that the object and image planes are located at a distance L_f from the transmitter and receiver slab waveguides, respectively. Both the input and output waveguides are positioned on the focal lines, which are circles of radius $L_f/2$. In Figure 2.12, x is the center-to-center spacing between the input waveguides, d is the spacing between the grating array waveguides, and θ is the diffraction angle in the input or output slab waveguide. The refractive indices of the star coupler and the grating array waveguides are n_s and n_c , respectively.

Since any two adjacent grating waveguides have same length difference ΔL , a phase difference $2\pi n_c \Delta L/\lambda$ results. Then, from phase-matching condition, the light emitted from the output channel waveguides must satisfy the grating equation

$$n_s d \sin \theta + n_c \Delta L = m \lambda \quad (2.5)$$

where the integer m is the diffraction order of the grating.

Focusing is achieved by making the path-length difference ΔL between adjacent array waveguides, measured inside the array, to be an integer multiple of the central design wavelength of the demultiplexer

$$\Delta L = m \frac{\lambda_c}{n_c}$$

where λ_c is the central wavelength in vacuum; that is, it is defined as the pass wavelength for the path from center input waveguide to the center output waveguide.

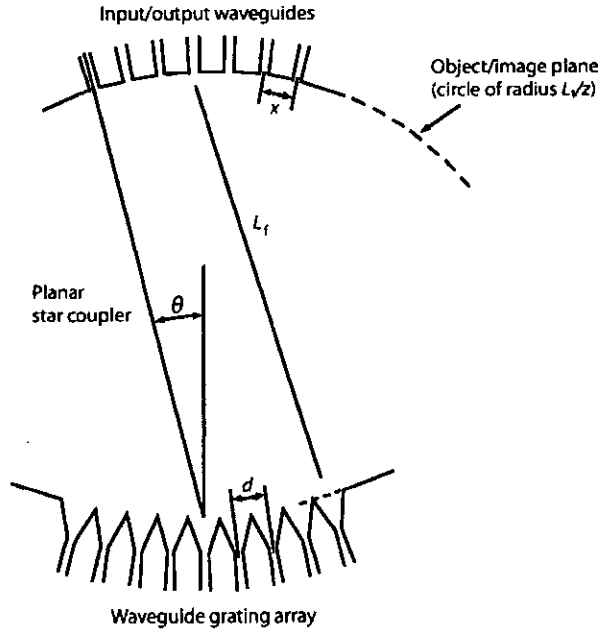


Figure 2.13: Geometry of the star coupler used in arrayed waveguide grating WDM device.

To determine the channel spacing, we need to find the angular dispersion. This is defined as the incremental lateral displacement of the focal spot along the image plane per unit frequency range, and is found by differentiating the grating equation with respect to frequency. Doing so, and considering the result in the vicinity of $\theta = 0$, yields

$$\frac{d\theta}{d\nu} = -\frac{m\lambda^2 n_g}{n_s c d n_c} \quad (2.6)$$

where the group index of the grating array waveguide is defined as

$$n_g = n_c - \lambda \frac{dn_c}{d\lambda} \quad (2.7)$$

In terms of frequency, the channel spacing $\Delta\nu$ is

$$\Delta\nu = \frac{x}{L_f} \left(\frac{d\theta}{d\nu} \right)^{-1} = \frac{x}{L_f} \frac{n_s c d n_c}{m\lambda^2 n_g} \quad (2.8)$$

or, in terms of wavelength,

$$\Delta\lambda = \frac{x}{L_f} \frac{n_s d n_c}{m n_g} = \frac{x}{L_f} \frac{\lambda_0 d n_s}{\Delta L n_g} \quad (2.9)$$

Thus the above equations define the pass frequencies or wavelengths for which the multiplexer operates, given that it is designed for a central wavelength λ_c . By making ΔL large, the device can multiplex and demultiplex optical signals with very small wavelength spacing.

2.8 Optical Amplifiers

In an optical communication system, the optical signals from the transmitter are attenuated by the optical fiber as they propagate through it. Other optical components, such as multiplexers and couplers, also add loss. After some distance, the cumulative loss of signal strength has to be restored. Prior to the advent of optical amplifiers over the last decade, the only option was to regenerate the signal, that is, receive the signal and transmit it. This process is accomplished by regenerators. A regenerator converts the optical signal to an electrical signal, cleans it up, and converts it back into an optical signal for onward transmission.

Optical amplifiers offer several advantages over regenerators. Regenerators are specific to the bit rate and modulation format used by the communication system. On the other hand, optical amplifiers are insensitive to the bit rate or signal formats. Thus a system using optical amplifiers can be more easily upgraded, for example, to a higher bit rate, without replacing the amplifiers. In contrast, in a system using regenerators, such an upgrade would require all the regenerators to be replaced. Furthermore, optical amplifiers have fairly large gain bandwidths, and as a consequence, a single amplifier can simultaneously amplify several WDM signal but we would need a regenerator for each wavelength. Thus optical amplifiers have become essential components in high-performance optical communication system.

Amplifiers are used in three different configurations as shown in Figure 2.2: power or booster amplifier, in-line amplifier, and preamplifier. An optical power or booster amplifier is used after a transmitter to increase an output power. An in-line amplifier is used typically in the middle of the link to compensate for link losses. A preamplifier is used just in front of a receiver to improve its sensitivity. The design of the amplifier depends on the configuration. A power amplifier is designed to provide the maximum possible output power. A preamplifier is designed to provide high gain and highest possible sensitivity, that is, the least amount of additional noise. A line amplifier is designed to provide a combination of all of these.

Amplifiers, however, aren't perfect devices. They introduce additional noise, and this noise accumulates as the signal passes through multiple amplifiers along its path due to the analog nature of the amplifier. The spectral shape of gain, the output power, and the transient behavior of the amplifier are also important considerations for system applications. Ideally we would like to have a sufficiently high output power to meet the needs of the application. We would also like the gain to be flat over the operating wavelength range, and for the gain to be insensitive to variations in input power of the signal. Figure 2.14 shows a basic operation of optical amplifiers.

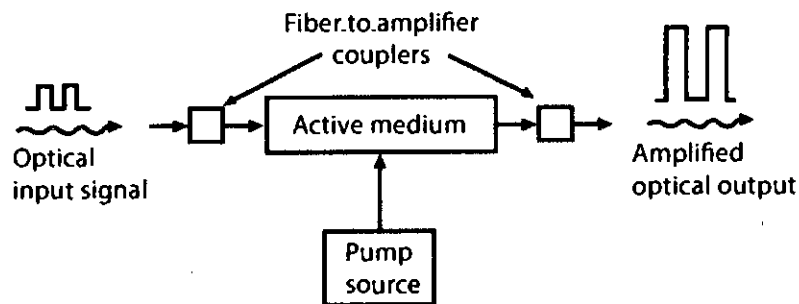


Figure 2.14: Basic operation of a generic optical amplifier.

We will consider three different types of amplifiers here:

- Semiconductor optical amplifiers
- Erbium-doped fiber amplifiers

•Raman amplifiers.

2.8.1 Semiconductor Optical Amplifiers

The two major types of semiconductor optical amplifiers (SOAs) are the resonant, Fabry-Perot amplifier (FPA) and the nonresonant, traveling-wave amplifier (TWA). In an FPA, the two cleaved facets of a semiconductor crystal act as a partially reflective end mirrors that form a Fabry-Perot cavity. The structure of a traveling-wave amplifier is the same as that of an FPA except that the end facets are either antireflection-coated or cleaved at an angle, so that internal reflection does not take place. Thus, the input light gets amplified only one during a single passthrough the TWA. These devices have been used more widely than FPAs because they have a large optical bandwidth, high saturation power, and low polarization sensitivity. Since the 3-dB bandwidth of TWAs is about the three orders of magnitude greater than that of FPAs, TWAs have become the SOA of choice for networking application. In particular, TWAs are used as amplifiers in the 1300 nm window and as wavelength converters in the 1500 nm region. Figure 2.15 shows the block diagram semiconductor optical amplifier.

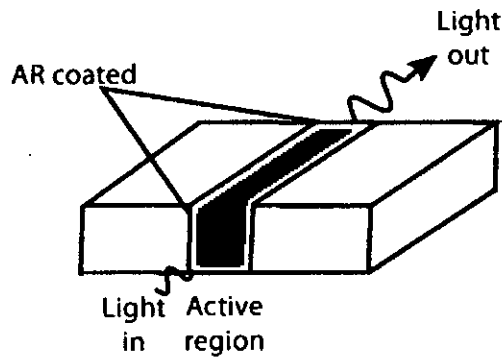


Figure 2.15: Block diagram of semiconductor optical amplifier (SOA).

2.8.2 Erbium-doped Fiber Amplifiers

An erbium-doped fiber amplifier (EDFA) is shown in Figure 2.16. It consists of a length of silica fiber whose core is doped with ionized atoms, Er^{3+} , of the rare earth element erbium. This fiber is pumped using a pump signal from a laser, typically at a wavelength

of 980 nm or 1480 nm. In order to combine the output of the pump laser with the input signal, the doped fiber is preceded by a wavelength-selective coupler.

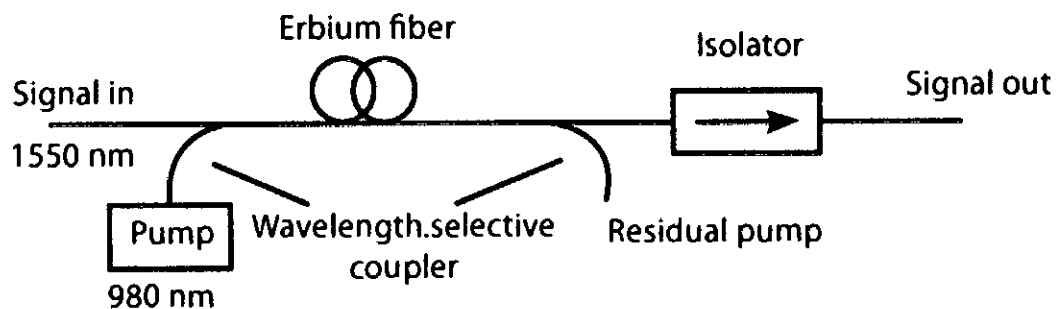


Figure 2.16: An erbium-doped fiber amplifier (EDFA).

At the output another wavelength-selective coupler may be used if needed to separate the amplified signal from any remaining pump signal power. Usually, an isolator is used at the input and/or output of any amplifier to prevent reflections into the amplifier.

A combination of several factors has made the EDFA the amplifier of choice in today's optical communication systems:

- (1) the availability of compact and reliable high-power semiconductor pump lasers;
- (2) the fact that it is an all-fiber device, making it polarization independent and easy to couple light in and out of it;
- (3) the simplicity of the device; and
- (4) the fact that it introduces no crosstalk when amplifying WDM signals.

2.8.3 Raman Amplifiers

Stimulated Raman scattering (SRS) is one of the nonlinear impairments that affect signals propagating through optical fiber. The same nonlinearity can be exploited to provide amplification as well. Figure 2.17 shows the Raman gain spectrum is fairly broad and the

peaks of the gain are centered about 13 THz below the frequency of the pump signal used. In the near-infrared region of interest to us, this corresponds to a wavelength separation of about 100 nm. Therefore, by pumping a fiber using a high-power pump laser, we can

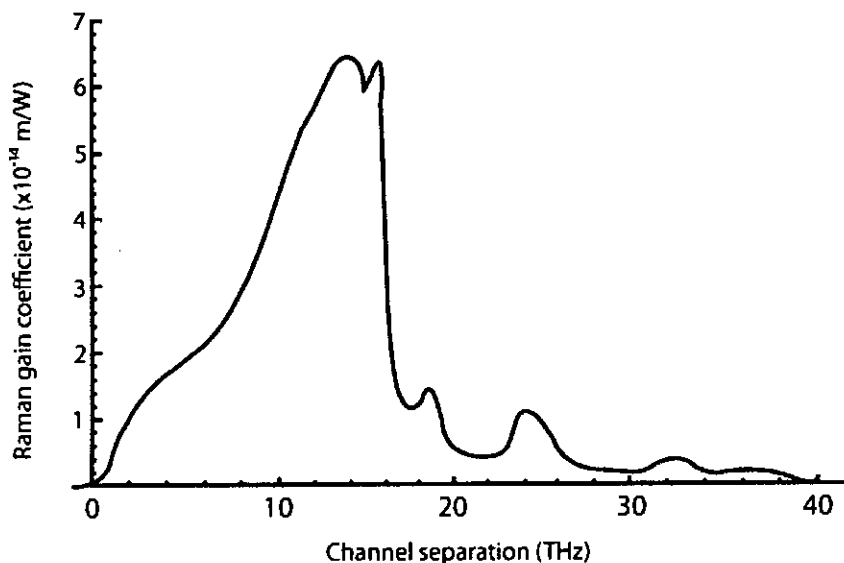


Figure 2.17: SRS gain coefficient as a function of channel separation.

provide gain to other signals, with a peak gain obtained 13 THz below the pump frequency. For instance, using pumps around 1460-1480 nm provides Raman gain in the 1550-1600 nm window.

A key attributes distinguish Raman amplifiers from EDFAs. Unlike EDFAs, we can use the Raman effect to provide gain at any wavelength. An EDFA provides gain in the C and L bands (1528-1605 nm). Thus Raman amplification can potentially open up other bands for WDM, such as the 1310 nm window, or the so-called S-band lying just below 1528 nm. Also, we can use multiple pumps at different wavelengths and different powers simultaneously to tailor the overall Raman gain shape.

Second, Raman amplification relies on simply pumping the same silica fiber used for transmitting the data signals, so it can be used to produce a lumped or discrete amplifier, as well as a distributed amplifier. In the lumped case, the Raman amplifier consists of a long spool of fiber along with the appropriate pump lasers in a package. In the distributed

case, the fiber can simply be the fiber span of interest, with the pump attached to one end of the span, as shown in Figure 2.18.

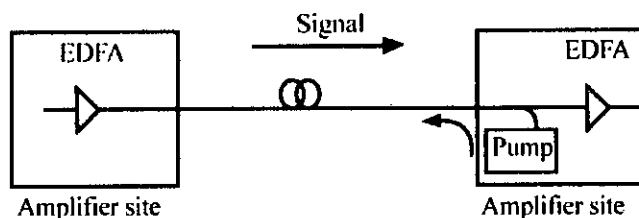


Figure 2.18: Distributed Raman amplifier using a backward propagating pump, shown operating along with discrete EDFAs.

The major concern with Raman amplifiers is crosstalk between the WDM signals due to Raman amplification. A modulated signal at a particular wavelength depletes the pump power, effectively imposing the same modulation on the pump signal. This modulation on the pump then affects the gain seen by the next wavelength, effectively appearing as crosstalk on that wavelength. Again, having the pump propagate in the opposite direction to the signal dramatically reduces this effect. For these reason, most Raman amplifiers use a counterpropagating pump geometry. Another source of noise is due to the back-reflections of the pump signal caused by Rayleigh scattering in the fiber. Spontaneous emission noise is relatively low in Raman amplifiers. This is usually the dominant source of noise because, by careful design, we can eliminate most of the other noise sources.

2.9 Summary

We studied WDM principle and many different WDM active/passive components and their characteristics in this chapter. After that we present different types of optical amplifier that are needed in WDM network for boosting the power levels of several signals simultaneously, where each signal uses a different wavelength.

CHAPTER THREE

WDM Networks

In this chapter, we will explore a brief architectural aspect of the network elements that are part of the WDM networks first. Then we will give brief description of some basic topologies that are possible for fiber optic WDM networks and examine the design tradeoffs among them.

3.1 WDM Network Elements

A WDM network consists of the following elements:

1. Optical Line Terminals;
2. Optical Add/Drop Multiplexer;
3. Optical Cross Connect.

3.1.1 Optical Line Terminals

Optical Line Terminals (OLTs) are relatively simple network elements from an architectural perspective. They are used at either end of a point-to-point link to multiplex and demultiplex wavelengths. Figure 3.1 shows the three functional elements inside an OLT: transponders, wavelength multiplexers, and optionally optical amplifiers. A transponder adapts the signal coming in from a client of the optical network into a signal suitable for use inside the optical network. Likewise, in the reverse direction, it adapts the signal from the optical network into a signal suitable for the client. The interface between the client and the transponder may vary depending on the client, bit rate, and the distance and/or loss between the client and the transponder.

The signal coming out of a transponder is multiplexed with other signals at different wavelength multiplexer onto a fiber. Any of the multiplexing technologies such as arrayed waveguide gratings, fiber Bragg gratings, can be used for this purpose. In

addition, an optical amplifier may be used to boost the signal power if needed. In the other direction, the WDM signal is amplified again, if needed, before it is sent through a demultiplexer that extracts the individual wavelengths.

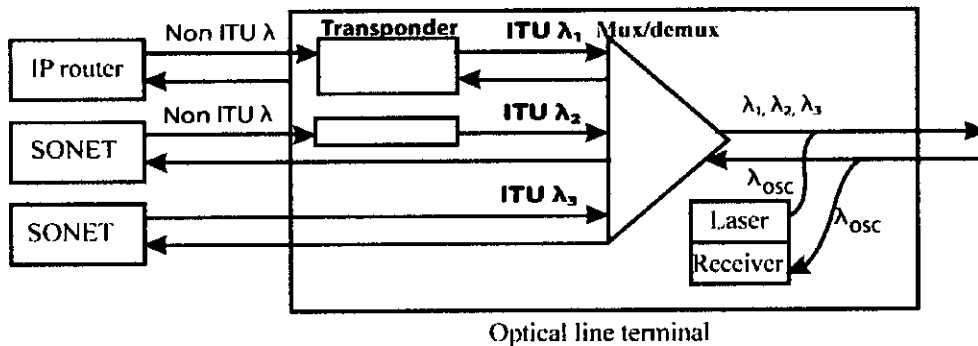


Figure 3.1: Block diagram of optical line terminal (OLT).

Finally, the OLT also terminates optical supervisory channel (OSC). The OSC is carried on a separate wavelength, different from the wavelengths carrying the actual traffic. It is used to monitor the performance of amplifiers along the link as well as for a variety of other management functions.

3.1.2 Optical Add/Drop Multiplexers

Optical add/drop multiplexers (OADMs) provide a cost-effective means for handling pass through traffic in both metro and long-haul networks. OADMs may be used at amplifier sites in long-haul networks but can also be used as stand-alone network elements, particularly in metro networks. Figure 3.2 shows three different OADM architectures. Figure 3.2 (a) shows the parallel architecture where all incoming channels are demultiplexed. Some of the demultiplexed channels can be dropped locally and others are passed through. So there are no constraints on what channels can be dropped and added. As consequence this architecture imposes minimal constraints on planning lightpaths in network. In addition, the loss in the OADM is fixed, independent of how many channels are dropped and added. Unfortunately, this architecture is not cost-effective for handling a small number of dropped channels because, regardless of how many channels are dropped, all channels need to be demultiplexed and multiplexed back together.

Some cost improvements can be made by making the design modular as shown in Figure 3.2 (b). Here, the multiplexing and demultiplexing is done in two stages. The first stage of the demultiplexing separates the wavelengths into bands, and the second stage separates the bands into individual channels. In addition to the cost savings in the multiplexers and demultiplexers realized, the use of bands allows signals to be passed through with lower optical loss and better loss uniformity. Several commercially available OADMs use this approach.

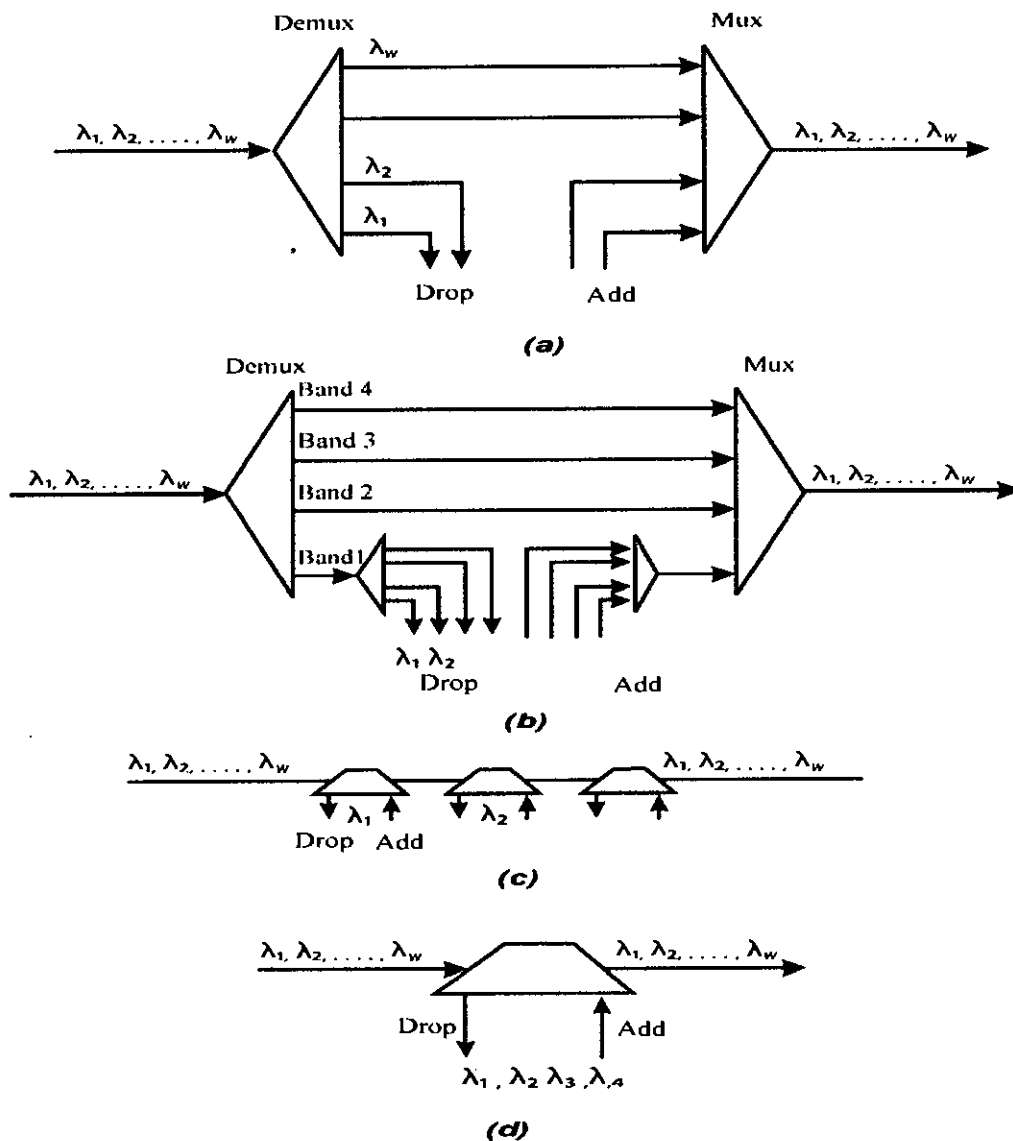


Figure 3.2: Different OADM architectures. (a) parallel; (b) modular version of the parallel architecture; (c) serial; and (d) band drop.

Figure 3.2 (c) shows the serial architecture of OADMs where a single channel is dropped and added from an incoming set of channels. This can be realized using fiber Bragg gratings dielectric thin-film filters. In drop and add multiple channels, several serial OADMs are cascaded. This architecture is highly modular in that the cost is proportional to the number of channels dropped. Therefore the cost is low if only a small number of channels are to be dropped. However, if a large number of channels are to be dropped, the cost can be quite significant since a number of individual devices must be cascaded. There is also an indirect impact on the cost because the loss increases as more channels are dropped, requiring the use of additional amplification.

Figure 3.2 (d) shows the band drop architecture of OADM where a fixed group channels is dropped and added from the aggregate set of channels. The dropped channels then typically go through a further level of demultiplexing where they are separated out. The added channels are usually combined together with simple couplers and added to the passthrough channels. This architecture tries to make a compromise between the parallel architecture and serial architecture. The maximum number of channels that can be dropped is determined by the type of band filter used. Within the group of channels, adding/dropping additional channels doesn't affect other lightpaths in the network as the passthrough loss for all the other channels not in this group is fixed.

3.1.3 Optical Cross Connects

OADMs are useful network elements to handle simple network. A high degree of path modularity, capacity scaling, and flexibility in adding or dropping channels at a user site can be achieved by introducing the concept of an optical cross connect (OXC) architecture in the physical path structure of an optical network. These OXCs operate directly in the optical domain and can route very high capacity WDM data streams over a network of interconnected optical paths. The use of dynamic routing solves the problem of a limited number of available wavelengths through the wavelength-reuse technique. The design and fabrication of OXCs has remained a major topic of research since the advent of WDM systems.

Figure 3.3 shows the generic design of an OXC schematically. The device has N input ports, each port receiving a WDM signal consisting of M wavelengths. Demultiplexers split the signal into individual wavelengths and distribute each wavelength to the bank of M switching units each unit receiving N input signals at the same wavelength. An extra input and output port is added to the switch to allow dropping or adding of specific channel. Each switching unit contains N optical switches that can be configured to route the signals in any desirable fashion. The output of all switching units is sent to N multiplexers, which combine their M inputs to form the WDM signal. Such an OXC needs N multiplexers, N demultiplexers, and $M(N+1)^2$ optical switches. Switches used by an OXC are 2×2 space-division switches which switch an input signal to spatially separated output ports using a mechanical, thermo-optic, electro-optic, or all-optical technique.

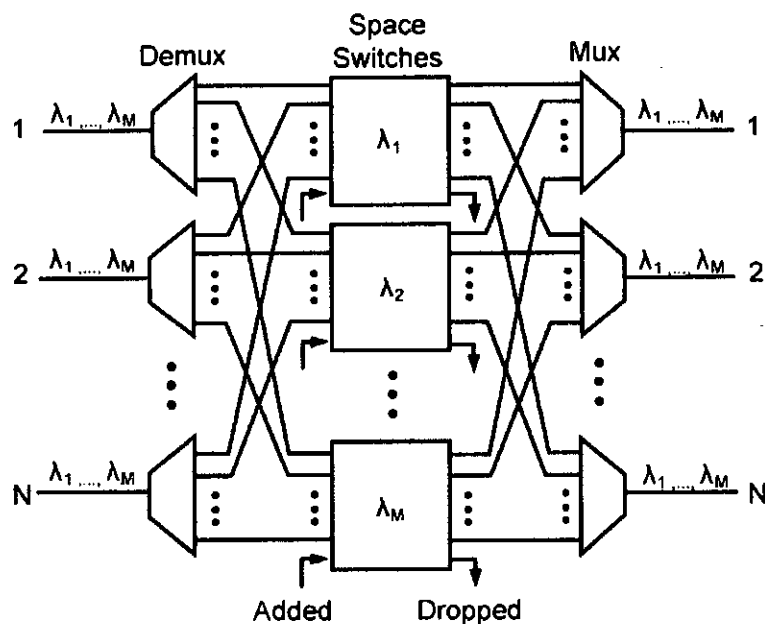


Figure 3.3: Schematic of optical cross-connect (OXC) based on optical switches.

Optical fibers themselves can be used for making OXCs if they are combined with FBGs and OCs which is a popular all-optical technique recently used in fiber-optic WDM network. Figure 3.13 shows the FBG-OC-based bidirectional OXC. Tunable FBG, which is one of the most versatile optical devices, is well suited for building such a small or medium-sized OXC. Particularly, its wavelength selectiveness enables the construction of

an OXC devoid of separate demultiplexers and multiplexers, which are indispensable to OXCs made up of color-blind-space-switch fabrics. As a consequence, structural simplicity as well as cost effectiveness is among the advantages of FBG-based OXC over the conventional space-switch-based OXCs [10].

3.2 Network Topologies

Networks are traditionally divided into the following three broad categories:

1. *Local-area networks* (LANs) interconnect users in a localized area such as a department, a building, an office or factory complex, or a university campus;
2. *Metropolitan-area networks* (MANs) provide user interconnection within a city or in the metropolitan area surrounding a city;
3. *Wide-area networks* (WANs) cover a large geographical area ranging from connections between nearby cities to connections of users across a country.

In this section first we will consider three basic network topologies such as linear bus, ring and star configurations used for fiber optic networks. Figure 3.4 shows the three common topologies used for fiber optic networks. Each has its own particular advantages and limitations in terms of reliability, expandability, and performance characteristics.

Optical bus networks employ optical fiber as the transmission medium. Fiber-optic based bus network is more difficult to implement. The impediment is that there are no low-perturbation optical-taps for efficiently coupling optical signals into and out of the main optical fiber trunk line. Access to the optical data bus is achieved by means of coupling element, which can be either active or passive.

In a ring topology, consecutive nodes are connected by point-to-point links that are arranged to form a single closed path. Information in the form of data packets is transmitted from node to node around a ring. The interface at each node is an active device that has the ability to recognize its own address in a data packet in order to accept messages. The active node forwards the messages that are not addressed to itself on its next neighbor.

In a star architecture, all nodes are joined at a single point called the central node or hub. The central node can be active or passive device. Using a active node, one can control all routing of messages in the network from the central node. In a star network with a passive central node, a power splitter is used at the hub to divide the incoming optical signals among all the outgoing lines to the attached stations.

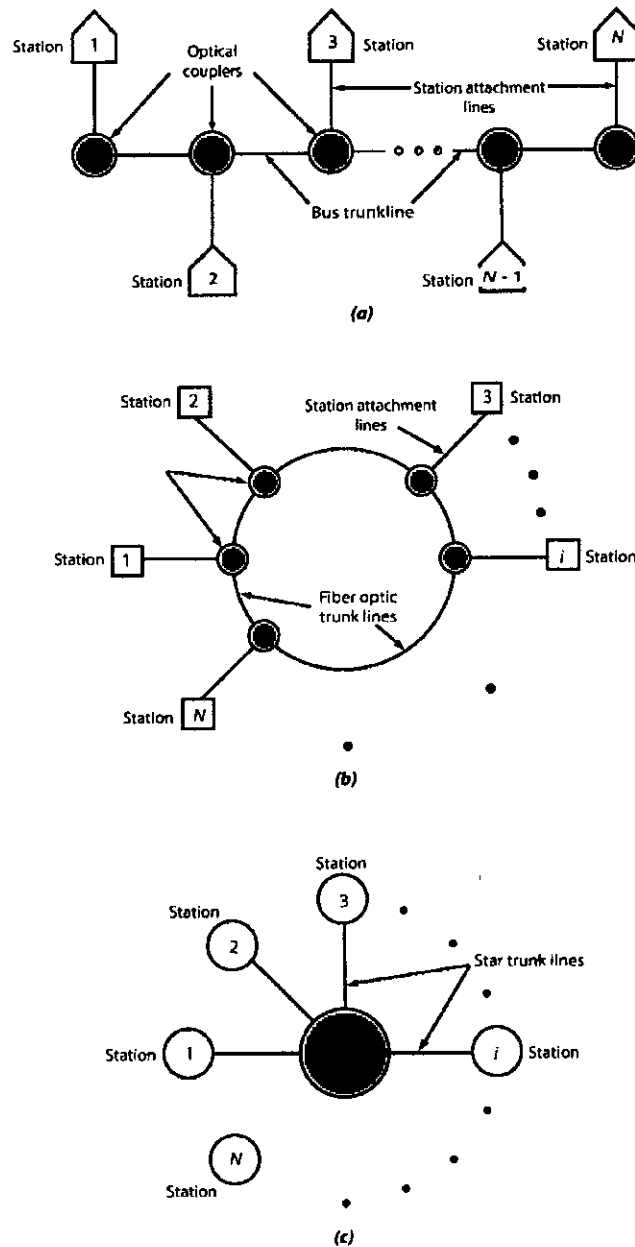


Figure 3.4: Three common topologies used for fiber optic networks (a) bus, (b) ring, and (c) star.

All three types of networks can get benefit from the WDM technology. They can be designed using bus, ring or star topology. A ring topology is most practical for MANs and WANs, while the star topology is commonly used for LANs.

3.3 SONET/SDH Networks

With the advent of fiber optic transmission lines, the next step in the evolution of the digital time-division multiplexing (TDM) scheme was a standard signal format called synchronous optical network (SONET) in North America and synchronous digital hierarchy (SDH) in other parts of the worlds. A key characteristic of SONET and SDH is that they are usually configured as ring architecture. This is done to create loop diversity for uninterrupted service protection purpose in case of link or equipment failures. The SONET/SDH rings are called self-healing rings, since the traffic flowing along a certain path can automatically be switched to an alternate or standby path following failure or degradation of the link segment.

Figure 3.5 shows generic configuration of a large SONET network consisting of linear chains and various types of interconnected rings. One can build point-to-point links, linear chains, unidirectional path-switched rings (UPSR), bidirectional line-switched rings (BLSR), and interconnected rings. The OC-192 four fibers BLSR could be a large

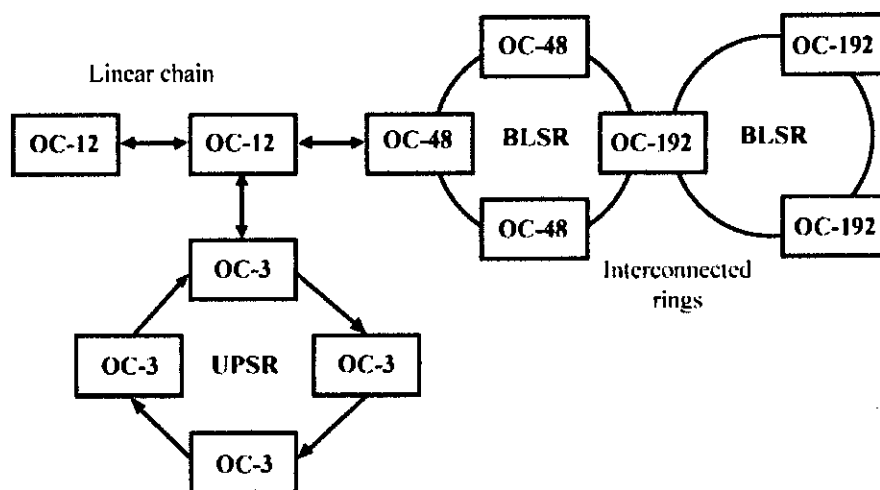


Figure 3.5: Generic configuration of a large SONET network consisting of linear chains and various types of interconnected rings.

national backbone network with a number of OC-48 rings attached in different cities. The OC-48 rings can have lower-capacity localized OC-12 or OC-13 rings or chains attached to them, thereby providing the possibility of attaching equipment that has an extremely wide range of rates and sizes.

The SONET/SDH architectures can also be implemented with multiple wavelengths. Figure 3.6 shows a dense WDM deployment on an OC-192 trunk ring for n wavelength.

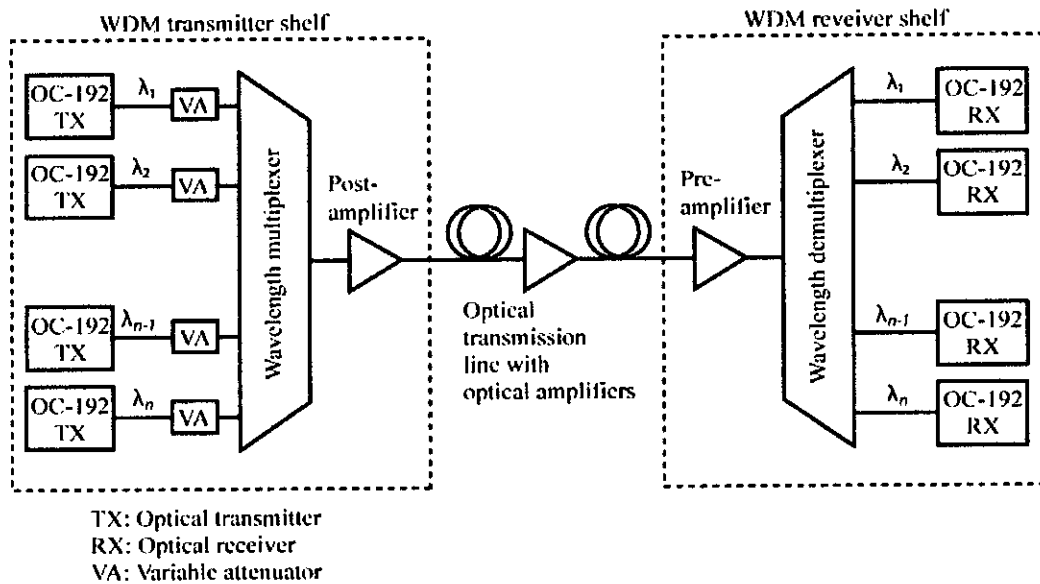


Figure 3.6: Dense WDM deployment of n wavelengths in an OC-192 trunk ring.

3.4 Broadcast-and-Select WDM Networks

As another step toward realizing the full potential of optical fiber transmission capacity, researchers have looked at all-optical WDM networks to extend the versatility of communication networks beyond architectures such as those provided by SONET/SDH. These networks can be classified as either broadcast-and-select or wavelength-routing networks. In general, broadcast-and-select techniques employing passive optical stars, buses, or wavelength routers are used for local network applications, whereas active components form the basis for constructing wide-area wavelength-routing networks. Broadcast-and-select networks can be categorized as single-hop or multi-hop networks.

3.4.1 Broadcast-and-Select Single-Hop WDM Networks

Single-hop refers to networks where information transmitted in the form of light reaches its destination without being converted to an electrical form at any intermediate point. Figure 3.7 shows two alternate physical architectures for a WDM-based local network. Here, N sets of transmitters and receivers are attached to either a star coupler or a passive bus. Each transmitter sends its information at a different fixed wavelength. All the transmissions from the various nodes are combined in a passive star coupler or coupled onto a bus and the result is sent out to all receivers.

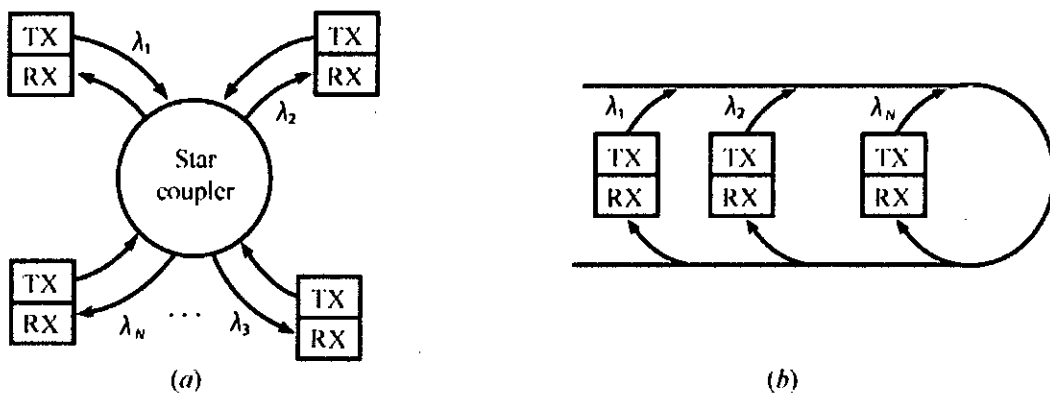


Figure 3.7: Two alternate physical architectures for a WDM-based local network: (a) star, (b) bus.

3.4.2 Broadcast-and-Select Multi-Hop WDM Networks

A drawback of single-hop networks is the need for rapidly tunable lasers or receiver optical filters. The designs of multihop networks avoid this need. Multihop networks generally do not have direct paths between each node pair. Each node has a small number of fixed-tuned optical transmitters and receivers. Figure 3.8 shows an example of a four-node broadcast-and-select multihop network where each node transmits on one set of two fixed wavelengths and receives on another set of two fixed wavelengths. Stations can send information directly only to those nodes that have a receiver tuned to one of the two transmit wavelengths. Information destined for other nodes will have to be routed through intermediate stations.

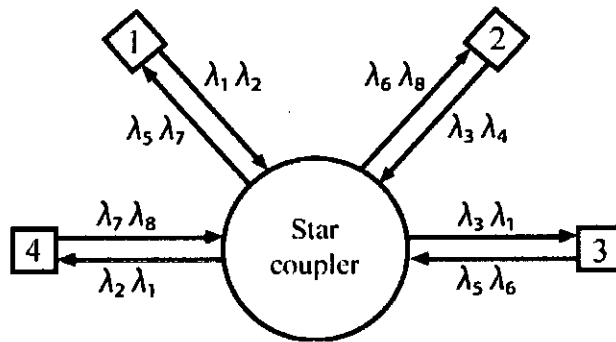


Figure 3.8: Architecture and traffic flow of a multihop broadcast-and-select WDM network.

3.5 Wavelength-Routed Networks

Two problems arise in broadcast-and-select networks when trying to extend them to wide-area networks. First, more wavelengths are needed as the number of nodes in the network grows. Typically, there are at least as many wavelengths as there are nodes, unless several nodes time-share a wavelength. Second, without the widespread use of optical booster amplifiers, a large number of users spread over a wide area cannot readily be interconnected with a broadcast-and-select network. This is because the network employs passive star couplers in which the splitting losses could be prohibitively high for many attached stations.

Wavelength-routed networks overcome these limitations through wavelength reuse, wavelength conversion, and optical switching. The physical topology of a wavelength-routed network consists of optical wavelength routers interconnected by pairs of point-to-point fiber links in an arbitrary mesh configuration as illustrated in Figure 3.9. Each link can carry a certain number of wavelengths, which can be directed independently to different output paths at a node. Each may have logical connections with several other nodes in the network, where each connection uses a particular wavelength. Provided the paths taken by any two connections do not overlap, they can use the same wavelength. Thereby the number of wavelengths is greatly reduced. For example in Figure 3.9, the connection from node 1 to node 2 and node 2 to node 3 can both be on λ_1 , whereas the connection between nodes 4 and 5 requires a different wavelength (λ_2).

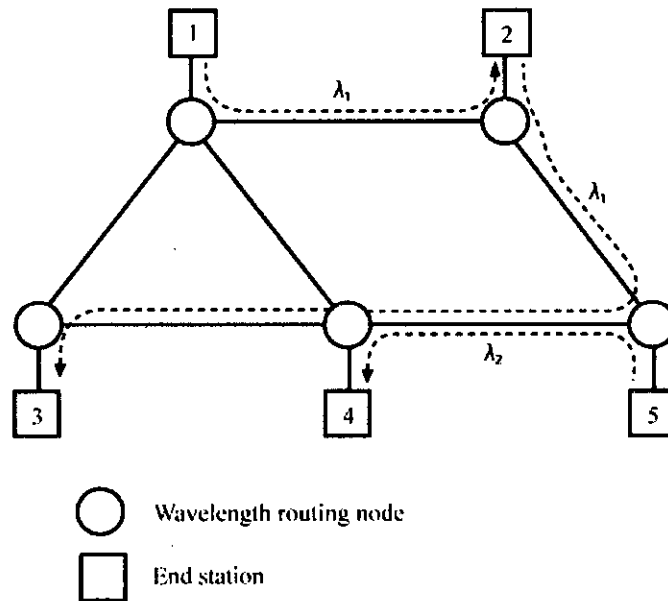


Figure 3.9: Wavelength reuse on a mesh network.

WDM systems can be designed to be transparent systems. This allows different wavelengths to carry data at different bit rates and protocol formats. This can be a major advantage in some cases.

Finally, WDM provides great flexibility in building networks. For example, if there is a network node at which most of the traffic is to be passed through and a small fraction is to be dropped and added, it may be more cost-effective to use a WDM optical add/drop element than terminating all the traffic and doing the add/drop in electrical domain.

3.6 Unidirectional versus Bidirectional WDM Networks

A unidirectional WDM system uses two fibers, one of each direction of traffic, as shown in Figure 3.10(a). A bidirectional system, on the other hand, requires only one fiber and typically uses half the wavelengths for transmitting data in one direction and the other half for transmitting data in the opposite direction on the same fiber, as shown in Figure 3.10(b). Both types of systems are being deployed and have their pros and cons. We will compare the two types of systems, assuming that technology limits us to a fixed number of wavelengths, say, W , per fiber in both cases.

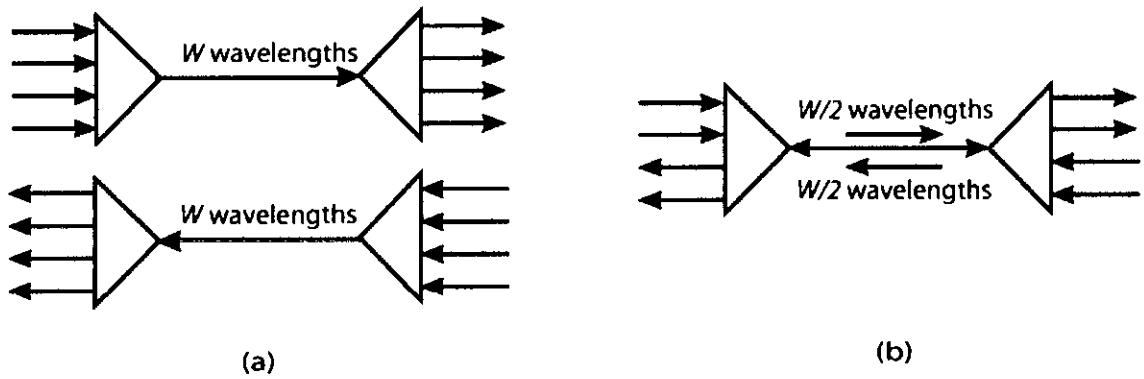


Figure 3.10: (a) Unidirectional and (b) bidirectional transmission systems.

1. A unidirectional system is capable of handling W full-duplex channel over two fibers. A bidirectional system handles $W/2$ full-duplex channels over one fiber. The bidirectional system, therefore, has half the total capacity, but allows a user to build capacity more gradually than a unidirectional system. Thus it may have a slightly lower initial cost.

2. If only one fiber is available, then there is no alternative but to deploy bidirectional systems. Implementing 1 + 1 or 1:1 configurations with unidirectional WDM systems requires a minimum of two pairs of fibers routed separately, but only requires two with bidirectional systems, as shown in 3.11.

3. Bidirectional systems can potentially be configured to handle asymmetric traffic. Given a total number of wavelengths in the fiber, more wavelengths could be used in one direction compared to the other.

4. Bidirectional systems usually require a guard band between the two sets of wavelengths traveling in opposite directions to avoid crosstalk penalties. However, high-channel-count unidirectional systems may also require guard bands due to the hierarchical nature of the multiplexing and demultiplexing in these systems. The guard band can be eliminated by interleaving the wavelengths in opposite directions, that is, by having adjacent wavelengths travel in opposite directions on the fiber. This also has the added advantage of effectively doubling the channels.

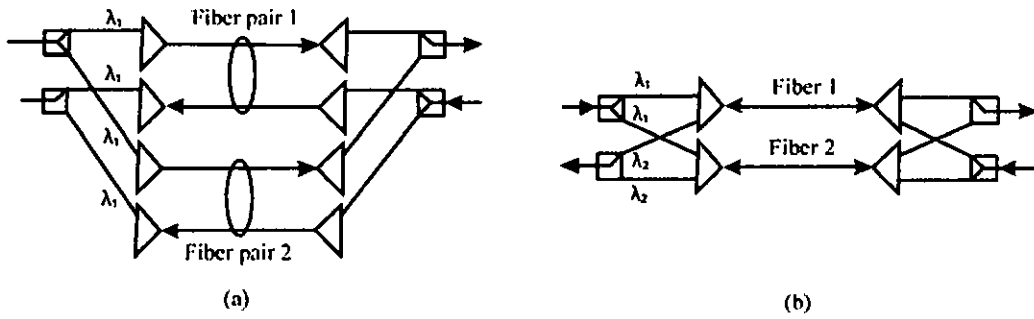


Figure 3.11: (a) Two unidirectional systems using four fibers, and (b) two bidirectional systems using two fibers.

3.7 System Model

Figure 3.12 shows a block diagram of a bidirectional WDM ring network (BWRN) in which small access ring networks are connected to a big metro-core ring network using BOXC. Recently a single-fiber BWRN emerge as a cost-effective and reliable topology for MANs. Therefore, bidirectional operation of the OXCs and wavelength add/drop multiplexers (BOADMs) are demanded. For a single BWRN, only bidirectional BOADM is needed at each node. As the BWRN evolves, demand to interconnect the BWRNs will occur. Figure 3.12 shows a diagram of a feasible MAN composed of BWRNs, in which small access ring networks are connected to a big metro-core ring network. At the node where multiple BWRNs are interconnected, we need a bidirectional OXC, which selectively interchanges wavelength channels among the BWRNs in both directions. Of course, BOXC should offer independent interconnectivity for each direction [7].

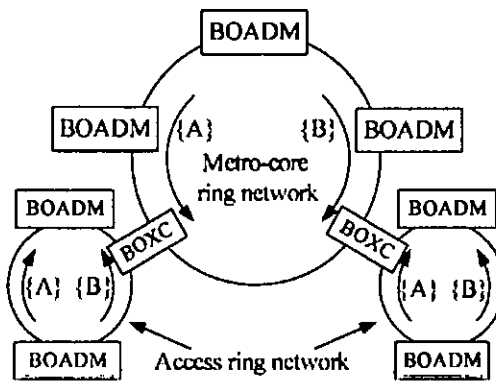


Figure 3.12: Bidirectional WDM ring networks interconnected by BOXCs.

Different configurations of BOXCs are given in [4]-[9]. Figure 3.13 shows a 2×2 BOXC based on rotatable OCs and fiber FBGs.

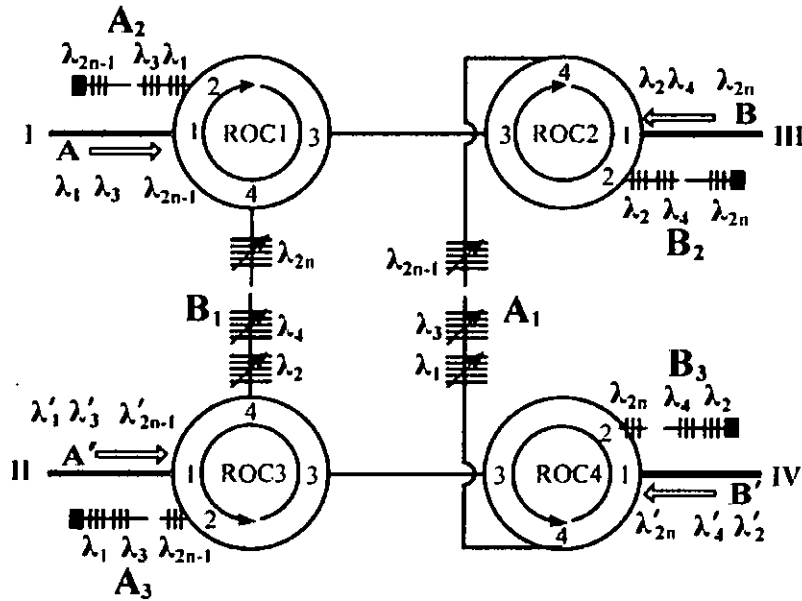


Figure 3.13: Schematic diagram of a 2×2 BOXC using four-port OCs and FBGs.

To extend a 2×2 BOXC to a generalized $N \times N$ BOXC, which can be constructed based on the Benes network structure using 2×2 BOXCs as a building blocks.

3.8 Summary

We studied the basic network elements constituting WDM networks and the design of various wavelength-routing networks by using network elements in this chapter. Then we compare unidirectional and bidirectional WDM systems and present a WDM system model which is made up of multiple ring networks interconnected by using BOXCs. Finally, how BOXC can be made and extended by using FBGs and OCs is given.

CHAPTER FOUR

Crosstalk Modeling and Analysis

This chapter is devoted to studying the various types of crosstalk introduced due to different types of WDM components used in a WDM network. Then try to establish analytical expression for the various types of crosstalk as well as their impact on transmission performance in a WDM system.

4.1 Introduction

The most important issue in the design of WDM networks is the crosstalk. Crosstalk is the general term given to the effect of other signal on the desired signal. Crosstalk can be introduced by almost any component in a WDM system, including optical filters, wavelength multiplexers and demultiplexers, optical switches, optical amplifiers, and fiber itself.

Two forms of crosstalk arise in WDM systems:

- Interband/interchannel crosstalk
- Intraband/intrachannel crosstalk

4.1.1 Interband Crosstalk

Interband crosstalk arises when an interfering signal comes from a neighboring channel that operates at a different wavelength. This nominally occurs when a wavelength-selecting device imperfectly rejects or isolates the signals from other nearby wavelength channels. Crosstalk then arises since these spurious neighboring signals could fall partially within the receiver passband. Interchannel crosstalk can arise from a variety of sources. Figure 4.1(a) shows an optical filter or demultiplexer that selects one channel and imperfectly rejects the others. Figure 4.1(b) shows an optical switch is switching

different wavelength where the crosstalk arises because of imperfect isolation between the switch ports.

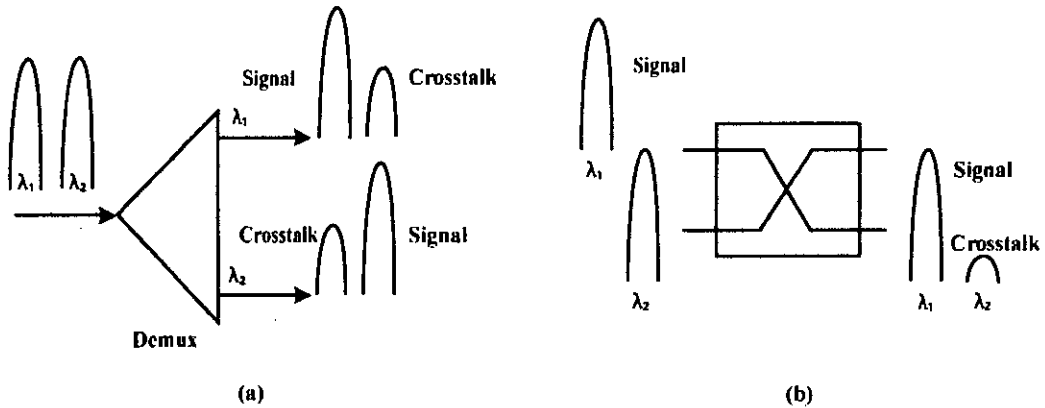


Figure 4.1: Source of interband crosstalk. (a) An optical demultiplexer, and (b) an optical switch with inputs at different wavelengths.

4.1.2 Intraband Crosstalk

Intraband crosstalk arises when the interfering signal is at the same wavelength as the desired signal. This effect is more severe than interchannel crosstalk, since the interference falls completely within the receiver bandwidth. Figure 4.2(a) shows the demultiplexer ideally separates the incoming wavelength to different output fibers. In reality, however, a portion of the signal at one wavelength, say λ_1 , leaks into the adjacent channel λ_2 because of nonideal suppression within the demux. When the wavelengths are combined again into a single fiber by the multiplexer, a small portion of the λ_1 that leaked into the λ_2 channel will also leaked back into the common fiber at the output. Although both signals contain same data, they are not in phase with each other, due to different delay encountered by them. This causes intrachannel crosstalk. Another source of this type crosstalk arises from optical switches, as shown in Figure 4.2(b), due to the nonideal isolation of one switch port from the other. In this case, the signals contain different data. Intrachannel crosstalk can be divided into coherent crosstalk and incoherent crosstalk. When the phase of the crosstalk signal is correlated with that of the main signal, it is called coherent crosstalk. When the phase of the crosstalk signal is not correlated with that of the main signal, it is called incoherent crosstalk. Crosstalk signal generated from

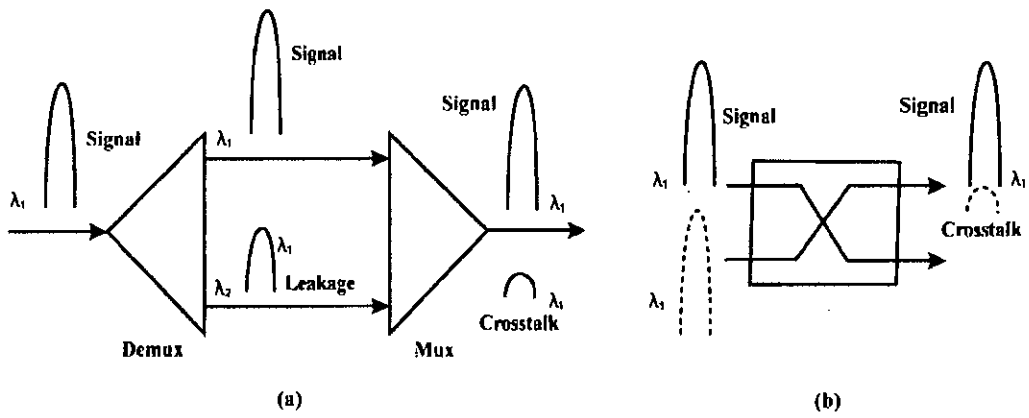


Figure 4.2: Sources of intraband crosstalk. (a) A cascaded wavelength demultiplexer and a multiplexer, and (b) an optical switch.

the same source are coherent crosstalk and crosstalk signals generated from different sources are incoherent crosstalk. Coherent crosstalk is believed not to cause noise but causes fluctuations of signal power [2].

4.1.3 Crosstalk in Optical Networks

Crosstalk suppression becomes particularly important in optical networks, where a signal propagates through many nodes and accumulates crosstalk from different elements at each node. Examples of such elements are muxes/demuxes and optical switches. Networks are very likely to contain amplifiers and to be limited by signal-spontaneous beat noise.

Interband crosstalk is the crosstalk situated in wavelengths outside the channel and since this crosstalk can be removed with narrow-band filters and it produces no beating during detection, so it is less harmful. Since the crosstalk within the same wavelength slot is called intraband crosstalk, so it cannot be removed by an optical filter and therefore accumulates through network. Since it cannot be removed, one has to prevent the intraband crosstalk [1]. Figure 4.3 shows the wavelength spectrum of interband and intraband crosstalk. In this thesis only intraband crosstalk is studied since the network performance will be limited by this kind of crosstalk. Moreover, within the intraband crosstalk, a distinction between incoherent and coherent crosstalk has to be made.

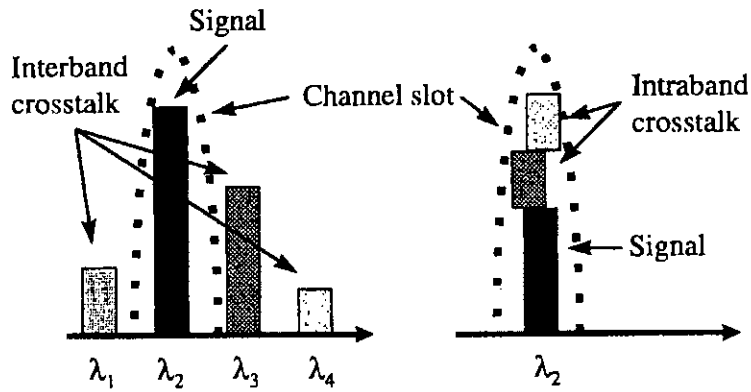


Figure 4.3: Wavelength spectrum of interband and intraband crosstalk.

4.1.4 Bidirectional Systems

In a bidirectional transmission system, data is transmitted in both directions over a single fiber. Figure 4.4 shows a bidirectional transmission system. Additional crosstalk mechanisms arise in these systems. Although the laws of physics do not prevent the same wavelength from being used for both directions of transmissions, this is not a good idea in practice because of reflections. A back-reflection from a point close to the transmitter at one end, say, end A, will send a lot of power back into A's receiver, creating a large amount of crosstalk. In fact, the reflected power into A may be larger than the signal power received from the other end B. Reflections within the end equipment can be

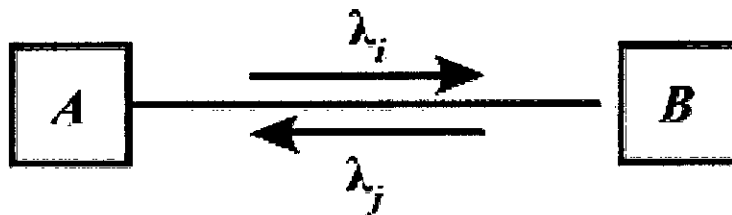


Figure 4.4: A bidirectional transmission system.

carefully controlled, but it is more difficult to restrict reflection from the fiber link itself. For this reason, bidirectional systems typically use different wavelengths in different directions. The two directions can be separated at the ends either by using an optical circulator or WDM mux/demux as shown in Figure 4.5.

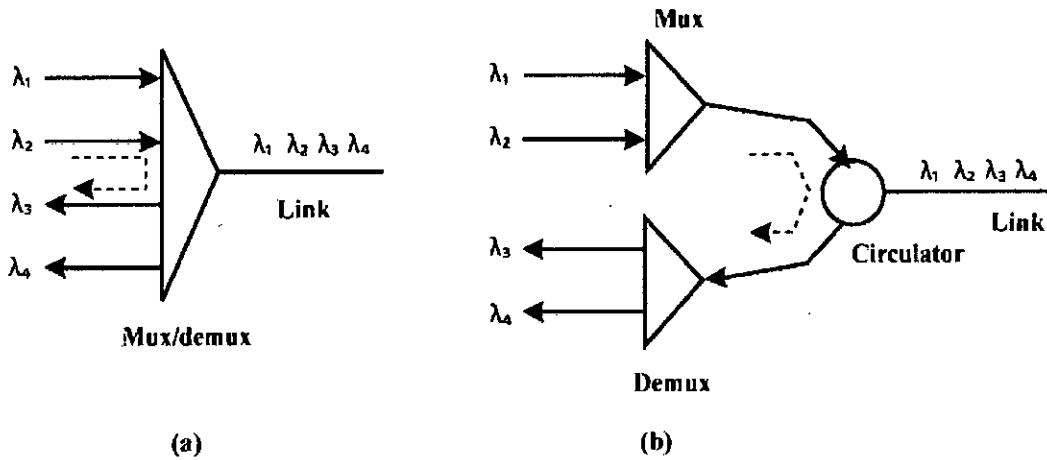


Figure 4.5: Separating the two directions in a bidirectional system: (a) using a WDM mux/demux, and (b) using an optical circulator (OC). Both methods can introduce crosstalk, as shown by dashed lines in the figure.

If a WDM mux/demux is used to handle both directions of transmission, crosstalk can also arise because a signal at transmitted wavelength is reflected within the mux into a port that is used to receive a signal from the other end, as shown in Figure 4.5(a). The mux/demux used should have adequate crosstalk suppression to ensure that this is not a problem. Likewise, if an optical circulator is used, crosstalk can arise because of imperfect isolation in the circulator, as shown in Figure 4.5(b).

Of the described above two methods, we will only focus on the FBG and optical circulator based bidirectional system due to lower insertion loss rather than arrayed waveguide grating based bidirectional system. The crosstalk caused by optical circulator is also ignored under the assumption that each optical circulator has sufficiently large isolation and return loss.

4.2 FBG-OC-Based BOXC Architectures

A 2×2 and 4×4 BOXC are considered and studied here. Figure 4.6 shows the schematic diagram of the proposed BOXC architecture. Two different sets of wavelength channels {A} and {B} propagate in opposite directions in each BOXC. If we use two separate wavelength bands for their respective directions and channels within a wavelength band

are densely spaced, the tuning range of FBGs has to be greater than the width of a wavelength band; while if we adopt the interleaved wavelength scheme, the tuning range of FBGs can be made as small as the wavelength channel spacing. To circumvent the constraint on the tuning range of FBGs, the interleaved wavelength scheme is adopted. We assume that a set of wavelengths $\{\lambda_{2n-1}\}$ (1, 2, ..., m), denoted as group A, and another set of wavelengths $\{\lambda_{2n}\}$ (1, 2, ..., m), denoted as group B, are transmitted in opposite directions.

Figure 4.6(a) shows the configuration of 2×2 BOXC using FBGs and six-port OCs [9]. There are two sets of tunable FBGs (A_1 and B_1) and four sets of fixed FBGs (A_2 , A_3 , B_2 , and B_3) are used in this configuration. Unwanted backscattered signals, including Rayleigh backscattering due to bidirectional transmission in the fiber and reflections at connectors and splices, can be slightly removed by the four sets of fixed FBGs with the optical isolator as light absorbers [9]. In the figure, we use A_i to denote the i th set of FBGs whose Bragg wavelengths are associated with the odd-number of wavelengths $\{\lambda_{2n-1}\}$ (1, 2, ..., m) of group A and B_i to present the i th set of FBGs whose Bragg wavelengths are associated with even-number wavelengths $\{\lambda_{2n}\}$ (1, 2, ..., m) of group B. The OCs used here are fully rotatable. A fully rotatable OC (ROC) can route the input signal from the last port back to the first port. The operation of this BOXC is described as follows. The WDM signals of group A at $\{\lambda_{2n-1}\}$ entering at port 1 of ROC1 are reflected by Set A_2 of fixed FBGs whose Bragg wavelengths are fixed and matched with the incoming WDM channels. These WDM signals will go through port 3 of ROC1 and encounter the tunable FBGs of Set A_1 . Note that a tunable FBG with Bragg wavelength $\{\lambda_{2n-1}\}$ only needs to be tuned to its adjacent Bragg wavelength λ_{2n} or λ_{2n-1} , and hence, the tuning range required is equal to the channel spacing. By tuning the Bragg wavelength of each tunable FBG, the incoming WDM signals will be either passed through or reflected back. A reflected signal will be coupled back to port 3 of ROC1 and exit at port 4 of ROC1, whose switching state in the BOXC is denoted as a “bar” state. On the other hand, a passed through signal will be coupled into port 3 of ROC2 and exit at port 4 of ROC2, whose switching state in the BOXC is denoted as a “cross” state. Similarly, for the WDM signals of group B at wavelength λ_{2n} that are launched into port 4

of ROC1, we can achieve the same independent switching by tuning the tunable FBGs of Set B₁.

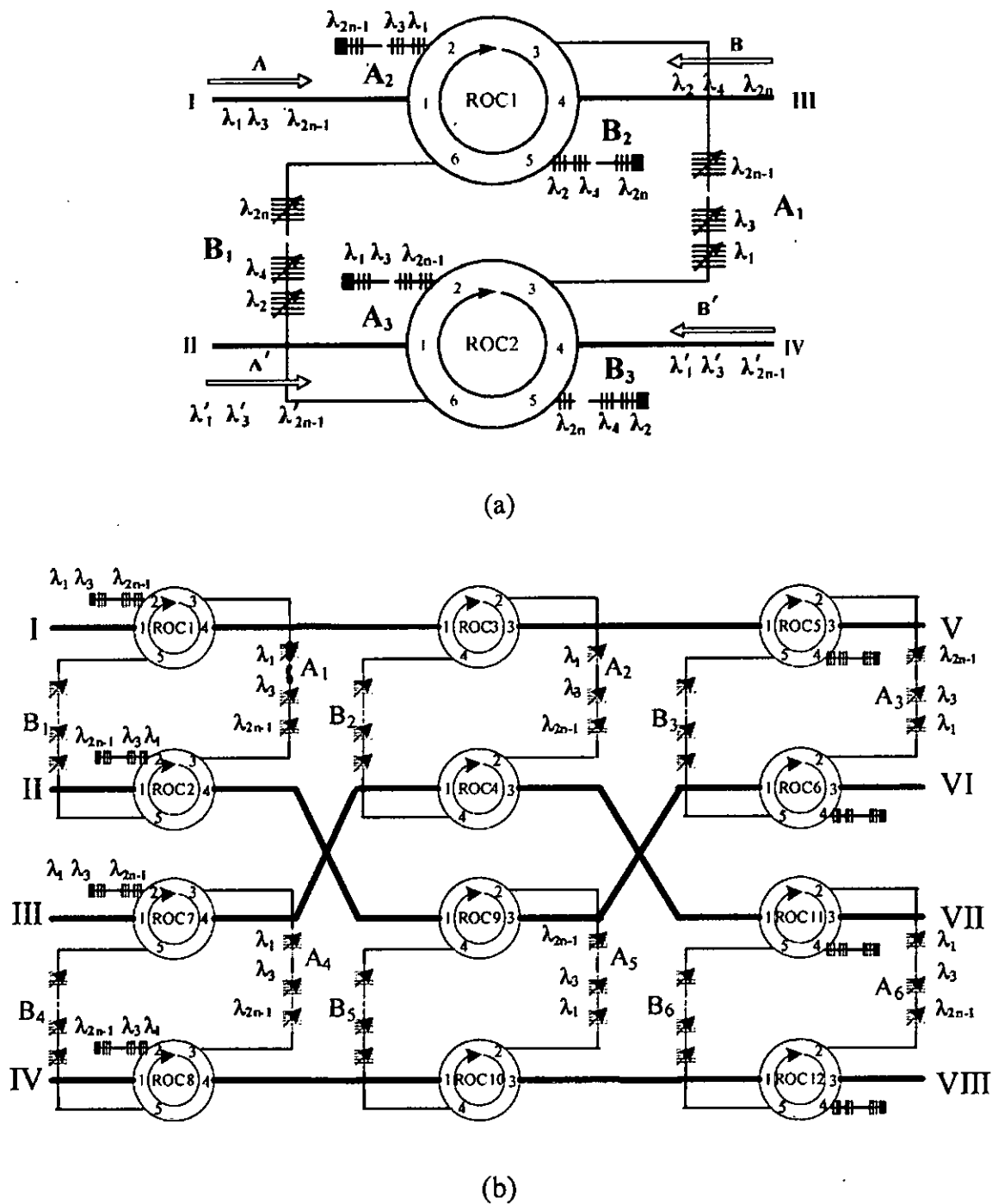


Figure 4.6: BOXCs based on FBGs and OCs. (a) 2 × 2 BOXC using six-port ROCs and FBGs, and (b) 4 × 4 BOXC consists of six 2 × 2 BOXCs.

Note that to achieve lower insertion loss and loss equalization for the bar state, the sequence of each set of FBGs should be arranged properly. As shown in Figure 4.6, FBGs in Set A_2 and FBGs in Set A_1 are arranged in the reverse order with respect to the WDM signals entering these two FBG sets. Similarly, FBGs in Set A_3 and FBGs in Set A_1 are also arranged in the reverse order. Thus, in the bar state, each input WDM signal entering from the left side will experience the same attenuation regardless of their wavelengths. In the cross state, the maximum insertion loss can be reduced, compared with the situation where FBGs in Set A_2 and FBGs in Set A_1 are arranged in the same order. Nevertheless, the loss equalization in the cross state cannot be achieved by this arrangement. To compensate the insertion loss difference among the individual channels caused by the proposed BOXC, a few dynamic commercially available gain equalizers can be used [9].

Figure 4.6(b) shows a 4×4 BOXC, which consists of six 2×2 BOXCs. Here we also used two separate wavelength bands in opposite directions as like as 2×2 BOXC described above. Since the main source of backscattering does not occur within the BOXC, we only need to place one set of fixed FBGs at each entry of the BOXC. Therefore, only eight sets of fixed FBGs are required.

4.3 Intraband Crosstalk arising from FBGs operation

In WDM networks employing a number of BOXCs, crosstalk arising from imperfect filtering or nonideal switching accumulates and grows rapidly through the path of networks, posing a severe limitation to the scale of transparent networks. Already we have described various types of crosstalk arise in WDM network in section 4.1.2. Figure 4.6 illustrates the mechanisms of intraband crosstalk generation when two signals, with the same wavelength λ , are simultaneously incident on the both sides of a single tunable FBG. In the reflection mode of FBG as shown in Figure 4.7 (a), the FBG is tuned to a wavelength λ and is supposed to reflect both signals. However, since the reflectivity of an FBG is usually less than 100% even at the center of the reflection bandwidth, small portions of signals are leaked and become crosstalk elements. Similarly, in the transmission mode of FBG as shown in Figure 4.7(b), due to imperfect transmissivity,

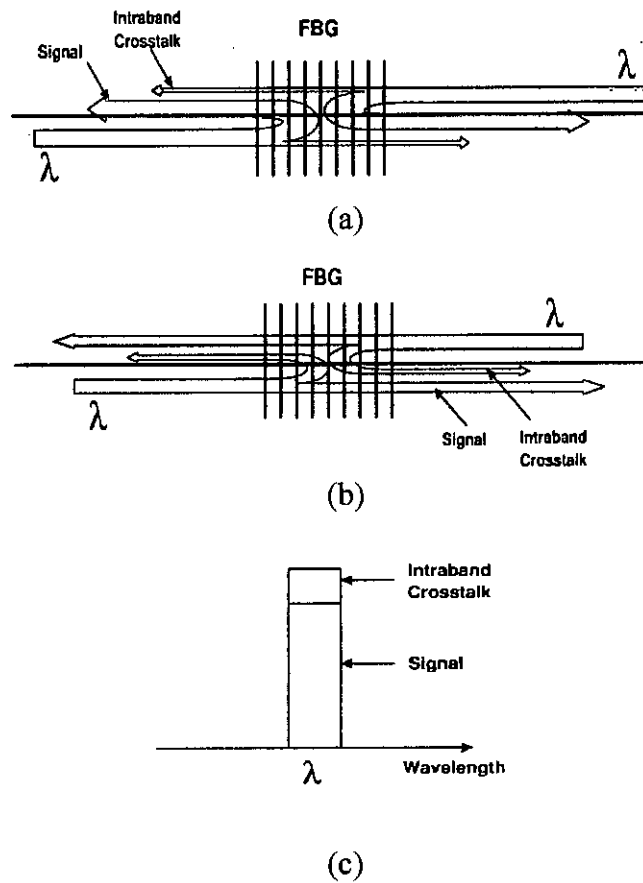


Figure 4.7: Illustration of the mechanism generating intraband crosstalk in the operation of tunable FBG. (a) The reflection mode of FBG, (b) The transmission mode of FBG, and (c) The consequent spectrum.

some portions of signals are also reflected by the FBG and become crosstalk elements. Sidelobe suppression ratio of an FBG is directly related to the amount of crosstalk in the transmission mode. The consequent spectrum after these imperfect reflection or transmission of signals can be conceptually described in Figure 4.7(c), where the spectrum of the crosstalk element is superimposed on the signal spectrum [10]. Theoretically, the isolation of FBGs for adjacent and nonadjacent channels is quite different, and it decreases significantly as the channel moves further away from the Bragg wavelength. However, the reflection spectra of practical FBGs are not good as shown in Figure 4.8. Some peak sidelobes may occur at the random position of FBGs spectra due to imperfect fabrication. Thus, here, we consider the highest sidelobe as the isolation of FBGs for both adjacent and nonadjacent channels i.e. the worst case is considered.

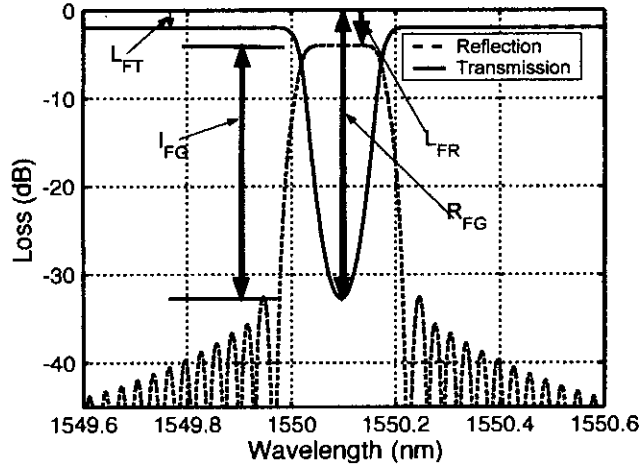


Figure 4.8: Transmission and reflection spectra of FBGs. (L_{FT} : Transmission loss outside the Bragg wavelength, L_{FR} : Reflection loss at the Bragg wavelength, R_{FG} : Reflectivity at the Bragg wavelength, I_{FG} : Isolation of FBGs).

4.4 Analysis of Intraband Crosstalk in BOXCs

We shall now analyze the crosstalk of the proposed BOXCs. We will focus on the BOXCs structure in Figure 4.6. We will assume that fixed FBGs are used to remove the RB noise. In the crosstalk analysis, we will ignore the insertion loss of the BOXC and only the first-order crosstalk fields that arise in the BOXC are considered, since the higher-order crosstalk fields are very weak and hence can be ignored. In the following discussion, we use λ_{2n-1} and λ_{2n} ($n = 1, 2, \dots, m$) to denote the main WDM channels with odd and even wavelength numbers, respectively, λ'_{2n-1} and λ'_{2n} to denote the corresponding crosstalk channels with the same odd and even wavelength numbers as the main WDM channels, respectively. With reference to Figure 4.6(a), let $\text{FBG}_{x,y}$ denote an FBG with Bragg wavelength y in FBG Set x . Considering a signal at wavelength λ_{2n-1} (its position number is n) that enters at port I and exits at port IV of the BOXC (i.e., the signal is in the cross state), due to imperfect FBG fabrication, a small portion of the λ_{2n-1} signal will be reflected by each of the $(n-1)$ FBGs in fixed FBG Set A_2 that are placed before the $\text{FBG}_{A_2, \lambda_{2n-1}}$ where the main signal is reflected, resulting in $(n-1)$ crosstalk fields. Since these $(n-1)$ crosstalk fields come from the same light source λ_{2n-1} , their phases are correlated with the main signal and are referred to as coherent crosstalk.

Similarly, a small portion of the signal at λ'_{2n-1} that enters at port II and exits at port III will be reflected by each of the m FBGs in tunable FBG Set A_1 when the λ'_{2n-1} signal passes through the tunable FBG Set A_1 , giving rise to m crosstalk fields, which will also combine with the main signal λ_{2n-1} . Since these m crosstalk come from another light source λ'_{2n-1} , their phases are not related with the main signal λ_{2n-1} and are referred to as incoherent crosstalk, but their phases are correlated with themselves because they are from the same light source λ'_{2n-1} .

As in the above discussion, for a signal at wavelength λ_{2n-1} that enters at port I and exits at port III of the BOXC (i.e., the signal is in the bar state), a small portion of the λ_{2n-1} signal will be reflected by each of the $(n-1)$ FBGs in fixed FBG Set A_2 that are placed before the $FBG_{A2, \lambda_{2n-1}}$ where the main signal is reflected, generating $(n-1)$ coherent crosstalk fields that will combine with the main signal λ_{2n-1} . Similarly, a small portion of the λ_{2n-1} signal will be reflected by each of the $(m-n)$ FBGs in tunable FBG Set A_1 that are placed before the $FBG_{A1, \lambda_{2n-1}}$ where the main signal is reflected, giving rise to $(m-n)$ coherent crosstalk fields that will also combine with the main signal λ_{2n-1} . In addition, a small portion of the signal λ'_{2n-1} that enters at port II and exits at port IV will leak through tunable FBG Set A_1 , generating one incoherent crosstalk field that will also combine with the main signal λ_{2n-1} .

Table 4.1 and 4.2 list the number of coherent and incoherent crosstalk fields that are generated in the 2×2 BOXC and combined with the main signal λ_{2n-1} for the bar and cross states, respectively, where m is the number of channels entering the BOXC for each

TABLE 4.1
NUMBER OF CROSSTALK FIELDS GENERATED IN THE 2×2 BOXC
AND COMBINED WITH THE MAIN SIGNAL λ_{2n-1}
FOR THE BAR STATE (PORT I TO PORT III)

Crosstalk Type	Light Source	Number of Crosstalk
Coherent Crosstalk	λ_{2n-1}	$n - 1$
		$m - n$
Incoherent Crosstalk	λ'_{2n-1}	1

TABLE 4.2
 NUMBER OF CROSSTALK FIELDS GENERATED IN THE 2×2 BOX
 AND COMBINED WITH THE MAIN SIGNAL λ_{2n-1}
 FOR THE CROSS STATE (PORT I TO PORT IV)

Crosstalk Type	Light Source	Number of Crosstalk
Coherent Crosstalk	λ_{2n-1}	$n - 1$
Incoherent Crosstalk	λ'_{2n-1}	m

TABLE 4.3
 NUMBER OF CROSSTALK FIELDS GENERATED IN THE 4×4 BOX
 AND COMBINED WITH THE MAIN SIGNAL λ_{2n-1}
 FOR THE BAR STATE (PORT I TO PORT V)

Crosstalk Type	Light Source	Number of Crosstalk
Coherent Crosstalk	λ_{2n-1}	$m - n$
		$n - 1$
		$n - 1$
		$m - n$
Incoherent Crosstalk	λ'_{2n-1}	1
		1
	λ''_{2n-1}	1
	λ'''_{2n-1}	0

TABLE 4.4
 NUMBER OF CROSSTALK FIELDS GENERATED IN THE 4×4 BOX
 AND COMBINED WITH THE MAIN SIGNAL λ_{2n-1}
 FOR THE CROSS STATE (PORT I TO PORT VI)

Crosstalk Type	Light Source	Number of Crosstalk	
Coherent Crosstalk	λ_{2n-1}	$m - n$	$m - n$
		$n - 1$	$m - n$
		$n - 1$	$n - 1$
Incoherent Crosstalk	λ'_{2n-1}	1	m
		m	1
	λ''_{2n-1}	1	1
	λ'''_{2n-1}	0	0

TABLE 4.5
 NUMBER OF CROSSTALK FIELDS GENERATED IN THE 4×4 BOXC
 AND COMBINED WITH THE MAIN SIGNAL λ_{2n-1}
 FOR THE CROSS STATE (PORT I TO PORT VII)

Crosstalk Type	Light Source	Number of Crosstalk	
Coherent Crosstalk	λ_{2n-1}	$m-n$	$m-n$
			$n-1$
			$n-1$
Incoherent Crosstalk	λ'_{2n-1}	m	1
		m	1
	λ''_{2n-1}	m	m
	λ'''_{2n-1}	0	0

TABLE 4.6
 NUMBER OF CROSSTALK FIELDS GENERATED IN THE 4×4 BOXC
 AND COMBINED WITH THE MAIN SIGNAL λ_{2n-1}
 FOR THE CROSS STATE (PORT I TO PORT VIII)

Crosstalk Type	Light Source	Number of Crosstalk	
Coherent Crosstalk	λ_{2n-1}	$m-n$	$m-n$
		$n-1$	$m-n$
Incoherent Crosstalk	λ'_{2n-1}	1	m
		m	1
	λ''_{2n-1}	m	m
	λ'''_{2n-1}	0	0

direction and n is the position number of each channel. Since the BOXC symmetric for is both directions, each row in Tables 4.1 and 4.2 is also applicable to the main signal with the even wavelength number λ_{2n} .

Similarly, we analyzed the 4×4 BOXC of Figure 4.6(b). We use λ_{2n-1} and λ_{2n} ($n = 1, 2, \dots, m$) to denote the main WDM channels with odd and even wavelength numbers, respectively, λ'_{2n-1} and λ'_{2n} , λ''_{2n-1} and λ''_{2n} , λ'''_{2n-1} and λ'''_{2n} ($n = 1, 2, \dots, m$) to denote the corresponding crosstalk channels with the same odd and even wavelength numbers as the main WDM channels, respectively. Tables 4.3, 4.4, 4.5 and 4.6 lists the number of

coherent and incoherent crosstalk fields are generated in the 4×4 BOXC and combined with main signal λ_{2n-1} for the bar and cross state, respectively, where m is the number of channels entering the BOXC for each direction and n is the position number of each channel. Since the BOXC is symmetric for both directions, each row in Tables 4.3, 4.4, 4.5 and 4.6 is also applicable to the main signal with the even wavelength number λ_{2n} . In the last column of Tables 4.4, 4.5 and 4.6 has two sub-column for the number of crosstalk which will combined with main signal λ_{2n-1} may follow either of the two paths to reach the destination port either of VI or VII or VIII during the cross state of the 4×4 BOXC.

The electrical field of the main signal after passing through the proposed BOXC can be written as

$$\vec{E}_s(t) = \sqrt{P_s b_s(t)} \exp[j(\omega_s t + \phi_s(t))] \vec{e}_s \quad (4.1)$$

If there are N_1 coherent crosstalk fields and N_2 incoherent crosstalk fields, they each can be written as

$$\vec{E}_k(t) = \sqrt{X_k P_s b_k(t)} \exp[j(\omega_k t + \phi_k(t))] \vec{e}_k \quad (4.2)$$

$k = 1, 2, 3, \dots, N_1$

$$\vec{E}_l(t) = \sqrt{X_l P_s b_l(t)} \exp[j(\omega_l t + \phi_l(t))] \vec{e}_l \quad (4.3)$$

$l = 1, 2, 3, \dots, N_2$

where all fields have the same nominal optical frequency ω , $\phi(t)$ represents the independent phase fluctuations of each optical source, P_s is the optical power of the main signal, and X_k and X_l are the power ratio of each coherent and incoherent crosstalk field relative to the power of the main signal ($X = P_x/P_s$), P_x is the crosstalk power, $b(t)$ is the binary symbols forming the ON-OFF keying (OOK) message where $b(t) \in \{r, 1\}$ ($0 < r < 1$), with r accounting for the extinction ratio, e_s, e_k, e_l are the unit polarization vectors of the main signal, coherent and incoherent crosstalk fields, respectively.

The resulting field E_{total} is given by the vector addition of the all individual crosstalk fields

$$\begin{aligned}
E_{total}(t) &= \vec{E}_s(t) + \sum_{k=1}^{N_1} \vec{E}_k(t) + \sum_{l=1}^{N_2} \vec{E}_l(t) \\
&= \sqrt{P_s b_s(t)} \exp[j(\omega_s t + \phi_s(t))] \vec{e}_s \\
&\quad + \sqrt{X_k P_s b_k(t)} \exp[j(\omega_k t + \phi_k(t))] \vec{e}_k \\
&\quad + \sqrt{X_l P_s b_l(t)} \exp[j(\omega_l t + \phi_l(t))] \vec{e}_l
\end{aligned} \tag{4.4}$$

Following square-law detection on a photodiode, the total photocurrent $I_1(t)$ is proportional to

$$\begin{aligned}
I_1(t) &\propto [E_{total}(t)]^2 \\
&\propto P_s \left[b_s(t) + \sum_{k=1}^{N_1} X_k b_k(t) + \sum_{l=1}^{N_2} X_l b_l(t) \right. \\
&\quad + 2 \sum_{k=1}^{N_1} \sqrt{X_k b_s(t) b_k(t)} \cos\{(\omega - \omega_k)t + \phi_s(t) - \phi_k(t)\} \vec{e}_s \times \vec{e}_k \\
&\quad + 2 \sum_{k=1}^{N_1} \sum_{l=1}^{k-1} \sqrt{X_k X_l b_k(t) b_l(t)} \cos\{(\omega_k - \omega_l)t + \phi_k(t) - \phi_l(t)\} \vec{e}_k \times \vec{e}_l \\
&\quad + 2 \sum_{l=1}^{N_2} \sqrt{X_l b_s(t) b_l(t)} \cos\{(\omega - \omega_l)t + \phi_s(t) - \phi_l(t)\} \vec{e}_s \times \vec{e}_l \\
&\quad \left. + 2 \sum_{l=1}^{N_2} \sum_{m=1}^{l-1} \sqrt{X_l b_l(t) b_m(t)} \cos\{(\omega_l - \omega_m)t + \Delta\phi_l(t)\} \vec{e}_l \times \vec{e}_m \right]
\end{aligned} \tag{4.5}$$

Since the main signal, all coherent and incoherent crosstalk come from same wavelength of sources, therefore, we can write

$$\omega = \omega_k = \omega_l = \omega_m$$

So, equation (4.5) can be expressed as

$$\begin{aligned}
I_1(t) \propto P_s \left[& b_s(t) + \sum_{k=1}^{N_1} X_k b_k(t) + \sum_{l=1}^{N_2} X_l b_l(t) \right. \\
& + 2 \sum_{k=1}^{N_1} \sqrt{X_k b_s(t) b_k(t)} \cos\{\omega t + \phi_s(t) - \phi_k(t)\} \vec{e}_s \times \vec{e}_k \\
& + 2 \sum_{k=1}^{N_1} \sum_{l=1}^{k-1} \sqrt{X_k X_l b_k(t) b_l(t)} \cos\{\omega t + \phi_k(t) - \phi_l(t)\} \vec{e}_k \times \vec{e}_l \\
& + 2 \sum_{l=1}^{N_2} \sqrt{X_l b_s(t) b_l(t)} \cos\{\omega t + \phi_s(t) - \phi_l(t)\} \vec{e}_s \times \vec{e}_l \\
& \left. + 2 \sum_{l=1}^{N_2} \sum_{m=1}^{l-1} \sqrt{X_l b_l(t) b_m(t)} \cos\{\omega t + \Delta\phi_l(t)\} \vec{e}_l \times \vec{e}_m \right] \quad (4.6)
\end{aligned}$$

It can be seen from the equation (4.6) that the photocurrent is composed of the following seven components:

- 1) the data signal;
- 2) an additive coherent crosstalk signal;
- 3) an additive incoherent crosstalk signal;
- 4) a beat term that exhibits between signal and coherent crosstalk dependence on relation between the time of optical propagation delay and duration of one message bit;
- 5) a beat term that exhibits between coherent and incoherent crosstalk;
- 6) a beat term between signal and incoherent crosstalk dependence on the phase difference;
- 7) a beat term between incoherent crosstalk.

The effect of crosstalk-crosstalk beating has been assumed to be negligible. All fields considered here are assumed to have co-polarized, represents the worst situation, giving the maximum crosstalk, causing the maximum BER degradation, and that all crosstalk products fall within the receiver bandwidth.



Following this assumption, considering normalized responsivity, the photocurrent can be expressed as

$$I_1(t) = P_s \left[b_s(t) + 2 \sum_{k=1}^{N_1} \sqrt{X_k b_s(t) b_k(t)} \cos\{\omega t + \phi_s(t) - \phi_k(t)\} \right. \\ \left. + 2 \sum_{l=1}^{N_2} \sqrt{X_l b_s(t) b_l(t)} \cos\{\omega t + \phi_s(t) - \phi_l(t)\} \right] \quad (4.7)$$

Since all coherent crosstalk come from same laser source, we can assume here that

$$\phi_s(t) = \phi_k(t)$$

Therefore equation (4.7) can be written as

$$I_1(t) = P_s \left[b_s(t) + 2 \sum_{k=1}^{N_1} \sqrt{X_k b_s(t) b_k(t)} \cos\{\omega t + \phi_s(t)\} \right. \\ \left. + 2 \sum_{l=1}^{N_2} \sqrt{X_l b_s(t) b_l(t)} \cos\{\omega t + \phi_d(t)\} \right] \quad (4.8)$$

where phase difference, $\phi_d(t) = \phi_s(t) - \phi_l(t)$ between the phase of the optical data signal and phase of the optical l th incoherent crosstalk at time t is represented by a uniform random variable distributed in $[0; 2\pi]$.

If the BOXC is not an integrated one but equipped with individual components, the optical path length difference between the main signal and coherent crosstalk may exceed the length of one bit period. Assuming the optical propagation delay (τ) is less than the coherence time (τ_c) of laser ($\tau < \tau_c$) but greater than of one bit duration (T) i.e. $\tau > T$ the second term in equation (4.7), $b_s(t)$ is incorrelated with $b_k(t)$ though they are come from same laser source.

Therefore, the second term in equation (4.8) is time-variant and cause noise to the signal. This noise power caused by coherent crosstalk is given by [2], [7]

$$\sigma_{co}^2 = \sum_{k=1}^{N_1} X_k P_s^2 \quad (4.9)$$

The third term of equation (4.8) represents signal-incoherent crosstalk beat term which is much more dominant and the noise power of this beat term can be expressed by [2], [7]

$$\sigma_{ico}^2 = \sum_{l=1}^{N_2} X_l P_s^2 \quad (4.10)$$

The total linear crosstalk noise variance which only present when both signal and crosstalk at carrying a data "1" is

$$\begin{aligned} \sigma_X^2 &= \sigma_{co}^2 + \sigma_{ico}^2 \\ &= \sum_{k=1}^{N_1} X_k P_s^2 + \sum_{l=1}^{N_2} X_l P_s^2 \\ &= N_1 X_k P_s^2 + N_2 X_l P_s^2 \end{aligned} \quad (4.11)$$

In FBG-OC-based BOXC, there are two types of crosstalk occurred in FBGs. Since the reflectivity of an FBG at Bragg-wavelength is usually less than 100% even at center of reflection bandwidth, small portions of signals are leaked and become crosstalk elements. Similarly, in the transmission mode of FBG, due to imperfect transmissivity, some portions of signals are also reflected outside Bragg-wavelength and become crosstalk elements [7].

We generally observed in our proposed BOXCs at bar-state that all inband coherent crosstalk from same laser source occurs due to the transmission mode of FBGs and at the same time all inband incoherent crosstalk from different laser sources occurs due to the reflection mode of FBGs. In the cross-state of considered BOXCs, all inband coherent crosstalk from same laser source and incoherent crosstalk from different sources occur only due to the transmission mode of FBGs. Rearranging FBGs transmission and reflection mode crosstalk with coherent and incoherent crosstalk in the equation (4.11), we can express the total component crosstalk noise power as

$$\begin{aligned} \sigma_X^2 &= \sigma_{re}^2 + \sigma_{tx}^2 \\ &= N_1 X_{kr} P_s^2 + N_2 X_{lt} P_s^2 \end{aligned} \quad (4.12)$$

107558

where X_{kr} and X_{lt} are the crosstalk coefficient of FBG during transmission and reflection mode, respectively.

For simplicity assuming FBGs transmission and reflection mode crosstalk are equal i.e. $X_{kr} = X_{lt} = X_F$ therefore, equation (4.12) can be express as

$$\sigma_x^2 = (N_1 + N_2)X_F P_s^2 \quad (4.13)$$

In a general bidirectional transmission system, unwanted backscattering such as Rayleigh-backscattering (RB) is generated by signals in both directions due to the inherent density fluctuations in the fiber core. Optical reflections will also be produced by fiber connectors and splices in the transmission path. In our proposed BOXC, although unwanted backscattered signals can be slightly removed by the fixed FBGs with light absorber, therefore, the noise power of the inband coherent crosstalk level due to RB can be calculated as [9]

$$\sigma_R^2 = X_R P_s^2 \quad (4.14)$$

where $X_R = G^2 R^2$, X_R is backscattering-induced crosstalk coefficient, G is the gain of the bidirectional amplifier and R is the RB level.

4.5 Expression of Bit-Error Rate

The performance of an optical communication system is judged by the bit-error rate, defined as the probability of incorrect identification of a bit by the decision circuit of the receiver. Most optical communication systems require BER to be $< 10^{-9}$. The BER depends on the signal-to-noise ratio (SNR) of the current generated at the receiver when an optical bit stream is converted into the electrical domain. The SNR, in turn, depends on various noise mechanisms such as shot noise, thermal noise, and ASE noise associated with the received signal.

The fluctuating electrical signal due to noise at the receiver is passed to the decision circuit, which samples it periodically at the bit rate to determine individual bits. The

sampled value I fluctuates from bit to bit around an average value I_1 or I_0 , depending on whether the bit corresponds to 1 or 0 in the bit stream. The decision circuit compares the sampled value with a threshold value I_D and calls it bit 1 if $I > I_D$ and bit 0 if $I < I_D$. An error occurs if $I < I_D$ for 1 bits because of receiver noise. An error also occurs if $I > I_D$ for 0 bits. Let P_{err1} and P_{err0} be the BER when the main signal is data “1” and “0”, respectively. Therefore the BER is obtained by combining all of the probability of error terms given by [8-9]

$$\begin{aligned}
 BER &= \frac{1}{2}(P_{err1} + P_{err0}) \\
 &= \frac{1}{2} \left\{ \frac{1}{2} \operatorname{erfc} \left(\frac{1}{\sqrt{2}} \frac{I_1 - I_D}{\sigma_1} \right) + \frac{1}{2} \operatorname{erfc} \left(\frac{1}{\sqrt{2}} \frac{I_D - I_0}{\sigma_{th}} \right) \right\} \quad (4.15)
 \end{aligned}$$

This rate depends on the decision threshold I_D . I_1 is the photocurrent of binary “1” and I_0 is the photocurrent of binary “0”. Generally, the decision threshold is chosen to minimize the bit-error-rate. In our analysis fixed decision threshold chosen for maximum BER which is

$$I_D = \frac{I_1}{2}$$

Assuming infinite extinction ratio ($r = \infty$), $I_0 = 0$, therefore, equation (4.15) can be approximately written as

$$BER \cong \frac{1}{2} \operatorname{erfc} \left(\frac{1}{2\sqrt{2}} \frac{I_1}{\sigma_1} \right) \quad (4.16)$$

4.6 Impact of Intraband Crosstalk induced by BOXC on BER

Intraband crosstalk induced by FBGs operation in BOXC is analyzed in section 4.4. Various kinds of modeling of signal-crosstalk beating noise have been proposed [2], as an attempt to estimate the effects of noise on optical transmission systems. Among them, the Gaussian approximation model is generally accepted as one of the most realistic ones,

and its theoretical and experimental verifications can be found in several prior works [7-9]. In the Gaussian approximation model, the probability density function (PDF) of the signal crosstalk beat noise is approximated as Gaussian.

It is assumed that “0” and “1” bits appear with equal likelihood and that all crosstalk terms are of equal power. Although the Gaussian approximation overestimates the homodyne crosstalk effect, as the number of crosstalk elements grows, the PDF of the signal power mixed with the multiple crosstalk elements gradually becomes Gaussian. Considering intensity modulation/direct detection (IM/DD) system and assuming both the beat noise and receiver noise have Gaussian probability density distribution according to central limit theorem [7].

In the presence of linear homodyne crosstalk induced in BOXC, backscattering-induced crosstalk in BOXC and receiver thermal and shot noises, the total noise power of the receiver is given by [7-8]

$$\sigma_1 = \sqrt{\sigma_0^2 + \sigma_X^2 + \sigma_R^2} \quad (4.17)$$

where σ_0^2 represents the thermal and shot noise power, σ_X^2 is the crosstalk noise power, and σ_R^2 is the backscattering-induced crosstalk noise power, respectively.

The thermal and shot noise power of the receiver are given by

$$\begin{aligned} \sigma_0^2 &= \sigma_{th}^2 + \sigma_s^2 \\ &= \frac{4kT}{R_L} B_e + 2eP_s B_e \end{aligned} \quad (4.18)$$

where k is the Boltzman constant (1.380658×10^{-23}), T is the Temperature in Kelvin, R_L is receiver load resistance in ohm, e is electron charge (1.603×10^{-19}) in Coulomb and B_e is the receiver bandwidth in Hz.

Since the photodetector current is proportional the optical power incident on it ($I_1=R_dP_s$) and assuming unit responsivity ($R_d = 1$) of photodiode, equation (4.16) can be expressed as

$$BER \cong \frac{1}{2} \operatorname{erfc} \left(\frac{1}{2\sqrt{2}} \frac{P_s}{\sigma_1} \right) \quad (4.19)$$

where P_s is the optical power of the main signal and σ_1 denotes the total noise power of the receiver.

4.6.1 PP due to Intraband Crosstalk induced by BOXC

In our proposed BOXCs, signals are reflected or transmitted by a number of FBGs and due to imperfect fabrication of FBGs a number of crosstalk elements are produced inside the BOXCs. During these operations, these crosstalk elements are added to the main signal. The amount of crosstalk is determined by the reflection and transmission characteristics of FBG employed in BOXC. The impact of the crosstalk in a WDM system may be quantified by considering the crosstalk PP. The crosstalk PP is defined as the additional power (in dB) needed for the signal to achieve the same BER as that without crosstalk [10]. We consider here an IM/DD system.

We assume here the case for high speed systems whose receiver bandwidths are wider than the signal-crosstalk beat noise spectrum. In equation (4.8), $b_i(t)$ is not synchronous with $b_s(t)$, we take the average of the integrations of $b_i(t)$ in bit periods to be 0.5. When $b_i(t) = 0$ and the lasers have infinite extinction ratio, there is no noise. With the fixed decision-threshold setting and assuming that all crosstalk elements of same optical power are mixed with the signal, the system PP is given by [7]

$$PP = -5 \log_{10} \left[1 - 4 \{ (N_1 + N_2) X_F + X_R \} Q^2 \right] (dB) \quad (4.20)$$

where X_F and X_R are the crosstalk coefficients of FBG and RB, and Q is the Q factor where $Q = 6$ at bit-error-rate (BER) of 10^{-9} [7].

4.6.2 BER and PP due to Optical Amplifier

Impact of crosstalk induced in BOXC on BER without considering amplifier in a WDM system has been discussed in section 4.6.1. In this section we will focus on the impact of optically amplified system on the BER and PP. All amplifiers degrade the signal-to-noise of the amplified signal because of spontaneous emission that adds noise to the signal during its amplification. For optically preamplified receivers at nodes in a WDM ring network, and/or long transmission distances through many optical amplifiers, signal-amplified spontaneous emission beat noise will dominate over the thermal receiver noise [13].

To understand the impact of amplifier noise on the detection of the received signal, consider an optical preamplifier system used in front of standard *pin* direct detection receiver. The photodetector produces a current that is proportional to the incident optical power. The signal current is given by [18-19]

$$I_1 = R_d G P_s \quad (4.21)$$

where R_d is responsivity of the photodetector, G denotes the optical amplifier gain and the P_s is the optical power of the main signal.

The photodetector produces a current that is proportional to the optical power. The optical power is proportional to the square of the electric field. Thus the noise field beats against the signal and against itself, giving rise to noise components referred to as the signal-spontaneous beat noise and spontaneous-spontaneous (ASE-ASE) beat noise, respectively. In addition, shot noise and thermal noise components are also present [18].

The variances of the thermal noise, shot-noise, signal-spontaneous beat noise, and spontaneous-spontaneous beat noise currents at the receiver are, respectively [15], [18-19],

$$\sigma_{th}^2 = \frac{4kT}{R_L} F_n B_e \quad (4.22)$$

$$\sigma_s^2 = 2eR_d [GP_s + n_{sp}hf_c(G-1)B_o]B_e \quad (4.23)$$

$$\sigma_{sig-sp}^2 = 4R_d^2 GP_s n_{sp} hf_c (G-1)B_e \quad (4.24)$$

and

$$\sigma_{sp-sp}^2 = 2R_d^2 [n_{sp}hf_c(G-1)]^2 (2B_o - B_e)B_e \quad (4.25)$$

where F_n is the front-end amplifier noise figure, n_{sp} is spontaneous emission factor, f_c is the carrier frequency, $h = 6.6261 \times 10^{-34}$ is a plank's constant, and B_o is the optical bandwidth.

Therefore, the total noise power of the receiver from equation (4.17) can be written as

$$\sigma_{1A} = \sqrt{\sigma_{th}^2 + \sigma_s^2 + \sigma_X^2 + \sigma_R^2 + \sigma_{sig-sp}^2 + \sigma_{sp-sp}^2} \quad (4.26)$$

Usually the amplifier gain is reasonably large (> 10 dB), the shot-noise and the thermal noise are negligible compared to the signal-spontaneous and spontaneous-spontaneous beat noise. In the bit error rate $< 10^{-9}$, these noise processes can be modeled adequately as Gaussian process. The spontaneous-spontaneous beat noise can be made very small by reducing the optical bandwidth B_o . This can be done by filtering the amplifier noise before it reaches the receiver. In the limit, B_o can be made as small as $2B_e$ which can reduce ASE noise induced by optical amplifier. So the dominant noise component is usually ASE beat noise [18].

Optical amplifiers are often cascaded to overcome losses in a long-haul optical communication system as well as a number of optical preamplifiers is used in a metropolitan ring network where a number of add/drop occurs in multiple nodes. The buildup of amplifier induced ASE noise is accumulates over many amplifiers in multiple nodes. If N_A is total number of amplifiers, the total noise power will be the ASE power multiplied by total number of amplifiers used in that system [19].

Assuming unit responsivity of the photodetector and using equations (4.21) and (4.26), BER of any amplified system can be determined by equation (4.19) and is given by

$$BER \cong \frac{1}{2} \operatorname{erfc} \left(\frac{1}{2\sqrt{2}} \frac{GP_s}{\sigma_{1A}} \right) \quad (4.27)$$

where G is the amplifier gain, P_s is optical power of the main signal, and σ_{1A} is the total amplified noise power of the receiver.

The power penalty occurs due to intraband crosstalk induced in BOXC for non-amplified system already discussed in section 4.6.1. In amplified optical systems, the dominant noise component is usually the signal-ASE beat noise. Mainly PP will be occurred due to this dominant signal-ASE noise power of optical amplifier used in a WDM system regardless of the other noise sources.

4.7 Summary

Theoretical study of intraband crosstalk arises due to FBGs in BOXCs is given in this chapter. How intraband crosstalk induced in BOXCs due to FBGs operation is explained and the total number of coherent and incoherent crosstalk induced in proposed BOXCs is given in tabular form. Detailed analytical expressions for the intraband crosstalk induced in the BOXC are developed. Finally the expression of BER and PP is modified using the effect of intraband crosstalk without and with the present of optical amplifier, respectively.

CHAPTER FIVE

Results and Discussion

In this chapter, BER performance and PP due to intraband crosstalk arises during FBGs operation in BOXCs of WDM system are investigated. BER and PP also investigated due to presence of optical amplifiers in a WDM system. Numerical computations are carried out to evaluate the results of BER and PP and discussion on those results are also presented.

5.1 Impact of Intraband Crosstalk

The detail analysis of intraband crosstalk is described in section 4.4. Figure 4.6 shows the architecture of 2×2 and 4×4 BOXCs and the intraband crosstalk such as coherent and incoherent crosstalk induced due to the FBGs operation in BOXCs is given by the equation (4.11). Due to bidirectional operation of the BOXCs, a backscattering-induced crosstalk is exist which is given by equation (4.13). The effect of intraband crosstalk and backscattering-induced crosstalk on BER is described in section 4.6. PP occurred due to intraband and backscattering-induced crosstalk is described in section 4.6.1. To observe the BER and PP performance of BOXCs, we simulated the equations (4.19) and (4.20) incorporating intraband crosstalk and backscattering-induced crosstalk into these equations.

To evaluate the expression of σ_0 as given by equation (4.18), we assumed $T = 300^0$ K, $k = 1.38 \times 10^{-23}$, $e = 1.603 \times 10^{-19}$, $B_e = 10^9$ Hz, and $R_L = 100 \Omega$. To evaluate the BER and PP, the following system parameters are chosen here: number of channels, $m = 32$, input power, $P_{in} = 0$ dBm, bandwidth, $B_e = 1$ GHz, FBGs crosstalk, $X_F = -20$ dB to -25 dB and backscattering-induced crosstalk, $X_R = -25$ dB. To find the power penalty (PP), we assume $Q = 6$ at $BER = 10^{-9}$, and the component crosstalk, $X_F = -20$ dB to -25 dB.

Figure 5.1 shows the BER against the received power with the different number of wavelength channels in the bar-state of 2×2 and 4×4 BOXCs, respectively. In both configurations, BER increases with the number of wavelength channels increases. It is

observed between these two configurations that more BER found in the 4×4 BOXC than 2×2 BOXC with the same number of wavelength channels.

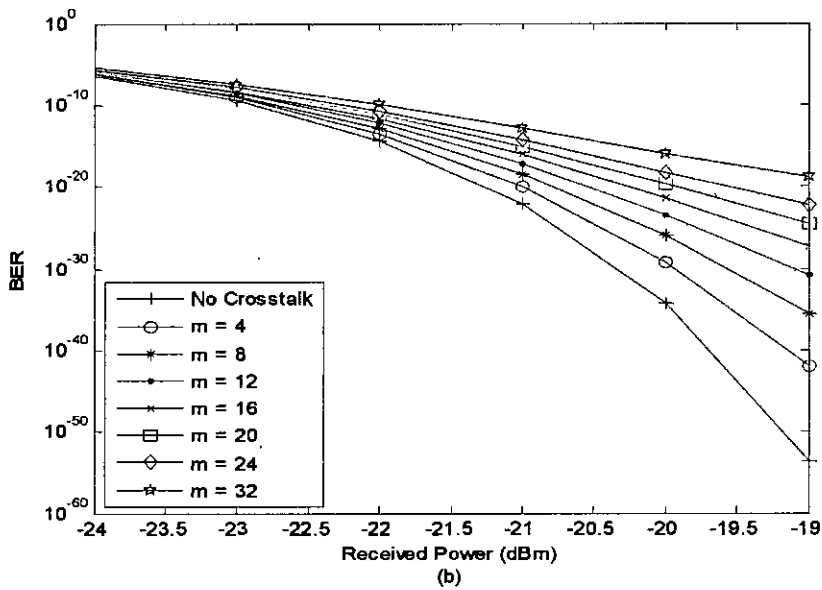
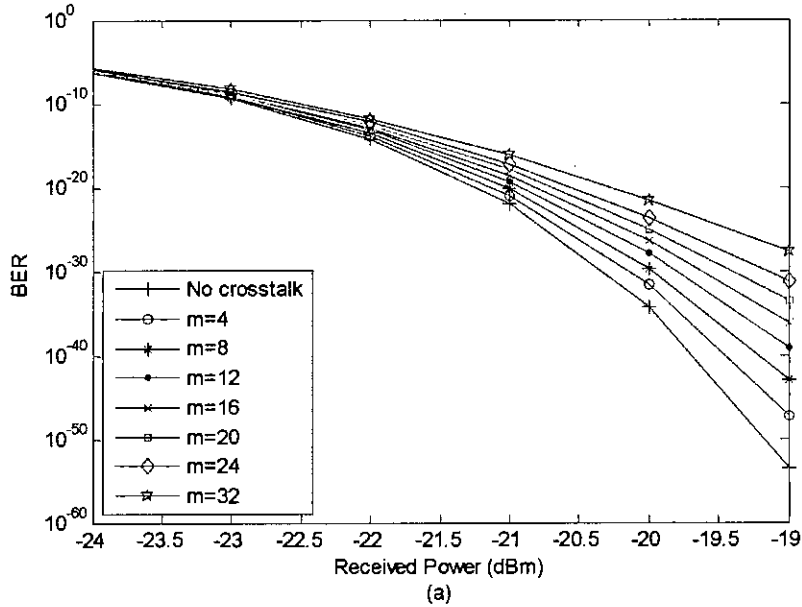


Figure 5.1: BER vs. received power at the bar-state of (a) 2×2 BOXC, and (b) 4×4 BOXC with the different number of wavelength channels, m . Component crosstalk, $X_f = -22$ dB and backscattering-induced crosstalk, $X_R = -25$ dB are assumed.

Figure 5.2 and 5.3 shows the BER against received power for different number of wavelength channels at different component crosstalk for the bar-state of 2×2 and 4×4 BOXCs, respectively. In each plot of Figure 5.2[(a)-(d)] and 5.3[(a)-(d)], number of wavelength channels, m varied from 8 to 32 with an increment of 8 wavelength channels

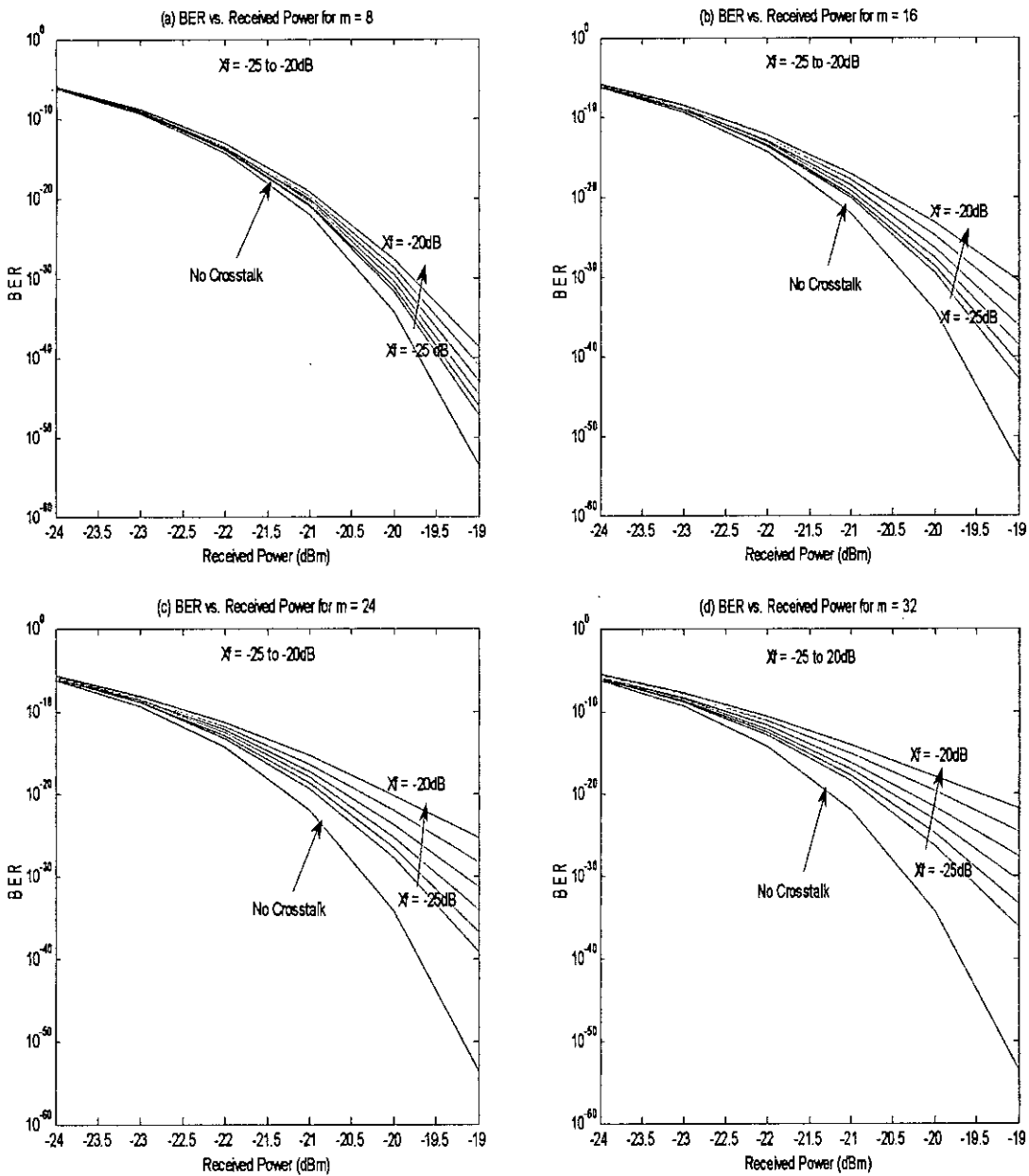


Figure 5.2: BER performance in presence of intraband crosstalk with varying number of wavelength channels, m with different component crosstalk, X_f in the bar-state of 2×2 BOXC. Backscattering-induced crosstalk, $X_R = -25\text{dB}$ is assumed.

per step and it is found that BER is significantly increases not only with the increasing number of wavelength channels but also with the component crosstalk increases.

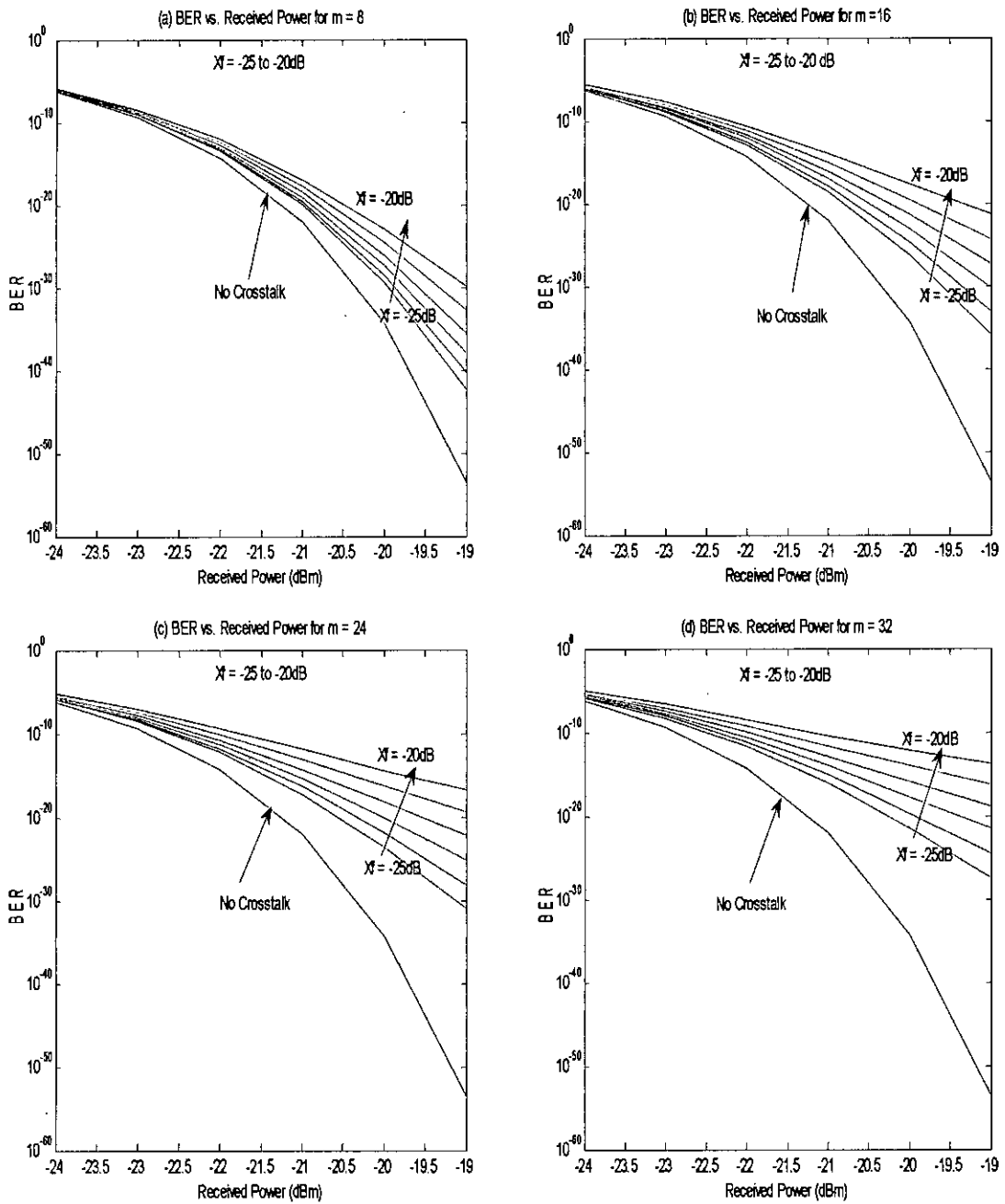


Figure 5.3: BER performance in presence of intraband crosstalk with varying number of wavelength channels, m with different component crosstalk, X_f in the bar-state of 4×4 BOXC. Backscattering-induced crosstalk, $X_R = -25\text{dB}$ is assumed.

Figure 5.4 shows the power penalty as a function the component crosstalk and Figure 5.5 shows the power penalty against different number of wavelength channels at bar-state of 2×2 and 4×4 BOXCs, respectively. We observed in both configurations that power penalty increases with the number of wavelength channels as well as the component crosstalk increases. But more power penalty occurs in 4×4 BOXC than 2×2 BOXC for the same number of wavelength channels as well as for the same amount of component crosstalk.

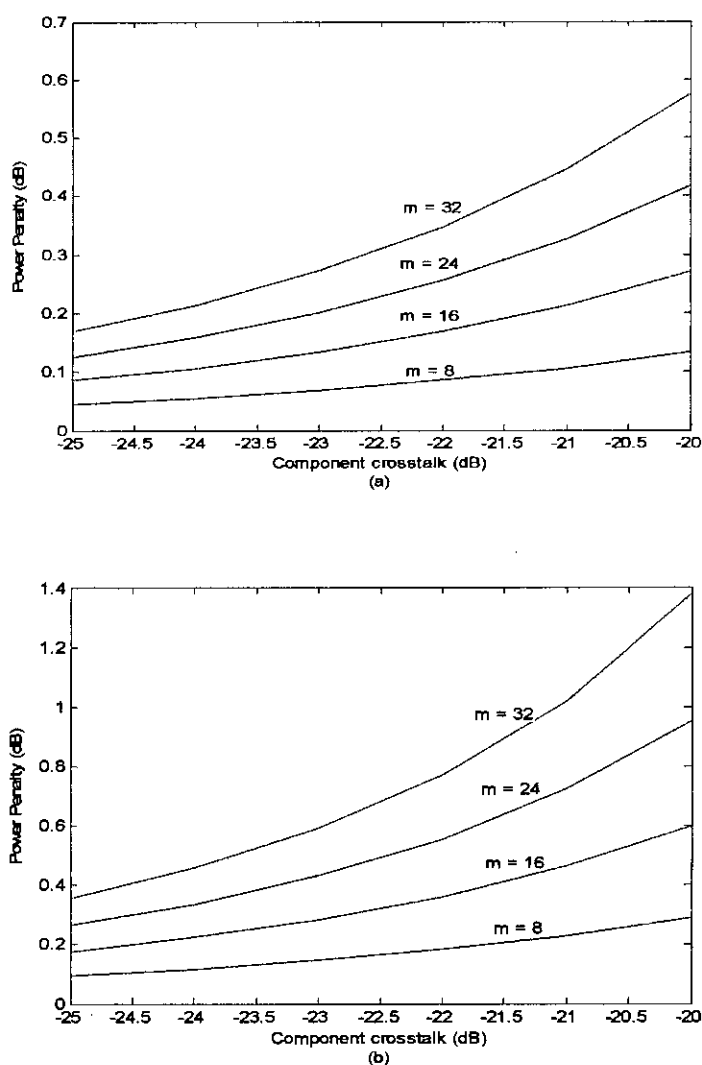


Figure 5.4: Power penalty as a function of component crosstalk at the bar-state of (a) 2×2 BOXC and, (b) 4×4 BOXC with the different number of wavelength channels, m .

BER = 10^{-9} is assumed.

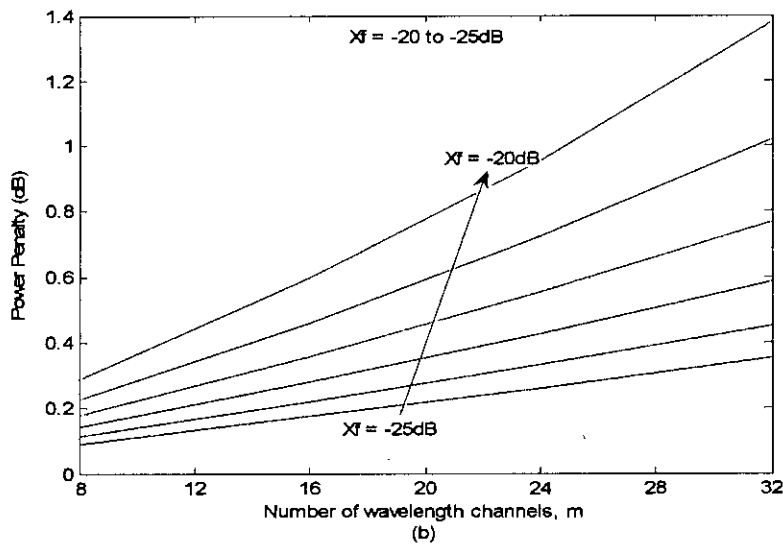
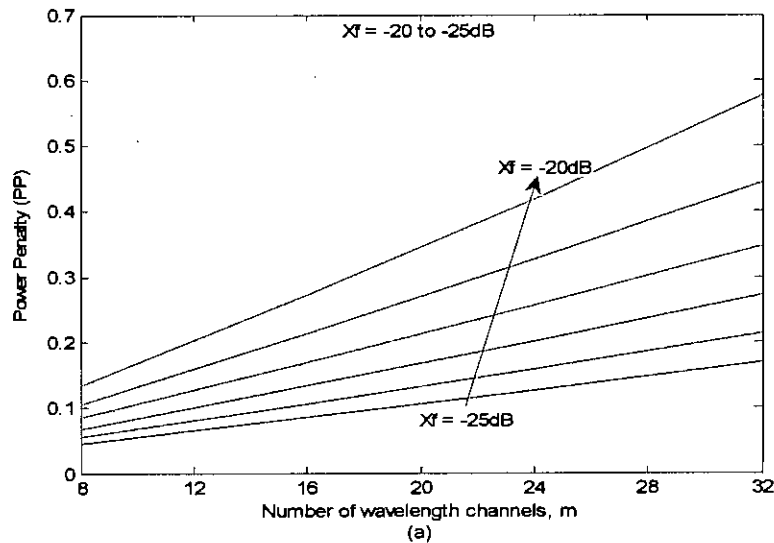


Figure 5.5: Power penalty as a function of wavelength channels, m at the bar-state of (a) 2×2 BOXC and, (b) 4×4 BOXC with the different number of component crosstalk, X_f . BER = 10^{-9} is assumed.

Figure 5.6 shows the BER against the received power with the various positions of the wavelength channels while the number of wavelength channels is fixed in cross-state of 2×2 and 4×4 BOXCs, respectively. It is found in both structures that BER of a channel not only increases with the number of wavelength channels increase but also increases with the position of the wavelength channels. In the bar-state of the BOXCs, we saw that

BER increases only with the number of wavelength channels but not with the positions of the channels. It is also observed that more BER occurs in 4×4 BOXC than 2×2 BOXC with the same position of the wavelength channels.

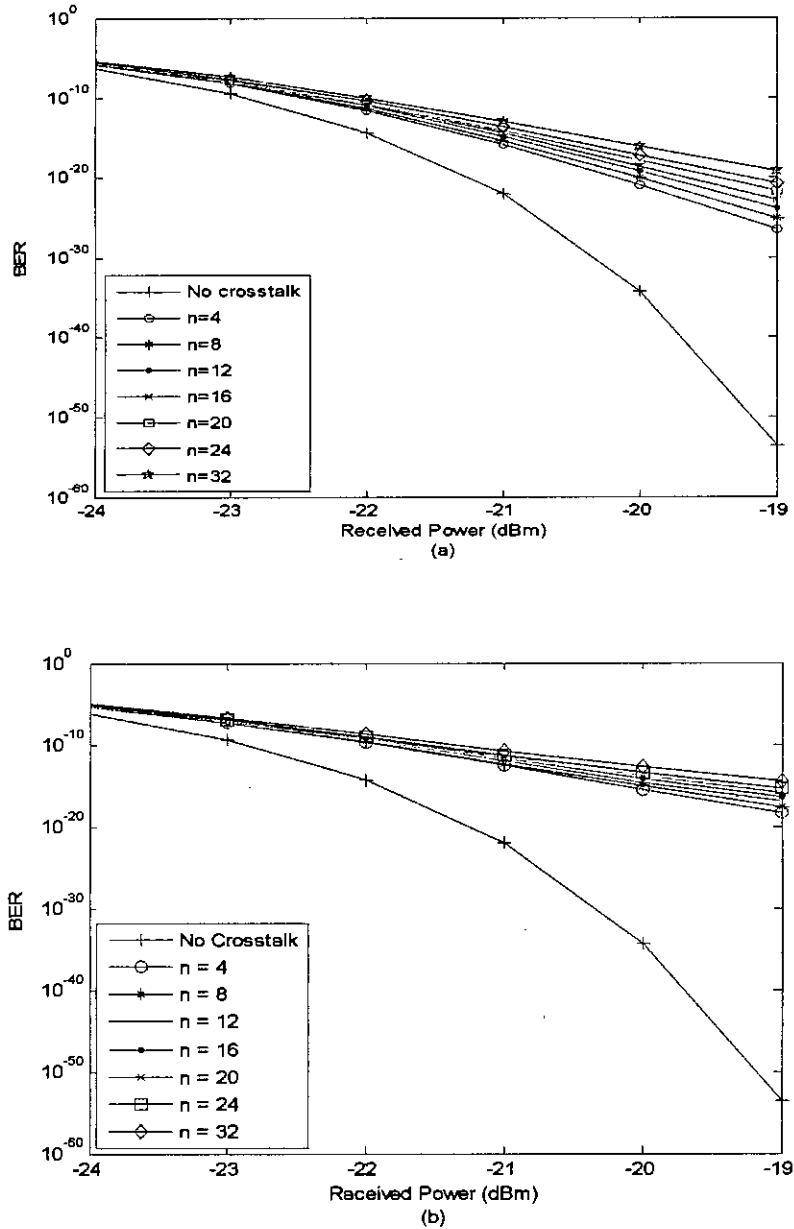


Figure 5.6: BER vs. received power at the cross-state of (a) 2×2 BOXC, and (b) 4×4 BOXC with the various positions, n of the wavelength channels while the number of wavelength channels, $m = 32$, is fixed. Component crosstalk, $X_f = -22$ dB and backscattering-induced crosstalk, $X_R = -25$ dB is assumed.

Figure 5.7 and 5.8 shows the BER as a function of received power for different position of wavelength channels at different component crosstalk for the cross-state of 2×2 BOXC and 4×4 BOXC, respectively. In each plot of Figure 5.7[(a)-(d)] and 5.8[(a)-(d)], positions of the wavelength channels, n varied from 8 to 32 with an increment of 8

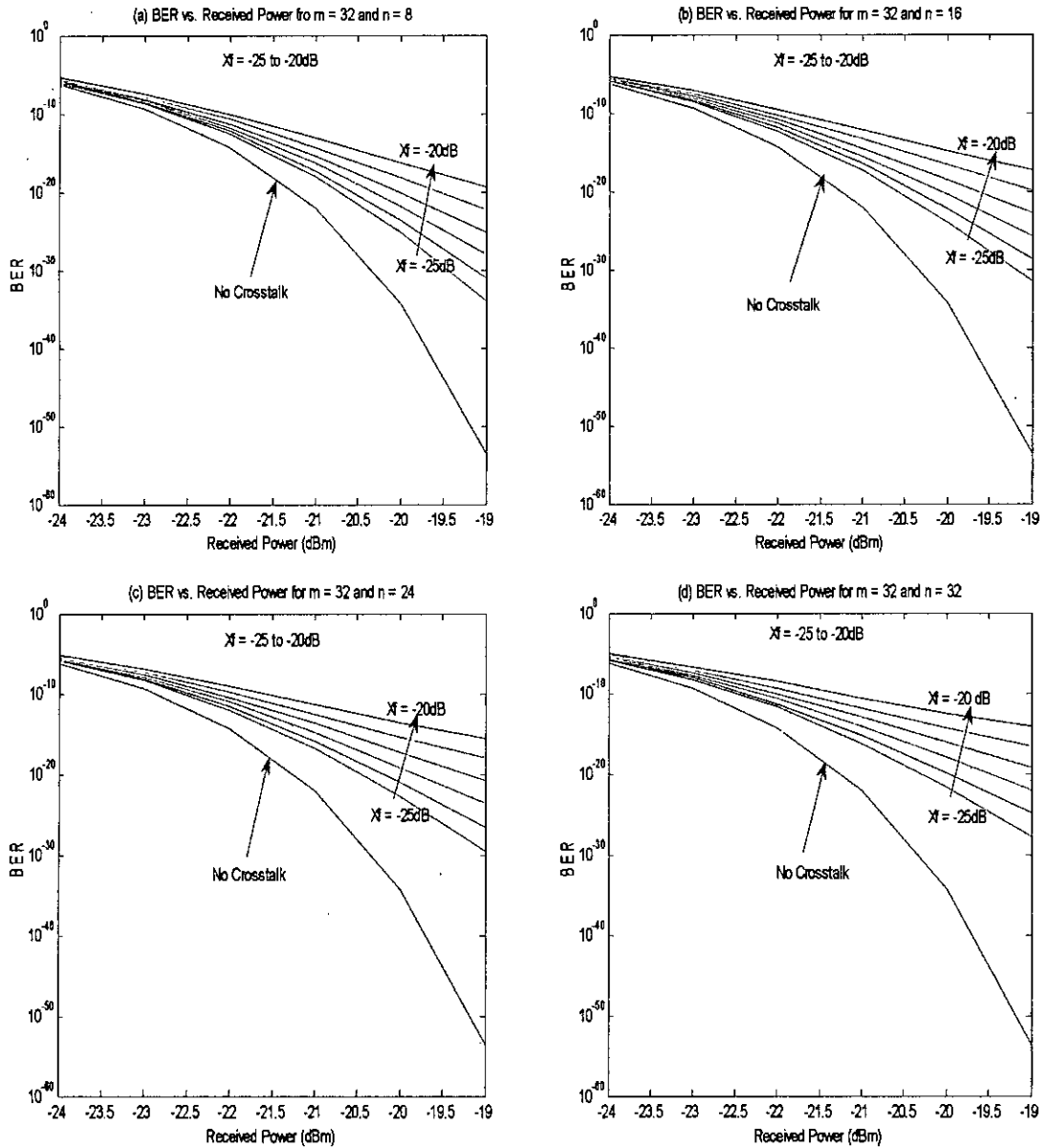


Figure 5.7: BER performance in presence of intraband crosstalk with various position of wavelength channels, n while the total number of wavelength channels, $m = 32$, is fixed with different component crosstalk, X_f in the cross-state of 2×2 BOXC. Backscattering-induced crosstalk, $X_R = -25$ dB is assumed.

wavelength channels per step while the total number of wavelength channels is fixed. Unlike the bar-state of BOXCs, it is found that BER is significantly increases not only with the increasing number of wavelength channels, but also with the position of the wavelength channels increases.

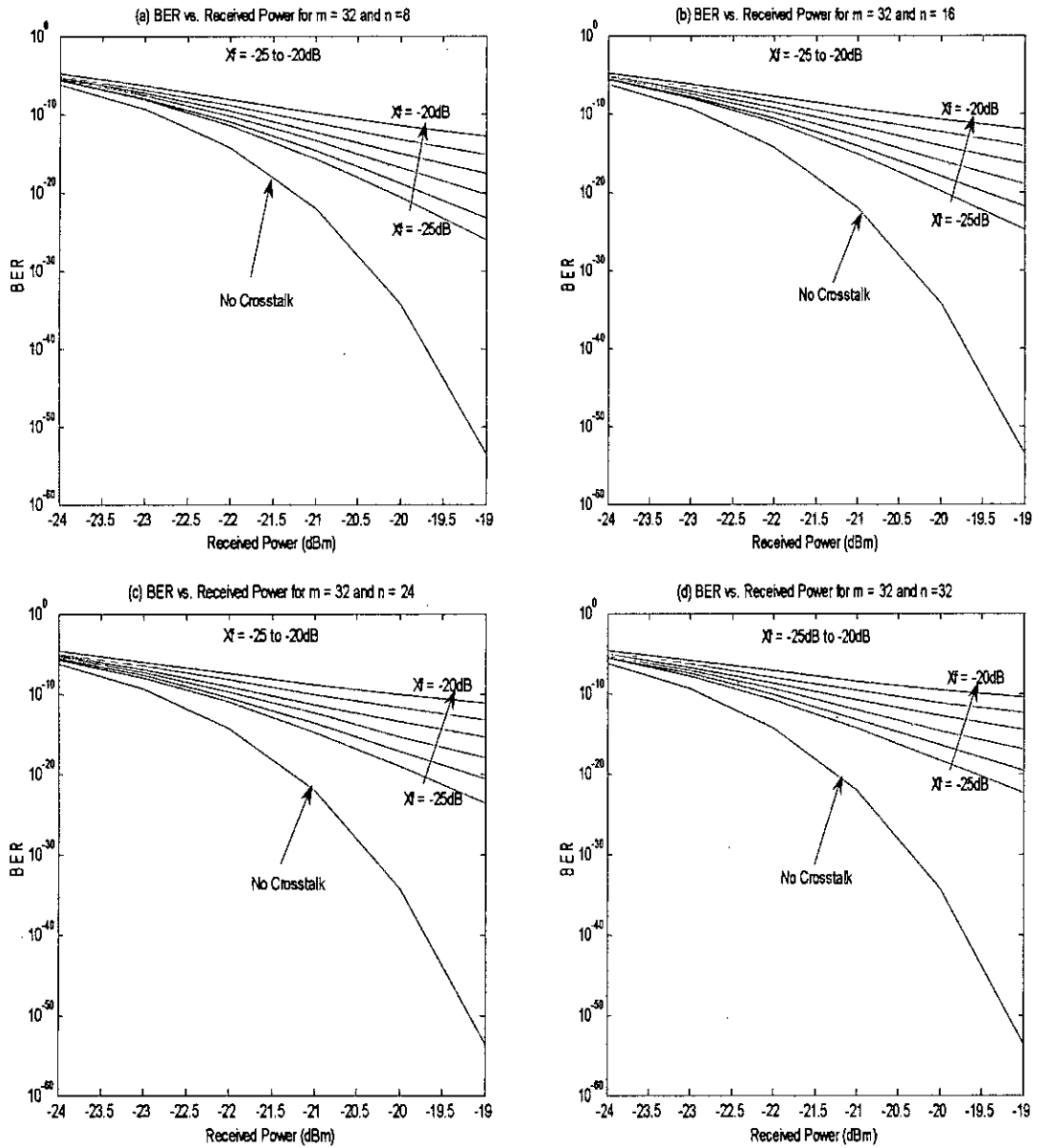


Figure 5.8: BER performance in presence of intraband crosstalk with various position of wavelength channels, n while the total number of wavelength channels, $m = 32$, is fixed with different component crosstalk, X_I in the cross-state of 4×4 BOXC. Backscattering-induced crosstalk, $X_R = -25$ dB is assumed.

Figure 5.9 shows the power penalty against the different component crosstalk and Figure 5.10 shows the power penalty as a function of various positions of the wavelength channels when the total number of wavelength channels is fixed at the cross state of 2×2 BOXC and 4×4 BOXC, respectively. Unlike the bar-state of BOXCs, it is found in both

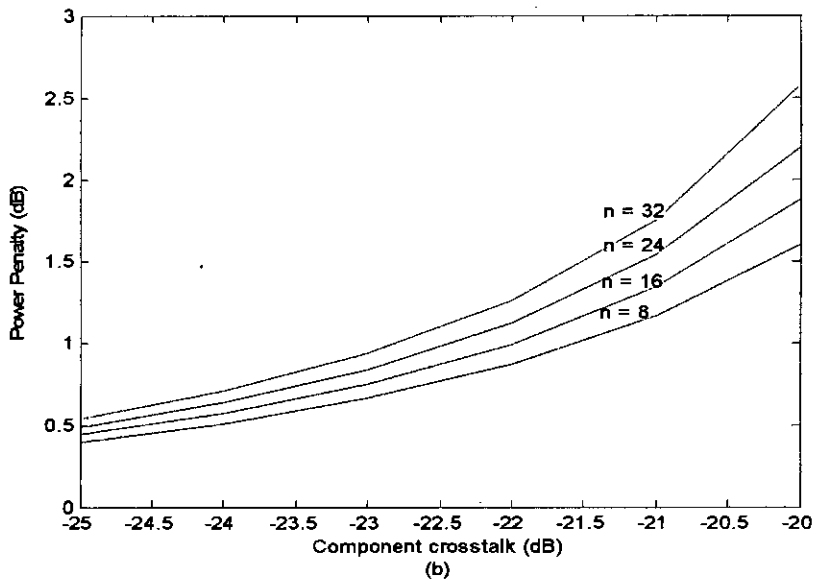
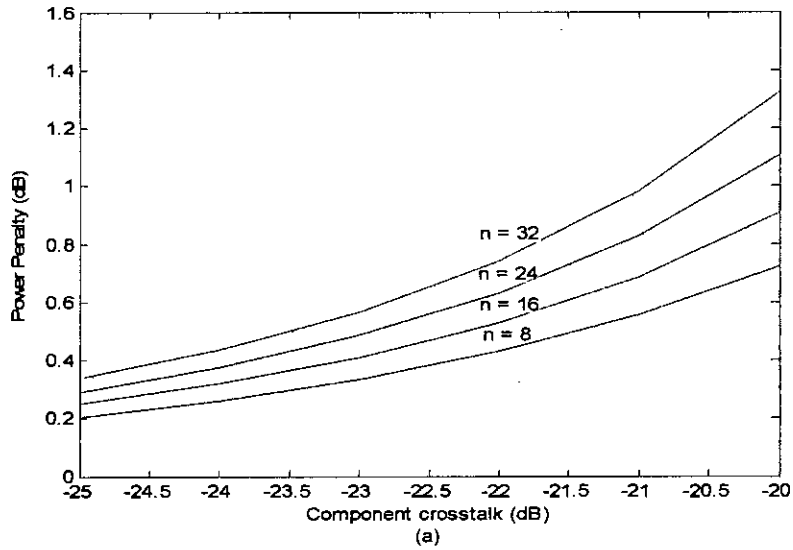


Figure 5.9: Power penalty as a function of component crosstalk at the cross-state of (a) 2×2 BOXC and, (b) 4×4 BOXC with the various positions of the wavelength channels, n while the number of wavelength channels, $m = 32$, is fixed. $BER = 10^{-9}$ is assumed.

structures that power penalty of a wavelength channel increases not only with the number of wavelength channels increases but also with the various positions of wavelength channels simultaneously. It is also found in cross-state of BOXCs that more power penalty occurs in 4×4 BOXC than 2×2 BOXC for the same number and position of the wavelength channels as well.

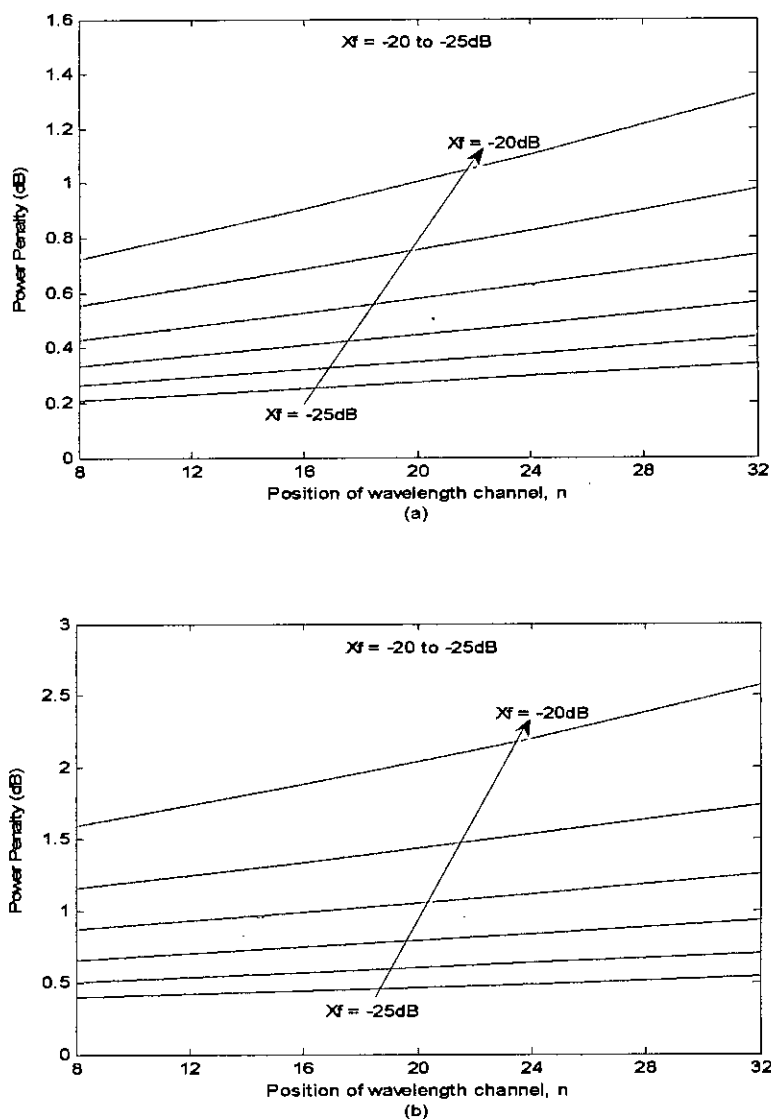


Figure 5.10: Power penalty as a function of position of the wavelength channels, n at the cross-state of (a) 2×2 BOXC and, (b) 4×4 BOXC with the different amount of component crosstalk, X_f , while the number of wavelength channels, $m = 32$, is fixed.

BER = 10^{-9} is assumed.

In the above discussion, at BER of 10^{-9} and component crosstalk of -22dB, we obtained the power penalty at the bar-state of 2×2 BOXC for 32-channel system is of 0.35dB for every wavelength channel in every position of the channel. But the power penalty in the cross-state of 2×2 BOXC for 32-channel system is different for different positions of the wavelength channel. In the cross-state of 2×2 BOXC, for the wavelength channel position 4 and 32, we get the power penalty of 0.38 dB and 0.74 dB, respectively.

TABLE 5.1
RECEIVED POWER AND POWER PENALTY DUE TO INTRABAND CROSSTALK IN
THE 2×2 BOXC

BER	X_f (dB)	X_R (dB)	m	n	Received Power (dBm)			Power Penalty (dB)	
					No Crosstalk	bar- state	cross- state	bar- state	cross- state
10^{-9}	-22	-25	32	4	-23.10	-22.75	-22.72	0.35	0.38
				8	-23.10	-22.75	-22.67	0.35	0.43
				16	-23.10	-22.75	-22.57	0.35	0.53
				24	-23.10	-22.75	-22.47	0.35	0.63
				32	-23.10	-22.75	-22.36	0.35	0.74

TABLE 5.2
RECEIVED POWER AND POWER PENALTY DUE TO INTRABAND CROSSTALK IN
THE 4×4 BOXC

BER	X_f (dB)	X_R (dB)	m	n	Received Power (dBm)			Power Penalty (dB)	
					No Crosstalk	bar- state	cross- state	bar- state	cross- state
10^{-9}	-22	-25	32	4	-23.10	-22.33	-22.29	0.77	0.81
				8	-23.10	-22.33	-22.23	0.77	0.87
				16	-23.10	-22.33	-22.11	0.77	0.99
				24	-23.10	-22.33	-21.98	0.77	1.12
				32	-23.10	-22.33	-21.84	0.77	1.26

Whatever the position of the channel at bar-state of BOXC, the power penalty is same for every wavelength channel for a 32-channel system and where as in the cross-state of BOXC for a 32-channel system, the power penalty increases with increasing the position of the channel. We also get the more power penalty in the cross-state than in the bar-state of 2×2 BOXC for the same number of wavelength channels. The reason for getting more PP is that the number of coherent and incoherent crosstalk fields induced in the bar-state remains unchanged due to fixed and tunable FBG set used in reverse order in the BOXCs, whereas the number of coherent crosstalk fields induced in the cross-state increases when the position of the wavelength channel increases.

Similarly, considering same BER and component crosstalk as 2×2 BOXC, it is found that the power penalty of 0.77dB at the bar-state for every wavelength channel of the 32-channel system and of 0.81dB and 1.26dB for the 4 and 32 position of the wavelength channels at the cross-state for 32-channel system of 4×4 BOXC. From the data obtained above it is clear that whatever the BOXC size more power penalty occur in cross-state than bar-state for the same number and position of the wavelength channel. We get about to double power penalty in 4×4 BOXC than in 2×2 BOXC for same number and position of the wavelength channel both in bar-state and cross-state, respectively.

The comparative analysis of received power and power penalty of 2×2 and 4×4 BOXCs with fixed number of wavelength channels using various position of wavelength channel in a 32-channel WDM system is given in Tables 5.1 and 5.2 at BER of 10^{-9} and component crosstalk of -22dB.

5.2 Impact of Optical Amplifier

Considering a metro ring network which has a single node without amplifier is discussed in the previous section. In a wavelength-routed metro ring network, a signal generated and launched at the departure node may traverse more than one node before it reaches its destination node. While traveling through the networks, the quality of the signal is affected by various signal degrading factors which are interrelated to one another. The effectiveness of one factor can vary according to the condition offered by others.

Therefore, how much the proposed BOXC influences the signal quality can be properly understood by investigating the signal transmitted in networks where not only the proposed BOXC, but also other network elements, such as fiber and optical amplifier, are present. Generally a metro ring network is to become a shorter span and the length of this network might be less than 100 km. Optical in-line amplifier need not to be used here due to the shorter span of the network. Along with proposed BOXC, we only consider a preamplifier in every node of such network ignoring degrading factors due to fiber and other elements. Analysis of the effect of optical amplifier on BER and PP in a WDM system is discussed in section 4.6.2. If there are N nodes, the amplified noise variance of receiver σ_{1A} is increased N times to become $N\sigma_{1A}^2$. We assume here that number of nodes (N) is equal to the number of preamplifier (N_A) used in WDM network. To observe the additionally induced BER and PP performance of a WDM system using optical preamplifier, we simulated the equation (4.27) incorporating signal-ASE beat noise, ASE-ASE beat noise along with intraband crosstalk and backscattering-induced crosstalk into this equation.

To evaluate the expression of σ_{th} as given by equation (4.22), we assumed $T = 300^0$ K, $k = 1.38 \times 10^{-23}$, $e = 1.603 \times 10^{-19}$, $B_e = 10^9$ Hz, noise figure, $F_n = 6$ dB, and $R_L = 100 \Omega$. To evaluate the BER, the following system parameters are chosen here: number of channels, $m = 32$, input power, $P_{in} = 0$ dBm, receiver bandwidth, $B_e = 1$ GHz, optical filter bandwidth, $B_0 = 2B_e$, plank constant, $h = 6.6261 \times 10^{-34}$, spontaneous emission factor, $n_{sp} = 2$, carrier frequency, $f_c = 193.55$ THz, gain of preamplifier, $G = 20$ dB, photodiode responsivity, $R_d = 1$, and component crosstalk, $X_F = -20$ dB to -25 dB.

Figure 5.11 shows the BER as a function of received power with the varying number of optical amplifiers used in a WDM ring network while the total number of wavelength channels is fixed in the bar-state of 2×2 and 4×4 BOXCs, respectively. In both configurations at the bar-state, usually BER increases with the number of wavelength channels increases. But in both structures, additional BER found only due to the noise induced by optical amplifier used in the network and BER increases with the number of optical amplifier increased since the amplifier induced noises accumulated through many nodes. It is observed between these two configurations that more BER found in the 4×4

BOXC than 2×2 BOXC with the same number of optical amplifiers and the same number of wavelength channels as well.

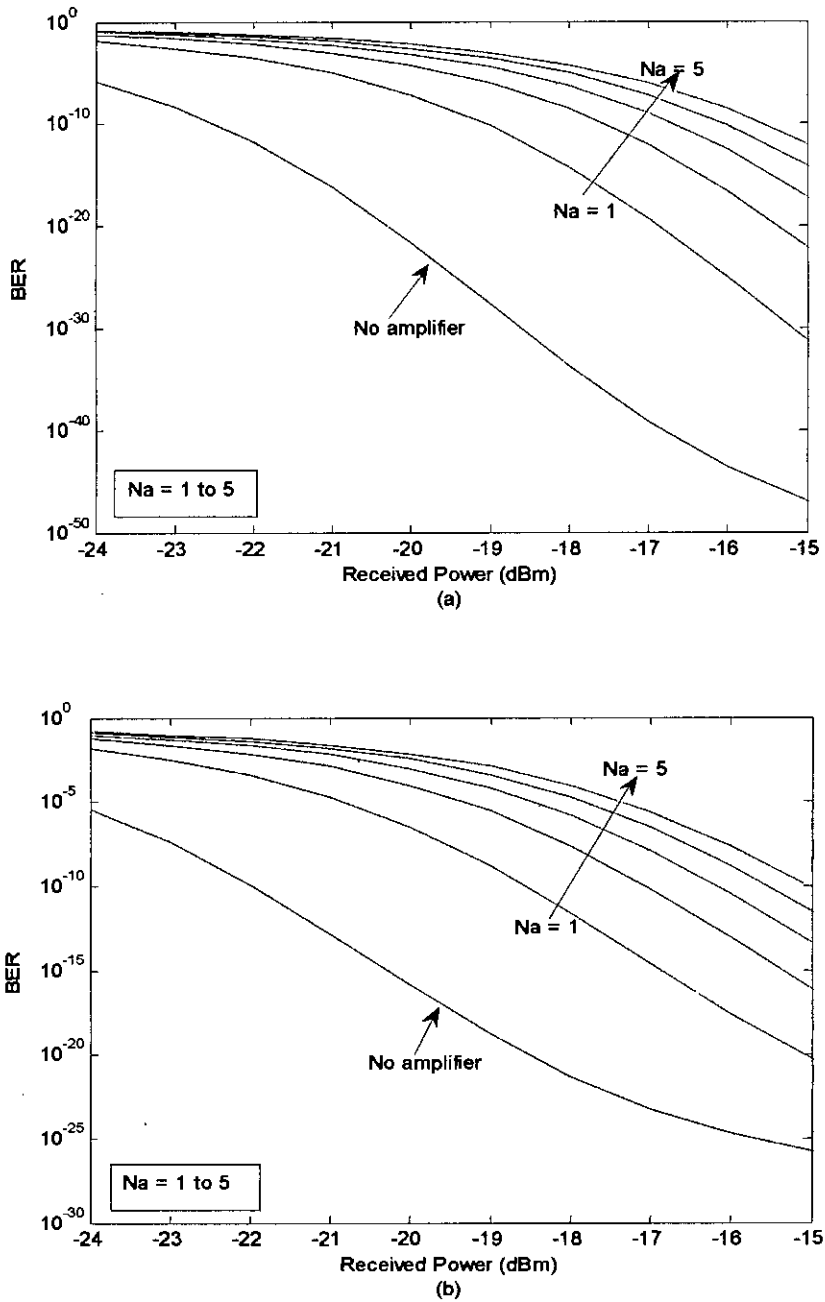


Figure 5.11: BER vs. received power at the bar-state of (a) 2×2 BOXC, and (b) 4×4 BOXC with the different number of optical amplifiers, N_a while the number of wavelength channels, $m = 32$, is fixed. Component crosstalk, $X_f = -22$ dB assumed.

Figure 5.12 shows the power penalty (PP) as a function of different number of amplifiers at bar-state of 2×2 BOXC and 4×4 BOXC while the number of wavelength channels is fixed. As the number of amplifier increases, additional receiver power penalty occurs since the receiver sensitivity decreased due to ASE-signal beat noise accumulation of optical amplifiers for maintaining the same BER. Whatever the positions of wavelength channel, PP will be the same for every channel position in the bar-state of BOXCs.

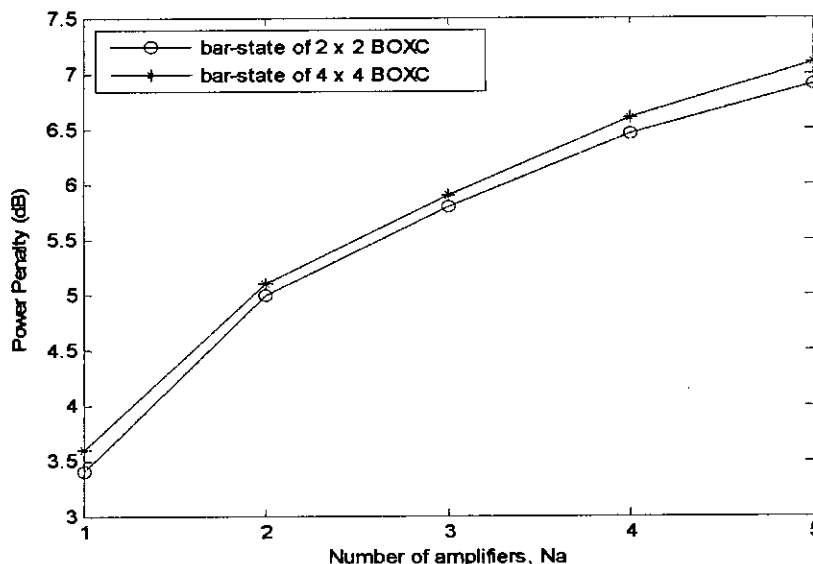


Figure 5.12: Power penalty as a function of number of optical amplifiers, N_a at the bar-state of (a) 2×2 BOXC and, (b) 4×4 BOXC with the number of wavelength channels, $m = 32$, is fixed. Component crosstalk, $X_f = -22\text{dB}$ and $\text{BER} = 10^{-9}$ is assumed. Data is obtained from the plot of figure 5.11.

Figure 5.13 shows the BER as a function of received power with the varying number of optical amplifiers used in a WDM ring network while the total number of wavelength channels and the channel's position is fixed in the cross-state of 2×2 and 4×4 BOXCs, respectively. In both configurations at the cross-state, usually BER increases not only with the number of wavelength channels increases but also with the channel's position increases. But in both structures, additional BER found only due to the optical amplifier used in the network and BER increases with the number of optical amplifier increased. It is observed between these two configurations that more BER found in the 4×4 BOXC

than 2×2 BOXC with the same number of optical amplifiers and the same number of wavelength channels as well as channel's position.

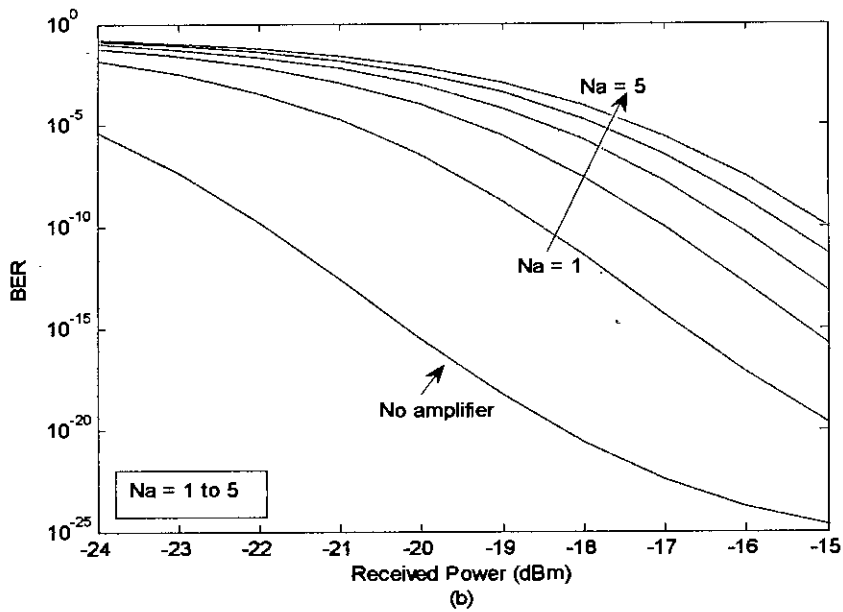
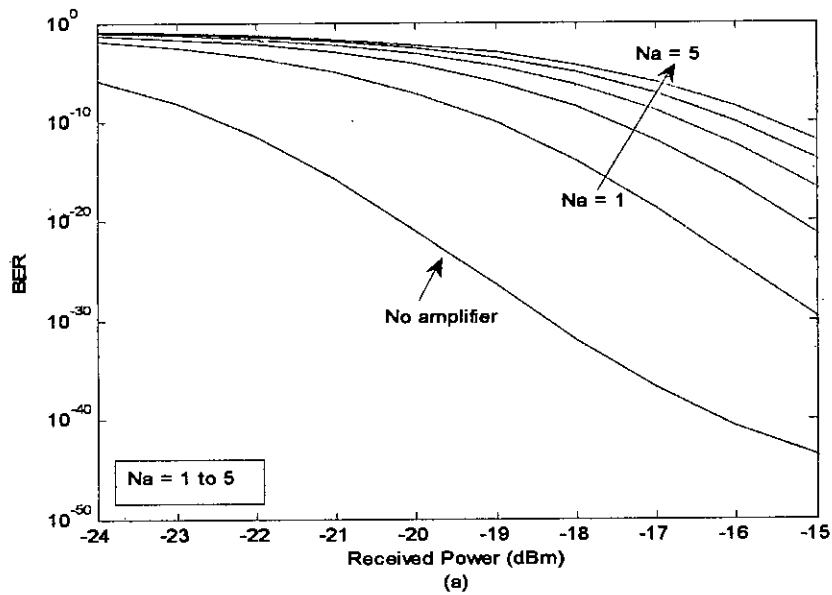


Figure 5.13: BER vs. received power at the cross-state of (a) 2×2 BOXC, and (b) 4×4 BOXC with the varying number of optical amplifiers, N_a while the wavelength channel position, $n = 4$, and the total number of wavelength channels, $m = 32$, is fixed.

Component crosstalk, $X_f = -22$ dB assumed.

Figure 5.14 shows the power penalty (PP) as a function of different number of amplifiers at cross-state of 2×2 BOXC and 4×4 BOXC while the number of wavelength channels and the position of the channel is fixed. As the number of amplifier increases, additional receiver power penalty occurs since the receiver sensitivity decreased due to signal-ASE beat noise accumulation of optical amplifiers for maintaining the same BER. Unlike the bar-state of BOXCs, PP also increases with the wavelength channel position increases.

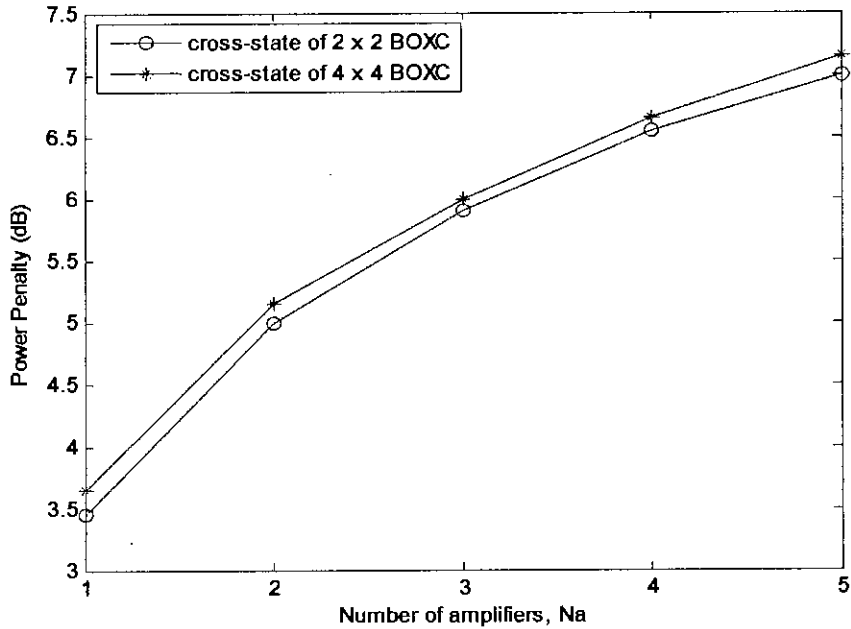


Figure 5.14: Power penalty as a function of number of optical amplifiers, N_a at the cross-state of (a) 2×2 BOXC and, (b) 4×4 BOXC with the number of wavelength channels, $m = 32$, and position of wavelength channel, $n = 4$, is fixed. Component crosstalk, $X_f = -22$ dB and BER = 10^{-9} is assumed. Data is obtained from the plot of figure 5.13.

In the above discussion at BER of 10^{-9} and component crosstalk of -22dB, receiver sensitivity decreases due to amplifiers noise accumulated both in bar and cross state of BOXCs. We have seen from the above simulation and from the Tables 5.3 and 5.4 that receiver sensitivity slightly lower in cross-state than in bar-state of the BOXCs i.e. slight additional power penalty occurs due to the position of wavelength channel since BER in cross-state of BOXCs not only depends on number of wavelength channels but also on

wavelength channel position. From Tables 5.3 and 5.4 that we have also seen that receiver sensitivity decreases i.e. PP increases with the increasing number of optical amplifier in a WDM system.

It is found in previous section that without using amplifier in a 32-channel WDM system, 0.35 dB and 0.38 dB power penalty occur for every channel in bar and cross state of 2×2 BOXC and 0.77 dB and 0.81 dB power penalty occur for every channel in bar and cross state of 4×4 BOXC, respectively. Using amplifier in a WDM system, PP significantly increases both in bar and cross state of BOXCs and PP increases as the number of amplifier increases. If only one amplifier used in 32-channel system, 3.4 dB and 3.45 dB PP found in bar and cross state of 2×2 BOXC and 3.6 dB and 3.65 dB PP found in bar and cross state of 4×4 BOXC, respectively. Comparing amplified WDM system with the unamplified WDM network, it is clear that additional PP occurs in amplified system due to receiver sensitivity degradation for additional noise accumulation on receiver. It is also found that more PP occurs in 4×4 BOXC than in 2×2 BOXC from the above analysis considering the same number and position of the wavelength channels. Unlike WDM system without optical amplifier discussed in previous section, we do not get about to double PP but slightly higher PP in 4×4 BOXC than in 2×2 BOXC since here signal-ASE beat noise power is more dominant noise power than other noise sources.

TABLE 5.3
RECEIVED POWER AND POWER PENALTY DUE TO OPTICAL AMPLIFIER IN
THE 2×2 BOXC

BER	X_f (dB)	m	n	N_a	Received Power (dBm)		Power Penalty (dB)	
					bar-state	cross-state	bar-state	cross-state
10^{-9}	-22	32	4	0	-22.8	-22.7	0.35	0.38
				1	-19.4	-19.25	3.4	3.45
				2	-17.78	-17.7	5.0	5.02
				3	-16.9	-16.8	5.8	5.9
				4	-16.35	-16.25	6.45	6.55
				5	-15.9	-15.7	6.9	7.0

TABLE 5.4
 RECEIVED POWER AND POWER PENALTY DUE TO OPTICAL AMPLIFIER IN
 THE 4×4 BOXC

BER	X_f (dB)	m	n	N_a	Received Power (dBm)		Power Penalty (dB)	
					bar-state	cross-state	bar-state	cross-state
10^{-9}	-22	32	4	0	-22.4	-22.35	0.77	0.81
				1	-18.8	-18.7	3.6	3.65
				2	-17.3	-17.25	5.1	5.15
				3	-16.5	-16.4	5.9	6.0
				4	-15.8	-15.7	6.6	6.65
				5	-15.25	-15.2	7.1	7.15

The comparative analysis of received power and power penalty of 2×2 and 4×4 BOXCs using varying number of optical amplifiers in a 32-channel WDM system is given in Tables 5.3 and 5.4 at BER of 10^{-9} and component crosstalk of -22dB.

5.3 Summary

In this chapter, performance analysis of FBG-OC based BOXCs has been carried out by examining the BER and power penalty due to linear crosstalk induced in BOXCs. Detail simulation is done to evaluate BER performance and PP that are occurred for receiver sensitivity degradation due to intraband crosstalk arises in BOXCs and also due to optical amplifiers used in a WDM network. Discussion and analysis are carried out considering the BOXCs without and with amplifier separately. Simulation is done based on analytical expressions developed in sections 4.4 and 4.6. The comparative effect of different system parameters on BER performance and PP is also discussed in this chapter.

CHAPTER SIX

Conclusion and Scope of Future Work

5.1 Conclusion

A highly channel-scalable FBG-OC-based BOXC is considered and its performances are investigated using numerical simulations. The effect of intraband crosstalk induced due to FBGs operation in BOXCs is considered. The effect of backscattering-induced crosstalk due to bidirectional operation of WDM network is also considered. FBG-OC-based two structures such as 2×2 BOXC and 4×4 BOXC are considered and analyzed for connecting two or more bidirectional WDM ring networks. Analytical expressions for BER and power penalty due to intraband and backscattering-induced crosstalk for BOXC have been developed. Considering optical amplifier in a WDM network, analytical expression of BER for BOXC has been modified. Numerical computation has been done regarding the calculation of BER and power penalty with the different number of system parameters for bidirectional WDM network considering without and with amplifier separately.

It is found in the analysis that BER and power penalty increased both in bar and cross state BOXCs with the number of wavelength channels increases. The main problem of such kind of BOXCs is that the BER and power penalty also increases significantly as the position number of channel increases in the cross-state while changing the position of the wavelength channels does not affect on BER and PP in the bar-state. Receiver sensitivity is significantly degraded which causes additional BER and power penalty due to signal-ASE beat noise induced in optical amplifiers. To achieve a particular network performance, we need to compromise with the different system parameters.

From the numerical simulations of signal transmission in the WDM networks employing the proposed FBG-OC based BOXCs, the signal-crosstalk beat noise in unamplified system and ASE-signal beat noise in amplified system are found to be most critical limiting factors of the BOXC size. However, the proposed FBG-OC-based BOXC can

play a key role in constructing the reconfigurable and upgradeable all-optical WDM networks by providing dynamic routing function and high-channel scalability.

5.2 Scope of Future Work

In this work, we have considered only linear crosstalk such as intraband crosstalk on BER performance and power penalty. Non linear crosstalk induced by fiber nonlinearities such as cross-phase modulation (XPM) and four-wave mixing (FWM) is not considered. Dispersion due to fiber as well as group velocity dispersion (GVD) due to FBGs for a signal are not taken into account. Polarization independent optical amplifier is considered but polarization dependent amplifier may cause performance degradation of the receiver which is not considered. Therefore, future work can be done considering all the above factors in the expression of BER and power penalty to observe the network performance.

Bibliography

- [1] Gyselings T., Morthier G., and Baets R., "Crosstalk analysis of multiwavelength optical cross connects," *J. Lightwave Technol.*, vol. 17, pp. 1273–1283, Aug. 1999.
- [2] Shen Y., Lu K., and Gu W., "Coherent and incoherent crosstalk in WDM optical networks," *J. Lightwave Technol.*, vol. 17, pp. 759–764, May 1999.
- [3] Wu X., Lu C., Ghassemlooy Z., and Wang Y. X., "Evaluation of intraband crosstalk in an FBG-OC-based optical cross connect," *IEEE Photon. Technol. Lett.*, vol. 14, pp. 212–214, Feb. 2002.
- [4] Simmons J. M. and Saleh A. A. M. *et al.*, "Optical cross connects of reduced complexity for WDM networks with bidirectional symmetry," *IEEE Photon. Technol. Lett.*, vol. 10, pp. 819–821, June 1998.
- [5] Park S. K. and Park J. W. *et al.*, "Multiwavelength bidirectional optical cross connect using fiber Bragg gratings and polarization beam splitters," *IEEE Photon. Technol. Lett.*, vol. 12, pp. 888–890, July 2000.
- [6] Kim J. and Lee B., "Independently switchable bidirectional optical cross connects," *IEEE Photon. Technol. Lett.*, vol. 12, pp. 693–695, June 2000.
- [7] Kim S., "Bidirectional optical cross connects for multiwavelength ring networks using single arrayed waveguide grating router," *J. Lightwave Technol.*, vol. 20, pp. 188–194, Feb. 2002.
- [8] Uddin M. J., "Analysis of crosstalk due to unidirectional and bidirectional optical cross-connects in a WDM network," *M.Sc. Thesis*, Dept. of Electrical and Electronic Engineering, Bangladesh University of Engineering and Technology, Bangladesh, 2008.

- [9] Yuan H., Zhong W. and Hu W., "FBG-based bidirectional optical cross connects for bidirectional WDM ring networks," *J. Lightwave Technol.*, vol. 22, pp. 2710–2721, Dec. 2004.
- [10] Moon N. S. and Kikuchi K. " $N \times N$ Multiwavelength optical cross connects based on tunable fiber Bragg gratings," *J. Lightwave Technol.*, vol. 21, pp. 703-718, March 2003.
- [11] Attard J. C., Mitchell J. E., and Rasmussen C. J., "Performance analysis of interferometric noise due to unequally powered interferers in optical networks," *J. Lightwave Technol.*, vol. 23, pp. 1692–1703, April 2005.
- [12] Chai T. Y., Cheng T. H., Ye Y., Liu Q., "Inband crosstalk analysis of optical cross-connects architectures," *J. Lightwave Technol.*, vol. 23, pp. 688–701, Feb. 2005.
- [13] Dods S. D., Anderson T. B., "Calculation of bit-error rates and power penalties due to incoherent crosstalk in optical networks using Taylor series expansions," *J. Lightwave Technol.*, vol. 23, pp. 1828–1837, April 2005.
- [14] Karfaa M. Y., Ismail M., Abbou F. M., Shaari S., "Performance evaluation of linear crosstalk in array waveguide grating router in WDM networks," *ELEKTRIKA*, vol. 9, no. 2, pp. 56-59, Faculty of Electrical Engineering, Universiti Teknologi Malaysia, 2007.
- [15] Olsson N. A., "Lightwave systems with optical amplifiers," *J. Lightwave Technol.*, vol. 7, pp. 1071–1082, July 1989.
- [16] Keiser G., "*Optical Fiber Communication*," 3rd Edition, McGraw-Hill Companies, Inc., 2000.
- [17] Agrawal G. P., "*Applications of Nonlinear Fiber Optics*," Academic Press, San Diego, CA, 2001.

- [18] Ramaswami R., Sivarajan K. N., “*Optical Networks: A Practical Perspective*,” 2nd Edition, Morgan Kaufmann Publishers, 2002.
- [19] Agrawal G. P., “*Fiber Optic Communication Systems*, 3rd Edition, John Willey & Sons, 2002.
- [20] Karim M. R., Majumder S. P., “Crosstalk modeling and analysis of FBG-OC-based bidirectional optical cross connects for WDM networks,” in proceedings *IEEE TENCON 2009* Singapore, Nov. 23-26, 2009.

Index

A

All-optical network, 4
Amplified spontaneous emission, 65, 68
Amplifier, 25
Amplifier noise, 64
Arrayed Waveguide Grating, 22
ASE-ASE beat noise, 68
ASE, 65, 68
AWG, 6

B

Back-reflection, 49
Backscattering, 6, 51
Bandwidth-length product, 2
Beat, 61, 68
BER, 6, 61, 63, 65, 70
Bidirectional, 42, 49
Bit-error-rate, 64
BOADM, 44
BOXC, 5, 44, 50
Bragg wavelength, 51
Broadcast-and-select, 39
Bus topology, 37
BWRN, 44

C

Circulator, 18
Coherent crosstalk, 56, 57, 58, 59, 61, 62
Coupler, 14
Crosstalk, 45, 48
Cross-phase modulation, 92

D

Demultiplexer, 22
Dense WDM, 20, 39
Directional coupler, 14

E

EDFA, 27
Erbium-doped fiber amplifier, 27
Extinction ratio, 65, 67

F

Fabry-Perot Filter, 26
FBG, 20, 45, 50
Fiber, 1
Fiber Bragg grating, 19, 63

Four-wave mixing, 92

G

Gain of optical amplifier, 64, 68

Gaussian distribution, 66

Group velocity dispersion, 92

GVD, 92

H

Heterodyne crosstalk, 6

Homodyne crosstalk, 6

I

Inband crosstalk, 6

Incoherent crosstalk, 56, 57, 58, 59, 61, 63

Interband crosstalk, 46

Interchannel crosstalk, 46

Intraband crosstalk, 47, 53, 67, 71

Intrachannel crosstalk, 47

Isolator, 20

L

LAN, 36

Linear crosstalk, 5

Local Area Network, 36

M

Mach-Zehnder Interferometers, 16

MAN, 36, 44

Multi-hop network, 40

Multiplexer, 16, 17

MZI, 16

N

Network Topology, 36

Noise, 63, 66

Noise figure, 69

Nonlinear crosstalk, 92

O

OADM, 32

OLT, 31

OC, 45

Optical circulator, 6, 45

Optical ADD/Drop Multiplexer, 31, 32

Optical amplifier, 25, 69, 82

Optical cross connects, 5, 31, 34

Optical fiber, 1

Optical line terminal, 31

OXC, 5

P

PBS, 6
PMD, 6
Power Penalty, 6, 67
Point-to-point link, 40
PP, 6, 67
Probability density function (PDF), 66

Q

Q-factor, 67

R

Raman amplifier, 28
Rayleigh backscattering (RB), 51, 64
Receiver, 68
Rotatable Optical Circulator (ROC),
51
Routing, 41
Responsivity, 67
Ring topology, 37, 38

S

SDH, 38
Semiconductor Optical Amplifier, 27
Signal-ASE beat noise, 6
Signal-to-noise ratio, 68
Single-hop network, 40
Shot noise, 64, 66, 68
SONET, 38
Star coupler, 15

Stimulated Raman Scattering (SRS), 29

T

Thermal noise, 64, 66, 68

U

Unidirectional, 42

W

Wavelength-routed network, 41
WDM, 4
WDM Mux/Demux, 49
WDM Network Elements, 32
WDM networks, 31

